5-25-2012

Spectral printing of paintings using a seven-color digital press

Simon Muehlemann

Spectral Printing of Paintings using a Seven-Color Digital Press

by

Simon Muehlemann

A Thesis Submitted in Partial Fulfillment
of the Requirements for the Degree of Master of Science
in the School of Print Media
in the College of Imaging Arts and Sciences
of the Rochester Institute of Technology

May 25, 2012

Thesis Committee:

Primary Thesis Adviser: Dr. Franziska Frey
Secondary Thesis Adviser: Dr. Roy S. Berns
Graduate Program Coordinator: Dr. Patricia Sorce

School of Print Media
Rochester Institute of Technology
Rochester, New York

Certificate of Approval

Spectral Printing of Paintings using a Seven-Color Digital Press

This is to certify that the Master's Thesis of

Simon Muehlemann

has been approved by the Thesis Committee as satisfactory
for the thesis requirement for the Master of Science degree
at the convocation of

May 2012

Thesis Committee:

_____
Dr. Franziska Frey, Primary Thesis Advisor

_____
Dr. Roy S. Berns, Secondary Thesis Advisor

_____
Dr. Patricia Sorce, Graduate Thesis Coordinator

_____
Chris Bondy, Administrative Chair, School of Print Media

Acknowledgements

I would like to thank Dr. Franziska Frey from the School of Print Media for serving as my primary thesis advisor. Dr. Frey guided me throughout my graduate study at RIT and my master's thesis.

My sincere thanks go to Dr. Roy S. Berns, Director of the Munsell Color Science Laboratory at RIT. His tireless inspiration, teaching and guidance taught me so much. This thesis would not have been possible without having Dr. Berns as an advisor. I enjoyed working with Dr. Berns, his faculty, staff and students at the Munsell Color Science Laboratory.

Professor Franz Sigg from the School of Print Media served as a technical advisor. His knowledge and experience in the area of print process control was very valuable for preparing the press runs.

My parents deserve my sincere thanks for all their support.

There are many people that supported and advised me throughout my master's thesis. Here I would like to name a few of them: The PhD students Max Derhak and Farhad Abed from the Munsell Color Science Laboratory for sharing their ideas and giving me advice; Lawrence Taplin for sharing results and code from his masters thesis; Susan Farnand for editing this document; Sarah and Roman Philipp for supporting me when I needed help writing C code. Jeremy Vanslette, Daniel Clark and Tim Richardson from the Printing Applications Laboratory at RIT for their help during the press runs; Mark Golden, Bob Gamblin, Mark Gottsegen and Thomas Bosket for sharing their knowledge about painting and artist materials.

Contents

List of Figures

List of Tables

Abstract

The human visual system is trichromatic and therefore reduces higher dimensional spectral data to three dimensions. Two stimuli with different spectral power curve shapes can result in the same cone response and therefore match each other. Color reproduction systems take advantage of this effect and match color by creating the same cone response as the original but with different colorants. ICC color management transforms all colors into a three-dimensional reference color space, which is independent from any input or output devices. This concept works well for a single defined observer and illumination conditions, but in practice, it is not possible to control viewing conditions leading to severe color mismatches, particularly for paintings. Paintings pose unique challenges because of the large variety of available colorants resulting in a very large color gamut and considerable spectral variability. This research explored spectral color reproduction using a seven-color electrophotographic printing process, the HP Indigo 7000. Because of the restriction to seven inks from the 12 basic inks supplied with the press, the research identified both the optimal seven inks and a set of eight artist paints which can be spectrally reproduced. The set of inks was Cyan, Magenta, Yellow, Black, Reflex Blue, Violet and Orange. The eight paints were Cadmium Red Medium, Cadmium Orange, Cadmium Yellow Light, Dioxazine Purple, Phthalo Blue Green Shade, Ultramarine Blue, Quinacridone Crimson and Carbon Black. The selection was based on both theoretical and experimental analyses. The final testing was computational indicating the possibility of both spectral and colorimetric color reproduction of paintings.

Chapter 1

Introduction

The human eye perceives color with cones ($\bar{l}_\lambda,\ \bar{m}_\lambda,\ \bar{s}_\lambda$) that are sensitive to long, medium and short wavelength light. This trichromatic nature of the human visual system reduces the dimensionality of spectral curves in the visible range to three dimensions. The amount of light reaching the cones (Φ_λ) is integrated and describes a color using only three dimensions (Equation 1.1). Two stimuli with different curve shapes can result in the same LMS cone response and therefore appear to be identical (Equation 1.2).

$$\begin{aligned} L &= \int \Phi_\lambda \bar{l}_\lambda d\lambda \\ M &= \int \Phi_\lambda \bar{m}_\lambda d\lambda \\ S &= \int \Phi_\lambda \bar{s}_\lambda d\lambda \end{aligned} \tag{1.1}$$

$$\begin{bmatrix} L \\ M \\ S \end{bmatrix}_1 = \begin{bmatrix} L \\ M \\ S \end{bmatrix}_2 \tag{1.2}$$

Current color reproduction systems take advantage of this principle and match colors by creating the same cone response as the original. In photography, for example, film uses three dyes and digital cameras use three color filters. The trichromatic concept is also implemented in ICC color management systems. The three primary cone responses are transformed to CIE XYZ tristimulus values, which are used to describe colors in a device-independent fashion. ICC color management is powerful because the input from different devices is transformed into a reference color space (more commonly referred to as a profile connection space, PCS), shown in Figure 1.1. The mapping from device coordinates to the reference color space, usually CIELAB, is depicted by the *T* box representing a transformation. From there, color can be transformed to different output devices. This allows a fully color managed workflow from input to output.

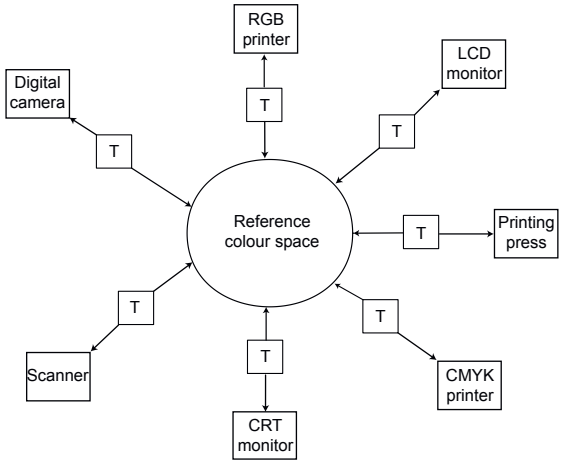

Figure 1.1: Use of reference color space in ICC profiles. Source: [ICC, 2010]

Color printing is based on this same trichromatic concept. However, printing processes use four primaries rather then the requisite three, commonly cyan, magenta,

yellow and black (CMYK). The addition of black ink has several purposes. First, most printed products use black ink to print text. Printing three-color text is impractical for print production. Black ink is also helpful for ink saving because in neutral tones, the gray component of CMY inks can be replaced with the less expensive black. This also reduces the total amount of ink used to print neutral tones. The human eye is very sensitive to small color differences in neutral tones. Using black ink in the separation helps to reduce the visibility of process variation in production. The flat spectral reflectance of black ink also reduces the sensitivity of neutral tones to color shifts when viewing conditions are changing. Despite all the advantages of using black, there are also some concerns. Using excessive gray component replacement in the separation can lead to grainy images and for some commercial systems, reduced chroma of colors. Graininess can also occur with only CMY because of the high contrast between cyan or magenta and white paper. Different systems were developed to reduce graininess for typical CMYK ink sets by adding light inks (e.g., light cyan, light magenta or light black). These additional inks improve the image quality of light colors but do not add any additional degrees of freedom for the separation algorithm.

These conventional color reproduction systems work well under controlled viewing conditions. The ICC specifications use Illuminant D50 and the CIE 1931 2° standard observer to define CIE L*a*b* values. In practice, however, it is not possible to control the viewing conditions under which the end-user is viewing the reproduction. There is no real D50 light source and a real observer is unlikely to have exactly the same cone

sensitivities as the CIE 1931 2° standard observer.

The consequence of uncontrolled viewing is the likelihood of poor color matching between an original and reproduction due to metamerism. This is of particular concern for artwork reproduction. Artist materials use a wide range of different pigments. CMYK color printing cannot represent such a wide range of paint pigments. A spectral match is impossible for most artist materials leading to color-mismatch under illuminants other than D50. The color gamut is insufficient to create a colorimetric match for many pigments by using CMYK. Adding additional colored inks can increase color gamut, e.g., Red, Green and Blue (CMYKRGB) [Küppers, 1993] or Orange and Green (CMYKOG) [Pantone, 1998]. Although these additional inks were developed to increase color gamut, they can also be used to improve the spectral matching of artwork.

For many years, the Munsell Color Science Laboratory (MCSL) at the Rochester Institute of Technology (RIT) has been conducting research in the field of spectral color reproduction [Kohler and Berns, 1993, Tzeng, 1999, Taplin, 2001, Urban et al., 2008]. Multi-ink printing was not only used for spectral color reproduction but also to improve image quality [Chen, 2006]. Using more than the standard CMYK inks can improve image quality and provides more degrees of freedom to reduce metamerism or implement spectral color matching. A spectral color match would provide an invariant color reproduction across all observers and viewing conditions.

This thesis explores the spectral reproduction of paintings. Reproducing paintings is a unique challenge because a very wide range of pigments are available to the artist. These

pigments not only span a huge color gamut, but also have very distinctive spectral curve shapes. Certain artist pigments are well known to cause problems in color reproduction (e.g., Ultramarine Blue, Cobalt Blue or Cadmium Orange). The spectral reproduction of such pigments would increase the accuracy of the reproduction under uncontrolled viewing conditions.

The HP Indigo printing process was selected for use in this research. This multi-ink digital printing system provides some unique opportunities as well as some constraints. It allows the printing of seven inks, which is unique for current electrophotographic presses. The seven ink units can either take one of the twelve primary inks or a custom mixed spot color. Printing with seven colors challenges the screening technology. Despite the seven inks, the system only offers four different screening angles.

For the purpose of this research, the ink set was limited to the existing twelve primary inks. The spectral properties of these primary inks were retrieved by printing them on the HP Indigo. Using seven inks does not provide enough degrees of freedom to match all artist paints. Therefore, a palette of artist paints and its corresponding ink set for spectral matching was defined. Evaluating paints and inks required spectral modeling of both the paints and the printing system. The spectral modeling allowed evaluation of inks required to match artist pigments. The evaluation of all paints and inks lead to the final ink and paint set. After completing the ink and paint selection, the printing process was characterized in a second press run. This allowed accurate spectral modeling of the printing process. The Cellular-Yule-Nielsen-Spectral-Neugebauer model was used to

predict the spectral reflectance of the print. This thesis is limited to a computational evaluation of the performance of the printing system. A custom paint target, gray metamers and synthetic spectral images were used to evaluate the performance of the system.

Chapter 2

Review of the Literature – Conventional Color Reproduction

2.1 Overview

This literature review provides the reader an overview about conventional color reproduction. Extensive literature is available for each topic. This review covers a few of the most relevant studies. From the principles of color reproduction, the reader is led to current color management workflows as they are implemented in the graphic arts industry today.

2.2 Introduction to Color Reproduction

Current color reproduction is based on colorimetric principles. The current systems take advantage of the human visual system, which is trichromatic. When the spectra of different colors generate the same cone signals, they are perceived as the same color. Tristimulus values are calculated from the color reflectance of the sample, the illumination

spectrum, and the color-matching functions of a standard observer. The integration underneath this curve delivers tristimulus values. Therefore, different curves can generate the same tristimulus values. These XYZ values can be transformed to different color spaces, such as CIELAB or RGB (Berns, 2000).

Color-mixing models are either additive or subtractive. Additive primary colors (i.e., red, green, and blue) mix by adding up to white. The corresponding secondary colors are cyan, magenta, and yellow. Subtractive primary colors (i.e., cyan, magenta, and yellow) add up to black. Red, green, and blue are the secondary colors in a subtractive color-mixing system. In real-world color reproduction, black is added to the subtractive system. Black is needed because the overprinting of all primaries do not appear as black because the pigments are not as perfect as they are in the theoretical system. Therefore, the use of black ink improves the color gamut. The theoretical color models RGB and CMYK are based on the idea of ideal pigments. These pigments do not have any reflection in the wavelengths of other primaries (Berns, 2000).

The effect of metamerism is used to generate a color reproduction that matches the original. Unfortunately, the use of metamerism for color reproduction is accurate for a specific observation condition only. These systems work only for one observer and illuminant combination (e.g., CIE illuminant D50 and the CIE 1931 standard observer). By changing the observer or the illuminant, the appearance of the reproduction becomes inconsistent. The problem of metamerism could be overcome by generating a spectral match between the original and the color reproduction (Berns, 2000).

2.3 Current Color Reproduction in Printing

None of the commercial printing processes used today are capable of generating true continuous tones. These systems are monochromatic and can print only solid tones or no color. Therefore, continuous tones are generated by applying screening technology. Halftoning technology can produce the appearance of continuous tones by taking advantage of the human eye's inability to resolve the small screening dots. Small dots placed on white paper are blended by the eye to become continuous tones. Different sizes of dots generate different tone values. Decades ago, the screens were made by exposing an extremely high contrast film through a glass plate with very fine opaque lines. After development, this film consisted almost entirely of black dots and white space. Color separations were built by using color separation filters. In multi-color printing, proper selection of the screening frequencies and angles is crucial to prevent artifacts, such as moiré. Currently, screening and separation are generated by using digital systems. Screening dots are generated by many exposure spots of the output device. The addressability of the system determines the number of tone values that a system can produce (Hunt, 2004).

Color reproduction with halftone screens was described in general by Neugebauer in 1937 [Neugebauer, 1937]. A three-ink system consists, for example, of cyan (c), magenta (m), and yellow (y). The area not covered by cyan is 1-c, the area not covered by magenta is 1-m, and the area not covered by yellow is 1-y per unit area of paper. The probability that an area of the paper is covered with cyan is c. The same applies to the other primary

colors. An area covered by all three inks has the probability of the product of c, m, and y. Any other point on the paper not covered with ink has the probability of the product of 1-c, 1-m, and 1-y. A color reproduction system with three inks would have $2^3 = 8$ Neugebauer primary colors. Figure 2.1 shows an example with two colors (Hunt, 2004).

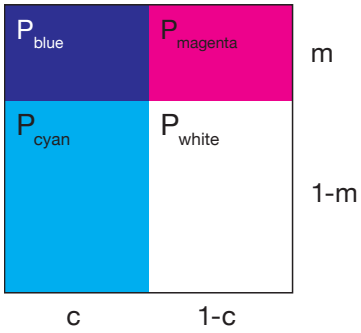

Figure 2.1: Neugebauer printing model with two colors (after Taplin 2001)

In current printing systems, the four primary colors (i.e., cyan, magenta, yellow, and black) are used. Multi-color presses apply the inks on top of each other in a very short time. Therefore, the previous ink film is not dry when the next is applied. Applying too much ink at one spot causes different problems in printing. Digital color separation allows the refinement of the color separations to avoid problems in printing. Two different concepts of reducing the total amount of ink placed on the paper are used. Under Color Removal (UCR) removes ink in dark tones to reduce the total area coverage (TCA). Gray Component Replacement (GCR) replaces the gray component of a tone (i.e., the smallest common amount of ink occurring in cyan, magenta, and yellow) with black ink. This leads to TCA reduction, better gray balance stability in printing, and ink saving. Both concepts are, again, based on the phenomenon of metamerism (Hunt, 2004).

2.4 Current Color Management Workflow

Several different color output devices are used in current workflows. The color of an image needs to be optimized for the output of every single device. Since the usage of ICC profiles, we have the ability to easily convert an image from one to another color space. The ICC specifications are published by the International Color Consortium, approved by ISO TC130, and published as ISO standards. (The latest ICC Version 4.3 is published as ISO 15076-1:2010.) The ICC profiles can be attached to a file to keep the description of the output intent within the file. This allows the conversion of the image to other color spaces with good color accuracy. ICC profiles are very well supported by nearly every software package used in current color management workflows. An ICC profile contains several color transformations in the form of look-up tables (LUT), matrices, or curves. The profile connection space (PCS) uses the output independent color spaces CIELAB and XYZ defined by the International Commission on Illumination (CIE). As illustrated in Figure 2.2, ICC profiles typically contain a source profile and a destination profile. Different rendering intents are implemented to allow an appropriate color gamut mapping for the output device. A color-matching module (CMM) is used to perform the interpolation of the LUT (Green, 2010).

There are two concepts of color rendering workflows: early binding and late binding. These terms are widely used in the graphics industry to describe when the color conversion/separation in a workflow is performed. In both cases, the image first is present in a color space, such as RGB or CIELAB. (Capturing directly to CMYK is rarely used

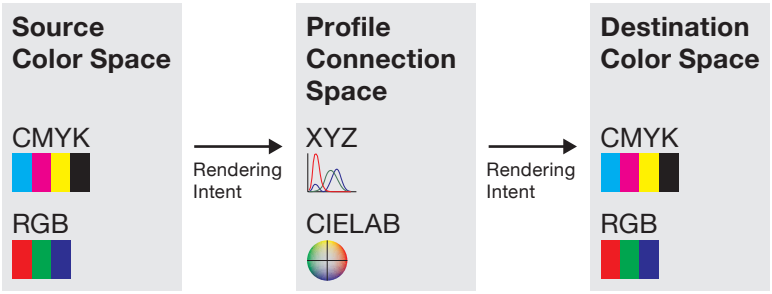

Figure 2.2: Basic structure of an ICC profile

today.) Early binding performs the color conversion/separation right after the image processing stage. This concept assumes that the output intent is already known. Late binding defers the conversion/separation to the device color space until the file reaches the output device. Both concepts have advantages and disadvantages. The usage depends on workflow, its capabilities, and the quality demand of the final product (Green, 2010).

Chapter 3

Review of the Literature – Spectral Color Reproduction

3.1 Overview

This literature review provides the reader with an overview of the topic of spectral color reproduction. Much research related to spectral color reproduction has been done in the past. A few of the most relevant studies are reviewed here. The reader is led to different aspects of spectral reproduction. Essential parts of spectral reproduction, such as challenges for the workflow, ink selection, ink overprint prediction, multi-color separation, and printing models, are covered.

3.2 Spectral Workflow

Implementing a spectral color reproduction workflow is a very complex process. From input to processing and output, spectral color reproduction requires new methods and technologies in the workflow. Handling the huge amounts of data is one of the biggest

challenges. The significant increase in dimensionality could be reduced by using an Interim Connection Space (ICS). A detailed investigation of the roadblocks leading to spectral color reproduction was made by Rosen [Rosen, 2003].

3.3 Spectral Capturing

Spectral printing requires input data in the form of spectral reflectance for every pixel. Spectral reflectance can be reconstructed by using a multi channel camera. A commercial camera equipped with two absorption filters can be used to reconstruct the spectral reflectance from only six camera channels. The developed matrix R method is based on the Wyszecki hypothesis and the matrix R theory and is explained by Zhao and Berns as follows: *The matrix R method can be used to generate spectra by combining the fundamental stimuli from the predicted tristimulus values with the metameric blacks from the estimated spectral reflectance factors based on the Wyszecki hypothesis.* This combination of a spectral and a colorimetric reconstruction is a big advantage because the high colorimetric accuracy is combined with an accurate spectral reconstruction. [Zhao and Berns, 2007]

3.4 Spectral Printing

3.4.1 Workflow of Spectral Color Reproduction

Implementing a spectral-based color reproduction workflow does incorporate some challenges. One of the main challenges is the huge amount of data produced in a spectral workflow. By using efficient methods, these data can be reduced. Research has been done that concluded that spectral imaging could be done with fewer channels than are currently implemented in spectral systems. The use of an Interim Connection Space (ICS) could reduce the bottleneck of dimensionality in processing. Much future work needs to be conducted before a realistic use of spectral reproduction will be possible. Nevertheless, with today's available processing power, spectral reproduction is possible and can be considered for use in different applications in the future [Rosen, 2003].

3.4.2 Reducing Metamerism

Existing multi-ink printing systems only focus on expanding color gamut. The goal of the separation of these multi-ink printing systems is to produce a colorimetric match. The problem of metamerism is not addressed. The use of more than the four process inks would increase the degrees of freedom, relative to what is currently provided. Tzeng (1999) addressed the problem of reducing metamerism by developing a spectral-based color separation algorithm. To reduce metamerism, it is important to have as much information as possible about the spectral properties of the inks used in the original object.

The spectral characteristics of the original can be captured by using a spectral capturing system, or a spectrophotometer. The selection of an optimal ink set is a complex task. The 18 basic colors used by Pantone to mix spot colors on presses would give 18,564 different combinations. The computational effort to construct 18,564 six-color printing models for the 18 ink combinations is unreasonable. Therefore, a robust ink selection algorithm was developed.

The ink selection algorithm was based on a vector correlation analysis, followed by a constrained regression analysis. After the selection of the ink set, the overprints of these inks needed to be predicted. A high spectral and colorimetric accuracy was achieved by using the Kubelka-Munk turbid theory. The results were evaluated by printing ink combinations on a proofing device. When the theoretical model was applied to real printing, many factors added uncertainty. The homogeneity of the ink film thickness, the uniformity of the paper, and measurement limitations were factors that affected the accuracy of the verification of the model [Tzeng, 1999].

For multi-ink color separation, a suitable printing model needs to be used. To do so, the Yule-Nielsen-Spectral-Neugebauer (YNSN) model was used for color separation. The overprinting of many inks causes problems in press. Ink trapping of more than four inks is limited by their physical nature. Despite the fact that some overprinting combinations are problematic, it was found that the YNSN color separation was capable of minimizing metamerism. The color separation was verified by printing the colors of the Gretag Macbeth Color Checker on a six-ink proofing system. The analysis showed that the

spectral and colorimetric accuracy of the color separation for the printing system used was good [Tzeng, 1999].

3.4.3 Color Gamut and Color Consistency

Research to enlarge the color gamut, to increase the color consistency, and to reduce the degree of metamerism was conducted by Chen in 2006. First, the relationship between predicted and measured area coverage was addressed. Using the Yule-Nielsen equation, the n value for each primary color was determined to reduce the spectral prediction error. To reduce the number of overprinting combinations, the non-realizable cellular primary colors were determined. The total area coverage is a physical limitation and is different for every printing system. This reduced the number of overprinting combinations significantly. To increase the prediction accuracy, the cellular enhanced YNSN model was evaluated, as well as the YNSN. It was found that using a synthesized spectra resulted in a 15% larger color space in CIELAB than was achieved by limiting the CYNSN model to printable cellular primaries. The printing model was verified by using six different inkjet printers. Test targets were printed on each printer. Even if the CYNSN model showed better results, the simpler YNSN model was preferred. The vast increase in complexity did not justify the small improvement in color accuracy. To predict the Neugebauer primaries, a virtual printing model was used. For the estimation of ink overprinting, the single constant simplified Kubelka-Munk equation was used.

Further, Chen (2006) designed inks to extend the printing gamut. It was shown that

additional inks can improve the color gamut significantly. However, the more inks that are used, the less the contribution of each ink to enlarge the color gamut. A relationship between ink shape and color inconsistency was found. The selection of an optimal ink set can reduce color inconsistency and metamerism.

3.4.4 Spectral Modeling of an Inkjet Printer

The evaluation of a spectral printing model needs to be done with a printer that has good repeatability. To achieve this, Taplin (2001) modified a six-color inkjet printer to have a continuous-feed ink system. This modified printer does not suffer from the problem of recalibrating the printer after cartridge changes. Orange and green inks were used, in addition to the process colors CMYK. The evaluation of the forward printing model was done by using two color combinations. When using six inks, fifteen two-ink combinations exist. It was found that the Yule-Nielsen-Spectral-Neugebauer (YNSN) model performed well for this CMYKOG inkjet printer. Similar results were seen for more complex, cellular models. Because the YNSN printing model is less complex, it was preferred over the others.

After the evaluation of the forward printing model, an algorithm was evaluated to invert the YNSN model. A printing model can only be inverted by using a nonlinear optimization-routine. An algorithm designed by Davidon, Fletcher, and Powel (known as the DFP model) performed best to invert the YNSN printing model. The DFP model is a quasi-Newton based algorithm. The algorithm performed best with assigned starting

values based on the Kubelka-Munk (KM) model. For the calculation of the starting values, it was assumed that the concentration is equivalent to the area coverage. The concentrations were found by using a non-negative least squares algorithm. The nonlinear optimization functions implemented in MATLAB were found to be very slow. To get better performance, the optimization function was recoded in C [Taplin, 2001].

The performance of the inverse model was evaluated by analyzing the end-to-end accuracy of the printing system. A combination of spectral and colorimetric evaluation was used. It was found that the results were as accurate as were the ones from previous research conducted by Tzeng using another printing system. Test prints showed that the metameric index could be decreased by using more inks. This was found by evaluating the spectral match between samples printed with three, four, and six inks. In addition to a decrease in the metameric index, the spectral RMS error decreased by using more inks.With six inks, the color gamut can be improved, while the spectral match reduces the color inconsistency. Spectral printing was successfully implemented using a multi-ink inkjet printer [Taplin, 2001].

3.4.5 Spectral Color Separation

Producing a spectral color separation can lead to larger visual color differences than a colorimetric reproduction. Urban (2008) developed a spectral gamut-mapping framework to address this problem. Optimizing the reproduction for multiple illuminants produced the spectral match. The optimization is taking the human color vision into account to

produce an accurate color match. An array of different illuminants is defined. The order of the illuminants defines the priority. The first one in the list is the base illuminant. For each illuminant, a CIELAB image is calculated from the multispectral image. The concept is to choose only spectra that are inside the printer's gamut. After producing a colorimetric match for the base illuminant, each CIELAB image is optimized for its corresponding illuminant. The optimization is based on producing the smallest CIEDE2000 for each illuminant [Urban et al., 2008].

3.4.6 Printing Models

For modeling a multi-ink printing system, it is important to predict the numerous overprinting combinations. Having an accurate overprinting model is especially important for ink selection and ink sequence determination. A comprehensive overview about many printing models was collected by [Viggiano, 2010]. The application of spectral printing to binary color printing is very complex. Printing models that work well in theory may fail when applied to halftone screening. Halftone screening can be divided into rotated screens (AM), dot-on-dot screens, and stochastic screening (FM). They depend differently on the registration of the colors in the press. Many printing models are reasonably accurate. Nevertheless, accuracy is not the most important issue. The number of measurements used for characterization and computational complexity of the model are also important. In general, the simplest model should be used. Before investigating more complex models, the Yule-Nielsen print model should be tested [Wyble and Berns, 2000].

3.4.7 Artist Paint Material Database

A database of artist paints has been developed at RITs MCSL [Okumura, 2005]. The database consists of spectral and colorimetric information about paint materials. To describe the characteristics of the paints, it was found that the two constant Kubelka-Munk Theory performed well. This theory is based on the assumption that, inside a paint layer, the light flux travels only up and down. The two constants are k and s, where k describes the absorption and s describes the scattering inside the paint layer. To convert measurement data to internal reflectance, the Saunderson correction was used. Okumara characterized not only the paints themselves, but also the effect of varnishing them. The process of characterizing the paint and varnish is described in detail by [Okumura, 2005]. More information can be found at www.art-si.org.

Chapter 4

Color Mixing Models

This chapter provides the reader with a detailed overview of the color mixing models used in this research.

4.1 Kubelka-Munk

The Kubelka-Munk Theory was developed by Paul Kubelka and Franz Munk. It is a concept of describing the absorption and scattering properties of a colorant film. The Kubelka-Munk method assumes that light flux only travels in two directions inside of the colorant film. Either up or down. Figure 4.1 shows a visualization of the two flux concept.

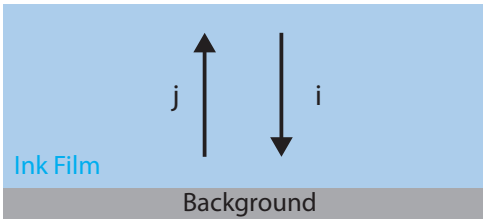

Figure 4.1: Two-Flux Kubelka-Munk Theory

4.1.1 Single Constant Kubelka-Munk (Masstone Approach)

The single constant model describes the absorption and scattering as one value for every wavelength which is described as the $\left(\frac{K}{S}\right)_\lambda$ coefficient. The $\left(\frac{K}{S}\right)_\lambda$ value is the ratio between the absorbed and the scattered light. This method assumes a colorant film with an infinite thickness. In practical applications, this is an opaque ink film. Equation 4.1 shows how the $\left(\frac{K}{S}\right)_\lambda$ coefficient is derived from the internal reflectance $R_{\lambda,i}$. The colorant mixing is performed by adding up the $\left(\frac{K}{S}\right)_{\lambda,colorant}$ values multiplied by their concentrations and adding white as shown in Equation 4.2. Going back from $\left(\frac{K}{S}\right)_\lambda$ to $R_{\lambda,i}$ is described in Equation 4.3.

$$\left(\frac{K}{S}\right)_\lambda = \frac{(1-R_{\lambda,i})^2}{2R_{\lambda,i}} \tag{4.1}$$

$$\frac{K}{S}_{(\lambda)sample} = c_1\left(\frac{K}{S}\right)_{\lambda,1} + c_2\left(\frac{K}{S}\right)_{\lambda,2} + ... + \left(\frac{K}{S}\right)_{\lambda,white} \tag{4.2}$$

$$R_{\lambda,i} = 1 + \left(\frac{K}{S}\right)_\lambda - \left[\left(\frac{K}{S}\right)_\lambda^2 + 2\left(\frac{K}{S}\right)_\lambda\right]^{1/2} \tag{4.3}$$

4.1.2 Two-Constant-Kubelka-Munk (Black and White Method)

The two-constant approach of the Kubelka-Munk model is known to deliver more accurate results for most applications. This specific two constant model requires colorant

films measured over a white and a black background. Absorption and scattering coefficients are calculated as shown in equations 4.4 to 4.7. A list describing the used variables is shown in Table 4.1. The variable X describes the thickness of the paint film that needs to be constant for the calculation.

Table 4.1: List of variables used in the two constant Kubelka-Munk Formulas

Variable	**Description**
R_w	Reflectance of paint film over white background
R_k	Reflectance of paint film over black background
R_{gw}	Reflectance of white background
R_{gk}	Reflectance of black background
X	Thickness of paint film
SX	Scattering coefficient for a specific paint film thickness
KX	Absorption coefficient for a specific paint film thickness

$$a = \frac{(R_w - R_k)(1 + R_{gw}R_{gk}) - (R_{gw} - R_{gk})(1 + R_wR_k)}{2(R_wR_{gk} - R_kR_{gw})} \tag{4.4}$$

$$b = \sqrt{a^2 - 1} \tag{4.5}$$

$$SX = \frac{1}{b}\left[coth^{-1}\left(\frac{a - R_k}{b}\right) - coth^{-1}\left(\frac{a - R_{gk}}{b}\right)\right] \tag{4.6}$$

$$KX = SX(a - 1) \tag{4.7}$$

The reflectance can be calculated by using equation 4.8. R_g is the background behind the ink layer, which in this case is the reflectance of the paper.

$$R = \frac{1 - R_g[a - b \cdot coth(b \cdot SX)]}{a - R_g + b \cdot coth(b \cdot SX)} \tag{4.8}$$

4.1.3 Saunderson Correction

When the light ray enters a colored layer, the refractive index changes between the air and the colored layer. This first surface reflection does not depend on the colorant absorption properties of the colored layer. Because this effect is not a colorant-dependent parameter, it will introduce errors into the Kubelka-Munk Theory. The Saunderson Correction is a method that accounts for this first surface reflection error. It converts the measured reflectance of a colorant layer into the internal reflectance. This conversion improves the linearity of the concentration prediction for the Kubelka-Munk theory. Equation 4.9 shows the calculation from measured to internal reflectance. The formula to get from internal to measured reflectance is shown in Equation 4.10. K_1 is a constant representing the surface reflection whereas K_2 is a constant that represents the internal reflection. These constants should be optimized for every type of colorant layer. [Kang, 2006]

$$R_{\lambda,i} = \frac{R_{\lambda,m} - K_1}{1 - K_1 - K_2 + K_2 R_{\lambda,m}} \tag{4.9}$$

$$R_{\lambda,m} = K_1 + \frac{(1-K_1)(1-K_2)R_{\lambda,i}}{1-K_2R_{\lambda,i}} \tag{4.10}$$

4.2 Neugebauer Printing Model

Viewing a halftone printed object from a distance leads to the apperance of a uniform colored area. Halftone printing takes advantage of the fact that the human eye can not resolve small dots from a certain distance. A closer look at the halftone pattern shows a large number of colored halftone elements. Where dots overlap, the ink is mixed by subtractive color mixing. Neugebauer showed that halftone printing can be described as a purely additive color mixing model [Neugebauer, 2005]. The color stimuli is produced by the paper white, the primary colors, and the subtractive mixed overprinting ink combinations. It is assumed that halftone elements are equally distributed (e.g. no moirée or dot on dot effects). A sample dot pattern of an amplitude modulated, round-dot halftone screened color is shown in Figure 4.2.

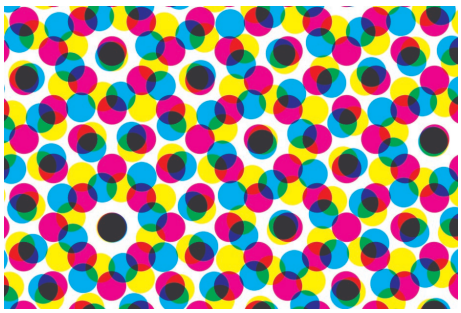

Figure 4.2: Screening Pattern

The primary inks (Cyan, Magenta and Yellow) produce solid ink elements, and two- and three-color overprints. Each one of these colors is referred to as a Neugebauer primary color. For an N-ink halftone printing system there are 2^N Neugebauer primary colors. The probability that an element is printed with ink 1 is p_1 and the probability of ink 2 is p_2. The probability that it is not overprinted by ink 1 is (1-p_1) and (1-p_2) for ink 2. An element printed with ink 1 but not with ink 2 has the probability of p_1(1-p_2). A general form for calculating p_i for N-inks is shown in Equation 4.11. For the three ink printing system showed in Figure 4.2, the $2^3 = 8$ Neugebauer primary color area coverages are calculated as shown in Equation 4.13. The probability that an ink amount is printed, can be derived from the area coverage (a_N) of the halftone dot.

$$p_i = \prod_{j=1 \to N} \begin{pmatrix} \text{If ink } j \text{ is in Neugebauer Primary } i\text{, then } a_j \\ \text{Else, } (1 - a_j) \end{pmatrix} \tag{4.11}$$

$$p_c = a_c(1 - a_m)(1 - a_y) \tag{4.12}$$

$$p_m = a_m(1 - a_c)(1 - a_y)$$

$$p_y = a_y(1 - a_c)(1 - a_m)$$

$$p_{m,y} = a_m a_y(1 - a_c)$$

$$p_{c,y} = a_c a_y(1 - a_m)$$

$$p_{c,m} = a_c a_m(1 - a_y)$$

$$p_{c,m,y} = a_c a_m a_y$$

$$p_{white} = (1 - a_c)(1 - a_m)(1 - a_y)$$

4.2.1 Spectral Neugebauer Model

As mentioned before, Neugebauer showed that these Neugebauer primary colors follow additive color mixing rules. The model can also be extended to a spectral model. When the spectral reflectance of the Neugebauer primary colors are known, summing up the reflectances multiplied by their probability of area coverage, the output of the Neugebauer equation is the spectral reflectance of the halftone pattern of the print. The spectral extension of the Neugebauer equation is shown in Equation 4.13.

$$\hat{R}_\lambda = \sum_{i=1}^{N} p_i R_{\lambda,i} \tag{4.13}$$

4.2.2 Effective Area Coverage Correction

In order to increase the accuracy of the model, an effective area correction can be used. The Murray-Davis equation can predict the effective dot area of a print. To extend the equation to a spectral model, a_{eff} is determined by a matrix calculation using least squares analysis (Equation 4.14) [Wyble and Berns, 2000]. Figure 4.3 shows the effective area correction for seven inks printed on an HP Indigo digital press. The curves show that by measuring the ramp at every digit count, the curve is somewhat noisy. This is not only because of limitations of the printing process, but also because of measurement precision and accuracy of the instrument. The gray vertical lines indicate that a curve can be estimated accurately by using only nine patches equally sampling the ink ramp.

$$a_{eff} = \mathbf{R_{tint-paper}} \mathbf{R^{T}_{solid-paper}} \left(\mathbf{R_{solid-paper}} \mathbf{R^{T}_{solid-paper}} \right)^{-1} \tag{4.14}$$

4.2.3 Yule-Nielsen extension of the Spectral Neugebauer Model

Yule and Nielsen analyzed light penetration and scattering in paper. As Figure 4.4 shows, there are four cases of how a light ray can behave when hitting halftone printed paper. In the first case, the light can hit a printed dot and reflect from it. In the second case the light is hitting the paper and exits through a printed dot. In the next case the light is hitting the paper and reflects without interacting with the ink. The last case describes the light hitting the printed dot and leaving through the paper. Yule and Nielsen found that this non-linear

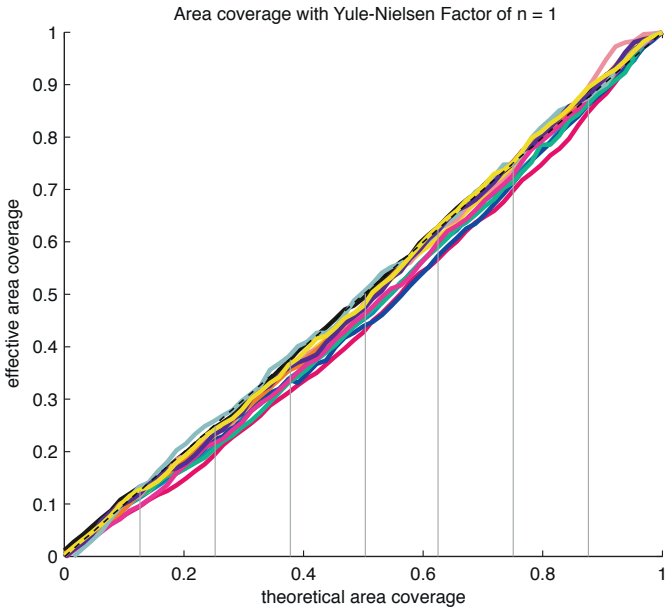

Figure 4.3: Effective Area Coverage for all Inks

relationship can be well described by a power function [Wyble and Berns, 2000]. The Yule-Nielsen n-value is added as an exponent to the Murry-Davis equation (Equation 4.15). This exponent accounts for the light spreading in the paper which improves the linearity of the model. The Yule-Nielsen-Spectral-Neugebauer equation is shown in Equation 4.16.

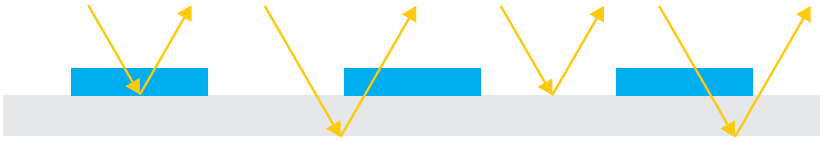

Figure 4.4: Effect of Light Scattering on Halftone Dots

$$\hat{R}_\lambda = \left[a_{eff} R_{\lambda,1}^{1/n} + (1 - a_{eff}) R_{\lambda,2}^{1/n} \right]^n \tag{4.15}$$

$$\hat{R}_\lambda = \left[\sum_{i=1}^{N} p_i R_{\lambda,i}^{1/n} \right]^n \tag{4.16}$$

4.2.4 Cellular extension of the YNSN

As described before, the Neugebauer primary colors are the solid ink patches and their overprinting combinations. Therefore, these patches circumscribe the printer gamut. The Neugebauer model is summing up all the fractions of each primary color. This interpolation can cause significant errors. As shown before, the Yule-Nielsen extension of the Neugebauer model can account for some of these errors. Nevertheless, interpolating across a large printer gamut implies some potential error. Heuberger, et al. and Rolleston and Balasubramanian extended the Neugebauer to the Cellular Neugebauer model [Wyble and Berns, 2000]. They improved the interpolation by adding more primary colors inside the gamut. Therefore, the distance over which a color is interpolated becomes smaller. By adding one node (e.g. 0%, 50% and 100%) the interpolation is going to be much more accurate. Figure 4.5 shows the cellular primary colors for a three ink system with three nodes for each ink. The number of cellular primary colors is increasing drastically. Whereas the Neugebauer model for three inks requires $2^3 = 8$ primaries, the cellular model with three nodes would require $3^3 = 27$ primary colors. Generally speaking, the more cells that are added, the higher is the accuracy of the interpolation. Accuracy and number of primary colors are a tradeoff which need to be evaluated. Especially for more than four color printing, the number of primaries explodes rapidly.

Also, the computational complexity should not be under estimated. Before the Neugebauer model can be applied, the corresponding subcell needs to be selected. Especially for a brute force inversion of the CYNSN model, this step needs to be repeated for every iteration. Once the subcell is selected, the 2^N primary colors can be used to perform the local interpolation inside of the subcell as shown in Equation 4.16.

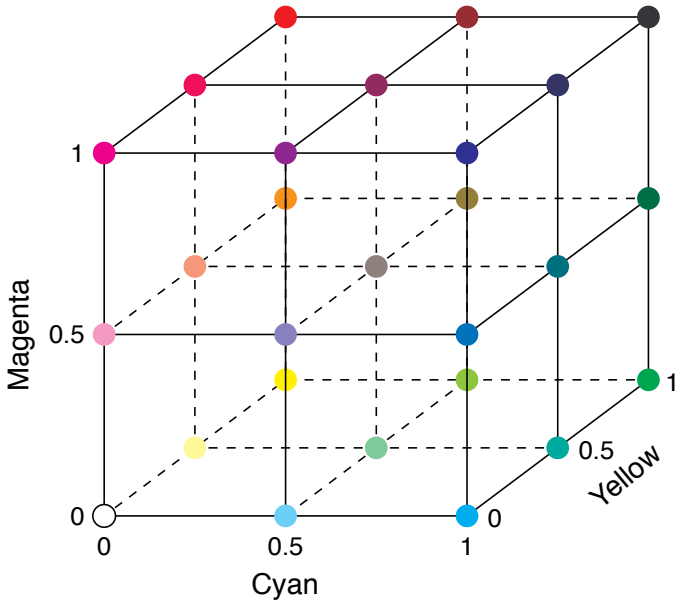

Figure 4.5: Cellular Neugebauer Model with Three Nodes and Three Inks

Chapter 5

Materials and Technologies

This chapter provides the reader with a description of the many different materials and technologies used in this research.

5.1 HP Indigo 7000

5.1.1 Printing Process

The HP Indigo 7000 is a digital press with the capability to print seven colors. Unlike many other electrophotographic digital presses, the HP Indigo is a liquid toner printing process. The inks are stored in cans containing toner powder dissolved in a paste. This paste is then fed to ink tanks and mixed with a clear imaging oil. The concentration of paste in the imaging oil tank determines the ink density of the printed color on the substrate. At this stage, the liquid toner does not have conductive properties. Therefore, a conductor liquid is added to the ink before it reaches the ink transfer system. The imaging

stage is a typical electrophotographic process. The writing head exposes the Photo Imaging Plate (PIP) (see Figure 5.1). The Binary Ink Developer (BID) then transfers the conductive liquid toner onto the charged PIP. From the PIP, the ink is transferred onto a blanket on the Intermediate Drum (ITM). From the ITM, the toner is transferred to the paper under heat and pressure. The toner transfer step also performs the fusing of the toner through the applied heat. Since each color is transferred sequentially, each color is fused separately. On one hand, this slows the printing process down – printing one ink is seven times faster than seven inks. On the other hand it allows the process to print each color on top of a fused toner layer. This enables print area coverages of 700 percent. Nevertheless, it is not recommended to do so because of adhesion problems with high ink coverages. HP Indigo is calling this system ElectroInk®. Because of the complex mixing, transfer and fusing system, it is not possible to take paste out of a can to create ink drawdowns. A schematic drawing of the printing process is shown in Figure 5.1.

5.1.2 Screening

Unlike conventional lithographic presses, digital presses suffer a much lower addressability of their imaging systems. The HP Indigo 7000 can image with an addressability of 812 spots per inch. The default screen ruling of this press is 180lpi. Doing the math clearly shows that this would not allow printing enough tone values for a 1-Bit amplitude modulated screening. In fact only about 20 tone values could be produced by using a conventional rational tangent screening. To overcome this limitation, a more

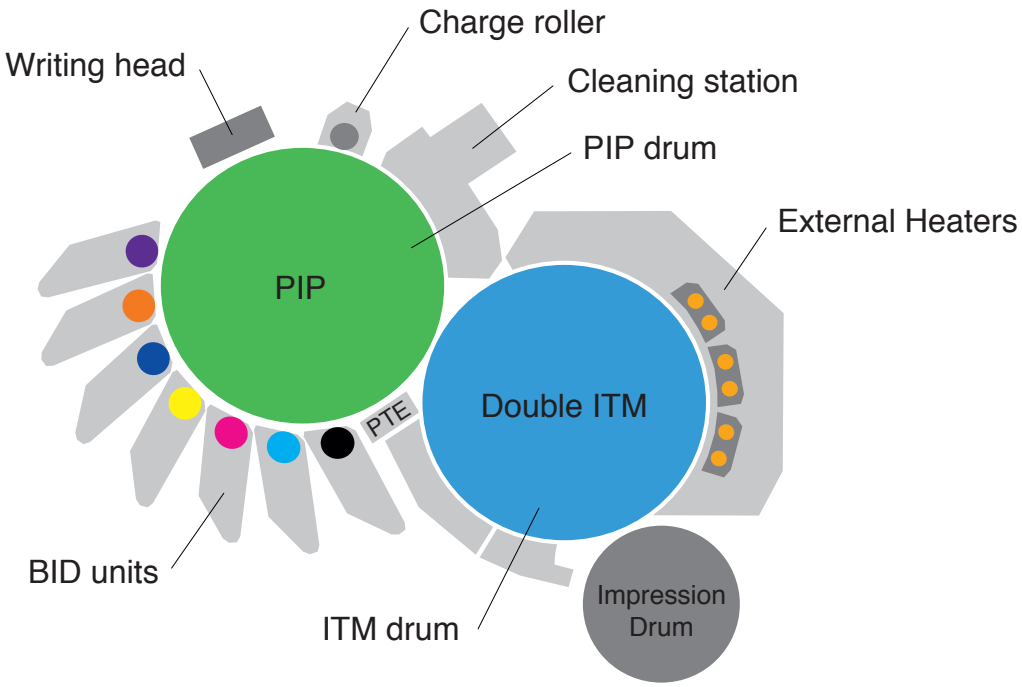

Figure 5.1: HP Indigo 7000 Printing Unit (drawing after HP)

complex screening technology is used in digital presses. No detailed information could be found about the screening methods used by HP Indigo. A closer look at the printed samples lead to the assumption that a complex mix of dithering, supercell screening and bit depth could be used. For this research project the screening has to be treated as a ”black box” system with very limited control. A further limitation is the available screening angles. Although the HP Indigo 7000 is a seven color press, it only offers four different screening angles. Since most printing jobs are printed CMYK and spot colors that do not interact with CMYK colors, screen angles can be shared without experiencing the effect of moiré. Frequency modulated (FM) screening systems would solve this problem because they do not need specific screen angles. Nonetheless, FM screening cannot be used due to the insufficient addressability.

5.2 HP Indigo ElectroInk® Set

The HP Indigo ink formulation system is based on a set of twelve primary colors. There is also white and transparent ink but they are not considered in this research. Beside the process inks Cyan, Magenta, Yellow and Black the system comprises eight additional chromatic colors. Some of these inks are meant to be printed pure (out of the can) or for ink formulation whereas others are only used for ink formulation. The light colors – Light Cyan and Light Magenta – are used in photorealistic printing to achieve smooth light tones. Orange and green inks have their application in Hexachrome printing. Violet and Orange in addition to CMYK are used for IndiChrome printing. HP Indigo is proposing

this setup to achieve a larger gamut for creating spot colors by screening rather than spot color ink formulation. Reflex blue, Rhodamine Red and Bright Yellow are inks used for ink formulation only. They are not meant to be installed pure in a press by the end-users.

The full set of HP Indigo inks is similar to the basic inks used in the Pantone system with some differences. Most distinctive is the difference of Reflex Blue. The pure HP Indigo Reflex Blue is lighter and more chromatic than the Pantone Reflex Blue. To match the Pantone Reflex Blue, the HP Indigo Reflex Blue needs to be mixed with Violet and Black. Rhodamine Red behaves similarly. To match its corresponding Pantone Color, Magenta needs to be added to the HP Indigo Rhodamine Red. Bright Yellow is quite similar to the Process Yellow but its properties are closer to an ideal (inflection point and short wavelength absorption) Yellow than the Process Yellow. The spectral reflectance of all HP Indigo primary inks is shown in Figure 5.2.

5.2.1 Retrieving the Spectral Properties of the Ink Set

Getting the spectral properties of the primary inks was not an easy process. As described before, the HP Indigo primary inks are pastes that are dispersed in a liquid. The complicated printing and fusing process can not be simulated outside of the press. Creating ink draw-downs or using a printability tester is a common process for other printing processes. Unfortunately, this does not apply to the HP Indigo technology. To retrieve the spectral properties of the inks, they had to be installed in the press and printed as a test target.

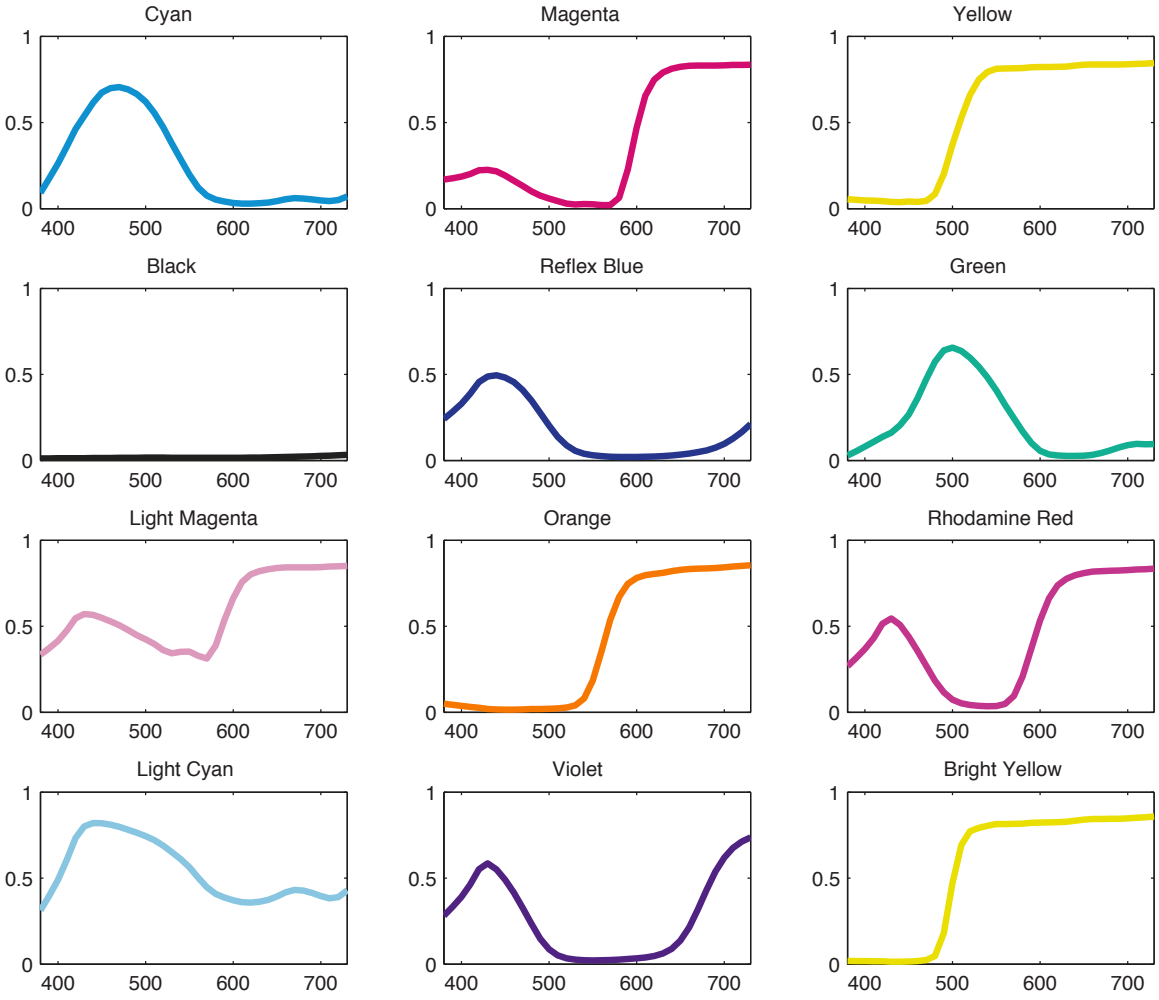

Figure 5.2: HP Indigo Primary Ink Set

Hence, the purpose of the first press run was to characterize the entire set of HP Indigo Primary Inks. To do so, a test target needed to be designed. The target was built for seven color printing. It incorporates an element of ink ramps with 4-digital-count steps and the full set of Neugebauer primary colors. There are 128 Neugebauer primary colors that span every possible combination of seven color overprints including paper white. This target was placed twice on the printed sheet: once with white backing and once with black ink in the background. Printing the black ink first would allow using this target for two constant Kubelka-Munk calculations with black and white backing. Spot colors are called Spot1, Spot2 and Spot3. Inks are allocated to the spot colors in the RIP at the press. The targets can be read automatically with the X-Rite iSis spectrophotometer. For process control, a control strip was designed. It consists of ray-targets, checkerboards and line patterns for each ink. These control elements are dynamic and adapt to the PostScript interpreter. The targets were written in Encapsulated PostScript (EPS). The control elements around the targets could be measured, but were only evaluated visually. The test target is shown in Appendix A.

Since the aim of this research is the implementation of spectral printing into a production environment, the press settings were chosen to be as close to the press manufacturers recommendations as possible. Therefore, the test targets were printed using the default screening of 180lpi. As output resolution, the native addressability of 812 spots per inch was used. Default screening angles were: Cyan: 4°, Magenta: 64°, Yellow: 18°, Black: 34°. An overview over the three press configurations is shown in Table 5.1

Table 5.1: Press Configurations Press Run 1

Press Configuration A		Press Configuration B		Press Configuration C	
Ink	**Screen Angle**	**Ink**	**Screen Angle**	**Ink**	**Screen Angle**
Cyan	Cyan	Cyan	Cyan	Cyan	Cyan
Magenta	Magenta	Magenta	Magenta	Magenta	Magenta
Yellow	Yellow	Yellow	Yellow	Yellow	Yellow
Black	Black	Black	Black	Black	Black
Reflex Blue	Black	Orange	Magenta	Orange	Magenta
Green	Cyan	Rhodamine Red	Black	Violet	Magenta
Light Magenta	Magenta	Light Cyan	Cyan	Bright Yellow	Black

5.3 Measurement instruments

5.3.1 X-Rite iSis

The i1 iSis is a 45°/0° spectrophotometer built by X-Rite to measure high volumes of color patches. The device can read substrates up to nine inches wide and 26 inches long. Up to 660 patches can be measured per minute. The iSis was used in combination with X-Rite ColorPort software version 2.0.1 and Measure Tool 5.0. Spectral reflectance is reported with a resolution of 10nm in the range of 380 to 730nm. As a light source the iSis is using white UV-Cut LEDs and UV LED. All measurements were taken according to ISO 13655 M2 (UV excluded).

Figure 5.3: EyeOne iSis (Source: X-Rite)

5.3.2 X-Rite i1Pro

The i1Pro is a 45°/0° handheld spectrophotometer built by X-Rite. This instrument was used for spot readings where automated measurements with the iSis were not possible. The iSis was used in combination with X-Rite ColorPort software version 2.0.1 and

Measure Tool 5.0. Spectral reflectance is reported with a resolution of 10nm in the range of 380 to 730nm. A gas-filled tungsten (Type A) light source is used to illuminate the sample. All measurements were taken according to ISO 13655 M0.

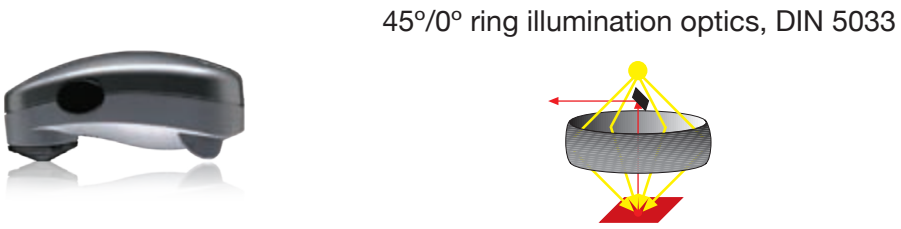

Figure 5.4: i1 Pro (Source: X-Rite)

5.4 Paint Database

5.4.1 Acrylic Colors

Acrylic artist colors, like the ones used in this research, are a relatively new material available to artists. Solvent-based acrylic paints were developed early in the twentieth century. Water based acrylic colors were first sold in 1955. Acrylic polymer resin, which is emulsified with water, is the main component of these paints. Pigment and Binder are other components that make an acrylic color. A superior property of acrylic colors is their ease of use. They can simply be mixed with water to be thinned. When wet, acrylics can easily be cleaned up with water. Once they are dry, acrylics adhere to a wide range of materials and are water resistant. Dried paint remains much more flexible than oil paint,

for example. Figure 5.5 shows the drying process of acrylic paint. The water emulsion evaporates into the atmosphere or absorbs into the substrate once the paint leaves its container. The polymerization process traps the pigments and forms a strong but fairly flexible paint layer. This process happens relatively quickly when the paint is exposed to the atmosphere. The mentioned properties made acrylic colors the preferred choice to perform experiments in this research.

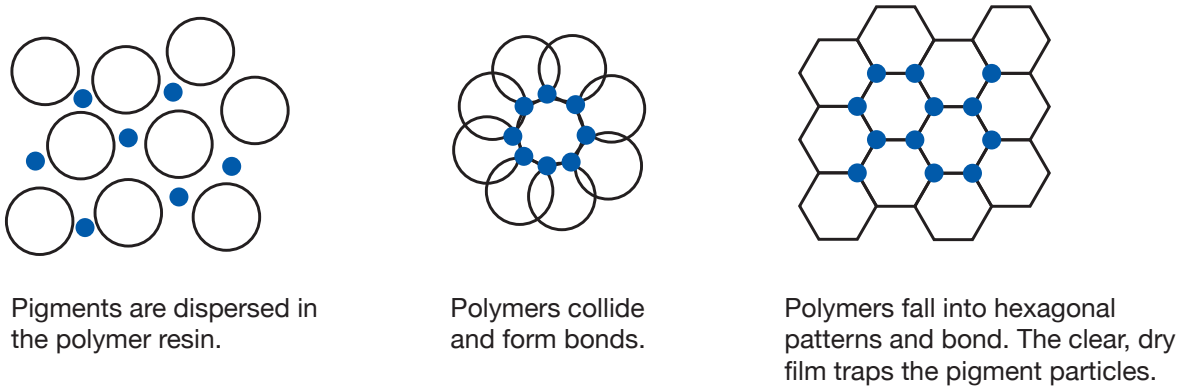

Figure 5.5: Polymerization process of Acrylic Paints. (graphic after: *The Acrylic Book* page 8, Liquitex)

Today, a wide range of acrylic paint can be bought, but getting spectral data of the paints is a time consuming process. Yoshio Okumura developed the GOLDEN Fluid Matte paint database at the Munsell Color Science Laboratory at RIT [Okumura, 2005]. At first, this database of 28 paints was used. It was found that this paint database does not include enough different pigments for the purpose of this research. Hence, more acrylic paints were added. Paints from GOLDEN Artist Colors and LIQUITEX were used. Primarily, single pigment paints were evaluated. Table 5.2 lists all acrylic paints that were

evaluated. For a better identification, the Pigment and the Chemical Description was added. The column O/T indicates the opacity or transparency where 1 indicates an opaque and 8 a transparent paint (This is the notation of GOLDEN Artist Colors).

5.4.2 Oil Colors

The use of oil colors goes back centuries. In the fifteenth century, oil colors started to be widely used. Oil colors are pigments that are dispersed in linseed or poppy oils. Unlike acrylics, oil colors do not dry by evaporation. There is no water in the paint that could evaporate. The properties of oil prevents it from evaporation. Oil colors dry by an oxidation process, which is started when the oil reacts with oxygen in the air. This oxidation caused the paint to harden. The drying process is a slow process taking days or even weeks.

5.4.2.1 GAMBLIN Oil Colors

The database of oil colors was built by measuring paint draw-downs provided by Robert Gamblin from GAMBLIN Oil Colors. These draw-downs were not made with the intention of being used for ink formulation. Therefore, the draw downs were not consistent in paint film thickness and opacity. Some draw-downs are fully opaque whereas others, especially transparent colors, show through a lot of the background substrate. Every color was measured three times with an X-Rite i1 Pro spectrophotometer and averaged. Some samples came out very dark. These dark samples are affected by noise of the instrument and were of limited use for the paint selection process. Some of the

Table 5.2: Database of Acrylic Pigments

Name	**Pigment**	**O/T**	**Chemical Description**
Hansa Yellow Light	PY3	6	Arylide Yellow
Bismuth Vanadate Yellow	PY184	3	Bismuth Vanadate
Cadmium Yellow Light	PY35	4	Cadmium Zinc Sulfide
Hansa Yellow Opaque	PY74	5	Arylide Yellow 5GX
Hansa Yellow Medium	PY73	7	Arylide Yellow
Diarylide Yellow	PY83	5	Diarylide Yellow HR-70
Cadmium Orange	PO20	3	Cadmium (Sulfo-Selenide)
Pyrrole Orange	PO73	5	Dipyrrolopyrrol
Pyrrole Red	PR254	3	Pyrrolopyrrol
Cadmium Red Medium	PR108	2	Cadmium (Sulfo-Selenide)
Primary Magenta	PV19	4	Quinacridone
Naphthol Red Medium	PR5	5	Naphthol ITR
Quinacridone Red	PV19	6	Quinacridone
Quinacridone Crimson	PR206, PR202	5	Quinacridone, Quinacridone
Quinacridone Magenta	PR122	7	Quinacridone
Dioxazine Purple	PV23	3	Carbazole Dioxazine
Ultramarine Blue	PB29	6	Polysulfide of Sodium-Alumino-Silicate
Cobalt Blue	PB28	3	Oxides of Cobalt and Aluminum
Cerulean Blue, Chromium	PB36:1	3	Oxides of Cobalt and Chromium
Anthraquinone Blue	PB60	2	Indanthrone Blue
Phthalo Blue / Green Shade	PB15:4	3	Copper Phthalocyanine
Turquois (Phthalo)	PB15:4, PG7	3	Copper Phthalocyanine Chlorinated Copper Phthalocyanine

Name	Pigment	O/T	Chemical Description
Phthalo Green / Blue Shade	PG7	3	Chlorinated Copper Phthalocyanine
Permanent Green Light	PY3, PG7	3	Arylide Yellow 10G Chlorinated Copper Phthalocyanine
Jenkins Green	PBk9 PY150 PG36	2	Amorphous Carbon produced by charring animal bones Nickel Complex Azo Brominated, Chlorinated Copper Phthalocyanine
Chromium Oxide Green	PG17	1	Anhydrous Chromium Sesquioxide
Green Gold	PY150 PG36 PY3	4	Nickel Complex Azo Brominated & Chlorinated Copper Phthalocyanine Arylide Yellow
Yellow Ochre	PY43	2	Natural Hydrated Iron Oxide
Raw Sienna	PY43	3	Natural Hydrated Iron Oxide
Red Oxide	PR101	1	Synthetic Red Iron Oxide
Burnt Sienna	PBr7	2	Calcined Natural Iron Oxide
Burnt Umber	PBr7	2	Calcined Natural Iron Oxide containing Manganese
Raw Umber	PBr7	1	Natural Iron Oxide containing Manganese
Carbon Black	PBk7	1	Nearly Pure Amorphous Carbon
Paynes Gray	PB29 PBk7	2	Polysulfide of Sodium-Alumino-Silicate Nearly Pure Amorphous Carbon
Titan Buff	PW6	2	Titanium Dioxide Rutile

GAMBLIN Oil Colors were used to evaluate pigments. Nevertheless, because Oil Colors are not easy to handle, mainly acrylic colors were used for detailed investigation.

Since this research is mainly interested in the spectral curve shapes of the pigments, the differences of Oil and Acrylic paints were neglected. This simplification is justified based on research by Staniforth. [Staniforth, 1985]:

> ”The shape of the reflectance curve is not significantly affected by the medium used to bind the pigment. ... The medium only affects the overall level and relative heights of maximum and minimum reflectance.” [Staniforth, 1985]

Chapter 6

Ink Selection

The evaluation of the ink set was approached from two different directions. First, the feasibility of formulating custom spot colors that spectrally match artist pigments was evaluated. Spectral matching primary inks would perform well to match all the paint mixtures of the corresponding ink and paint set. The second approach performs the evaluation of a set of pure primary inks that match a palette of artist pigments when mixed by halftone screening in the press. But first, the section *Structure of Artist Palette* is investigating how paint mixing is performed by artists. Understanding the structure of an artist palette is an important step for the later evaluation of the ink set.

6.1 Structure of Artist Palette

Artist colors follow the rules of subtractive color mixing. Three ideal primary colors as shown in Figure 6.1 would be sufficient to mix a very large color gamut. Unfortunately, real primary colors with these curve shapes do not exist. Using real physical pigments

makes paint mixing much more complex than using ideal primary colors. Therefore, more than three primary colors are needed to create a palette with a large color gamut. Hence, mixing these paints requires a good understanding of their properties. Paint mixing without knowing the paint properties can be a frustrating experience. Novice painters often experience that mixtures turn out very different than what they expected. Understanding the structure of artist palettes and the spectral curve shapes of pigments greatly enhances the gamut that can be achieved when mixing paints.

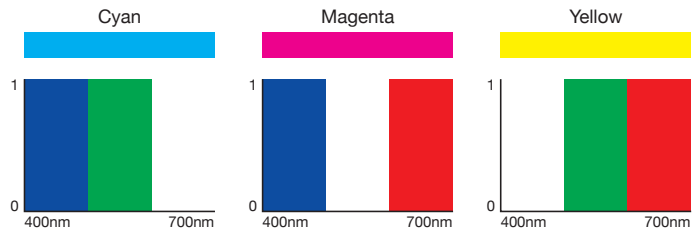

Figure 6.1: Ideal Subtractive Primary Colors

A good guide about mixing artist paints can be found on the website of Gamblin Artist's Oil Colors [Gamblin, 2011]. A color wheel as shown in Figure 6.2 represents the structure of an artist palette. At first, the circle is separated into six hues. Ideally, in each hue segment, there are at least two colors: a warmer and a cooler color. The cool–warm interaction changes at two locations of the color wheel. There is only one location where two warm colors meet. This occurs between orange and red. Two cool colors also meet only once – between blue and green. Understanding this structure is crucial for the selection of artist pigments to build a paint palette. Theoretically, mixing red and blue paint results in violet. With real world pigments, this only works when a warm blue and a

cool red are mixed. Mixing a warm red with a cool blue would result in a dark, low chromatic and almost brown mixture – far away from the intended violet. To achieve a large color gamut, the pigments need to be selected carefully.

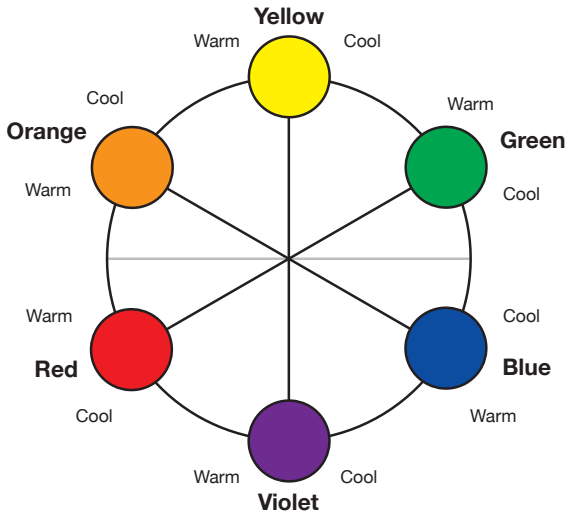

Figure 6.2: Structure of Artist Palette [Gamblin, 2011]

In order to understand the structure of paint palettes, experiments were performed with acrylic paints to gain a better understanding of what artists experience. The book *Blue and Yellow Don't Make Green* is also a helpful guide to get started with paint mixing [Wilcox, 1994]. Different paint mixing experiments are shown in Figures 6.3, 6.4 and 6.5 to demonstrate the outcome of bad pigment selection when mixing certain colors. The first figure shows that mixing a cool yellow and a warm blue does not yield a good green. The Phthalo Green Blue Shade shown as a reference clearly shows that the mixed green is much less chromatic than the green pigment. As shown in the right graph of Figure 6.3, the yellow paint absorbs light below 500nm and the blue paint between 540 and 650nm.

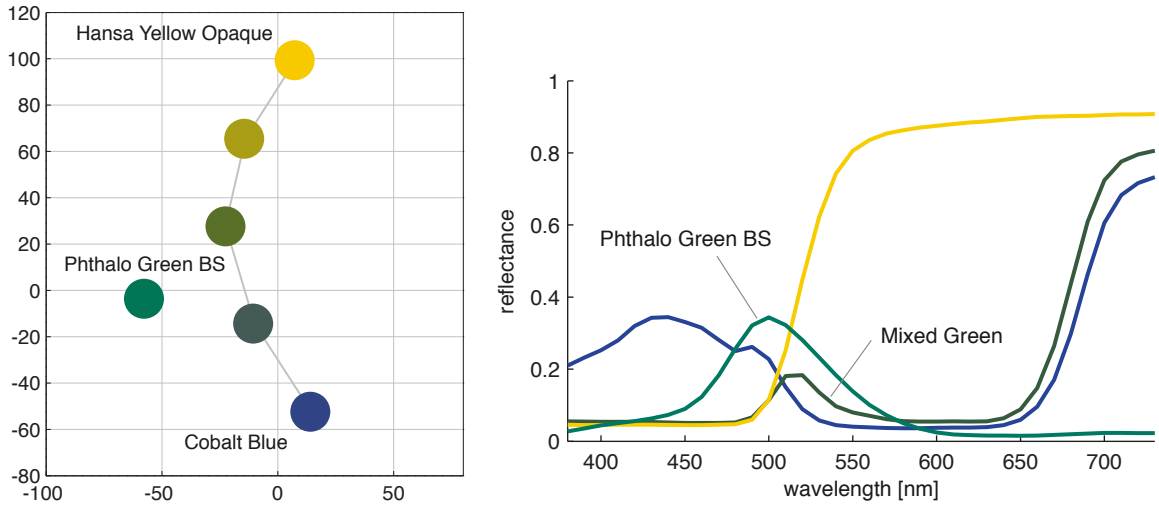

Figure 6.3: Mixing Green Paint with Cobalt Blue and Hansa Yellow Opaque

This leaves only a small range of reflection between 500nm and 540 nm to build a green mixture. Because both paints reflect light above 650nm, the long-wavelength tail of the Cobalt Blue is maintained.

An other example is visualized in Figure 6.4. The result of mixing a cool yellow with a cool red is far away from matching Cadmium Orange paint. A significant portion of the light is absorbed by the red paint. This reduces the reflectance of the mixed orange at medium and long wavelengths. The mixture is less chromatic and as the curve shape indicates, also highly metameric to the orange pigment.

The last Figure (6.5) of this mixing series shows that Cerulean Blue and Cadmium Red Medium mix to a brown color rather than the desired purple. To better visualize the curve shape of Dioxazine Purple, the 80% mixture with Titanium white is shown. (The masstone is very dark and does not visualize the reflectance in the short wavelength

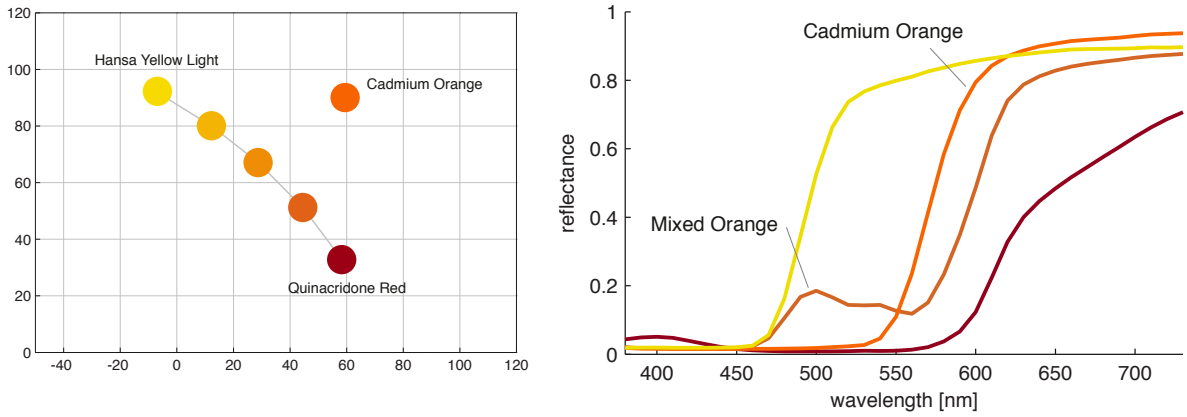

Figure 6.4: Mixing Orange with Hansa Yellow Light and Quinacridone Red

range.) Due to the strong absorption of the red paint, all the short wavelengths are absorbed in the mixture. The only significant scattering of the mixture occurs above 650nm where the human eye is less sensitive. In the range where the human eye is most sensitive, the spectral curve of the mixture is flat with some reflectance towards longer wavelengths. This explains the very low chromatic mixtures shown in the left graph of Figure 6.5.

These three mixtures show how important knowing the spectral properties of pigments is to assemble a paint palette with a large gamut.

6.2 Ink Formulation to match Paints of an Artist Palette

The three approaches to perform spectral ink formulation in this project are the single- and two-constant Kubelka-Munk theory and the use of commercial software (which also uses Kubelka-Munk internally). To characterize the ink set, the printed ink ramps and solid

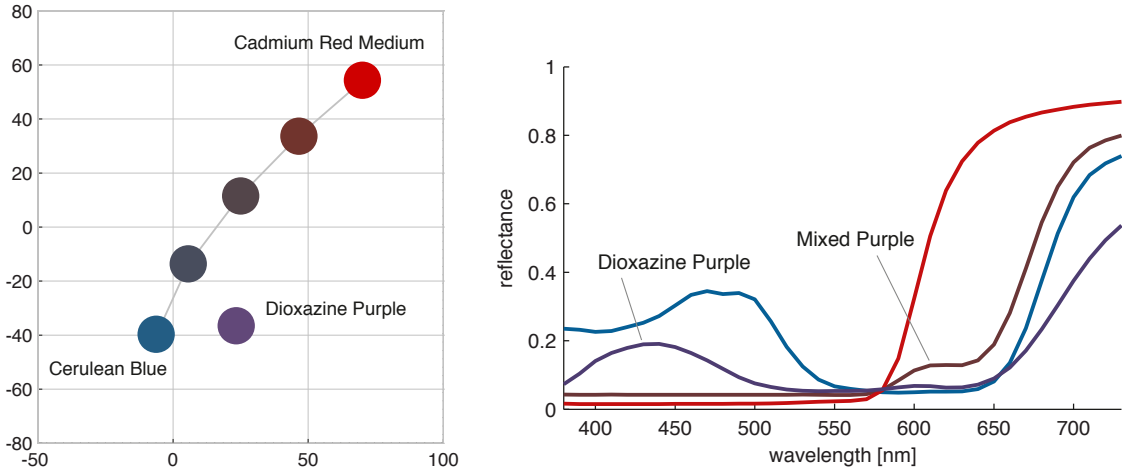

Figure 6.5: Mixing Purple with Cadmium Red Medium and Cerulean Blue

tones were used. The researcher was aware of the fact that this is not the ideal way to train the system. Nevertheless, this approach was chosen because the HP Indigo Ink system cannot be used to make ink draw-dawns. A test set of spot colors was used to verify the performance of the system. This set consisted of 20 Pantone® colors from the ink formulation database of the Printing Application Laboratory at RIT. The reflectance data were measured from printed samples and the mixtures were extracted from the database.

6.2.1 Single-Constant-Kubelka-Munk (Masstone Method)

At first the simplest calculation method was evaluated. The Single-Constant-Kubelka-Munk method is also referred to as the masstone method because only a masstone and no tints are required. In order to work properly, this method would require fully opaque samples. Since it is not possible to print fully opaque masstones on the HP Indigo system,

the 100% solid tones were used and opacity was assumed. Not using fully opaque samples will introduce some error into the calculations. Before a more complex method was tested, the magnitude of the error was evaluated. The absorption and scattering $(K/S)_\lambda$ values were calculated from the spectral reflectance of the solid tones. The prediction of the sample spot colors showed that the calculations were highly inaccurate. Spectral, colorimetric and concentration error were far too big to deliver reasonable results. Therefore, no further analysis was done for this method.

6.2.2 Two-Constant-Kubelka-Munk (Black and White Method)

Since the Single-Constant-Kubelka-Munk model performed poorly with the available input data, a more complex model was tested. As input data, the chromatic inks printed on white paper and on black ink were used to calculate the KX and SX values as described in Section 4.1.2. This more complex mixing model delivered better results than the single constant Kubelka-Munk method for most systems. Nevertheless, the accuracy of the calculations was still not good enough to be useful. No further analysis was done for this method.

6.2.3 Commercial Ink Formulation Software

In addition to building a custom ink formulation tool, the use of commercial software was also considered. Therefore, the X-Rite ColorMaster 8.4 software was evaluated. To build the database of primary colors, ColorMaster requests tint ramps (Primary ink mixed with

white) to characterize the absorption and scattering properties of the ink. Creating tint ramps just by mixing a color with white is not feasible with the present set of HP Indigo ElectroInk®. Therefore, the assumption to use printed halftone ramps instead of tints was made. Measured samples with known concentrations were used to verify the prediction. As expected, the input data was not reliable to calibrate the system. The ColorMaster ink formulation software did not deliver a useful performance due to the bad input data.

6.2.4 Performance of Ink Formulation Methods

Unfortunately, each of the three approaches to formulate artist colors by mixing printing inks failed. This is not due to a poor performance of the used software and formulas – each method demonstrated good performance for other ink mixing applications. The HP Indigo ElectroInk® is a complex system that would require further research to find a feasible process to characterize the mixing properties of these inks.

6.3 Ink Selection to Match Artist Palette

Finding an ink set to match an artist palette requires not only the selection of inks but also the selection of paints. Matching all paints in the database will not be possible. Therefore, the selected paints need to build a good paint palette and the selected inks need to be able to match this paint palette.

For the ink and paint selection, colorant mixing and printing models were used to predict spectral reflectance. These are two very different models. One is the Kubelka-Munk Masstone Approach and the other is the Yule-Nielsen-Spectral Neugebauer (YNSN) model. The researcher was aware of the fact that both models do not deliver accurate predictions of concentrations for the given input data. At this stage of the research, the interest is in evaluating spectral curve shapes and not so much accurate concentration.

6.3.1 Spectral Prediction using Kubelka-Munk

The Kubelka-Munk Masstone approach is known to work well when fully opaque samples can be used to characterize the colorant. Opaque samples could be produced for the paint, but not for the ink samples. Before the absorption and scattering coefficients were calculated, the Saunderson Correction was applied to the spectral curves. For the Saunderson Correction, the K1 and K2 values were optimized and resulted in 0.04 and 0.6, respectively.

6.3.2 Spectral Prediction using YNSN

The Neugabauer model was used to predict the spectral reflectance of the selected inks. The Neugebauer model is described in detail in Section 4.2. There are 2^{ink} Neugebauer Primary colors in a printing system. For seven inks this results in $2^7 = 128$ Neugebauer primaries. The Yule-Nielsen factor is used to improve the accuracy of the model. Equation 6.1 describes the Spectral Neugebauer model enhanced with the Yule-Nielsen correction.

$$R(\lambda) = \left[\sum a_i R_i(\lambda)^{\frac{1}{n}}\right]^n \tag{6.1}$$

Due to the many ink overprinting combinations, it was not possible to print all Neugebauer primary colors during the first press run. Therefore, the overprinting ink combinations have to be predicted. To do so, the Viggiano Trap Equation showed good results for the HP Indigo System [Sigg and Viggiano, 2011]. This Equation is shown in Equations 6.2 and 6.3. For Neugebauer primaries with more than two overprinting inks, the equation is used iteratively.

$$D_{12,\lambda} = D_{1,\lambda} + T_v \frac{D_{2\infty,\lambda} - D_{1,\lambda}}{D_{2\infty,\lambda} - D_{P,\lambda}} (D_{2,\lambda} - D_{P,\lambda}) \tag{6.2}$$

$$D_{2\infty,\lambda} = D_{P,\lambda} + b + c(D_{2,\lambda} - D_{P,\lambda}) \tag{6.3}$$

$D_x = log(1/R_x)$

$D_{12} =$ Spectral density of the overprint

$D_1 =$ Spectral density of first ink down

$D_2 =$ Spectral density of second ink down

$D_{2\infty} =$ Saturation density of the second ink down

$D_P =$ Density of the unprinted substrate

$T_v =$ Viggiano equation trap (0.8) (optimized for smallest error)

$b = 2.1$ (optimized for smallest error)

$c = 1$

6.3.3 Graphical User Interface (GUI)

6.3.3.1 GUI Functions

To support the ink and paint selection, a graphical user interface was designed. Due to the complexity of the many ink and paint combinations, the GUI played an important role in the ink and paint selection process. The Graphical User Interface is shown in Figure 6.7. The prediction models can be selected from a drop-down menu. The drop-down menu allows the user to select a database of paints. After selecting the prediction model and the paint database, the user can select inks from the ink list. Any number of inks between one and twelve can be selected. As a next step, the user can select the paint ramp that should be matched. After clicking the *Plot* button, the result is calculated and displayed. Beside the spectral plot comparing the measured ramp with the prediction, the ramps are

visualized on the right side of the GUI. The ramps are rendered for Illuminant D65 and A and displayed in the sRGB color space. Out-of-gamut colors are clipped to the sRGB color gamut. For a better visual comparison, a CIECAT02 chromatic adaptation was applied to the ramps shown under Illuminant A.

6.3.3.2 Optimization

The graphical user interface (GUI) allows the user to choose four different minimization methods. The default value, where none of the check boxes is selected, optimizes each ramp for the smallest spectral reflectance root mean square error (RMS). Selecting the *weight* check box, uses the diagonal of the N by N dimensional matrix R (Figure 6.6) as a weighting function for the root mean square error (RMS). As shown in Equation 6.4, the matrix R is computed from the N by 3 matrix A, which represents a tristimulus weighting function.

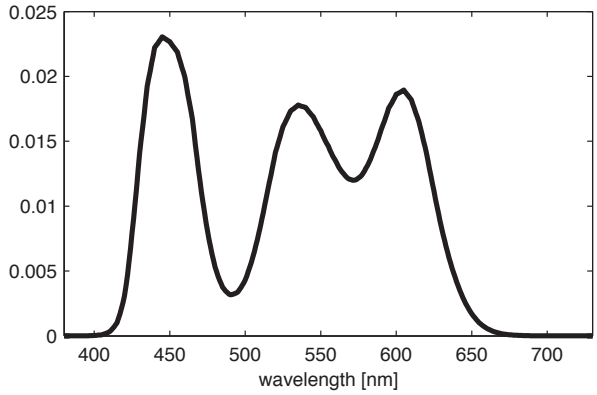

Figure 6.6: Diagonal of Matrix R

Checking *dE 94* uses the ΔE^*_{94} color difference formula to minimize color difference. The GUI also allows to select a weighed color difference measure. Equation 6.5 shows the weighted color difference function $(where: S_L = 1\ ;\ S_C = 1 + 0.045\sqrt{a_1^2 + b_1^2}\ ;\ S_C = 1 + 0.015\sqrt{a_1^2 + b_1^2})$. Note the similarity to ΔE_{94}. This formula pays more attention to the Hue angle error than ΔE_{94}.

$$\mathbf{R} = \mathbf{A}(\mathbf{A}'\mathbf{A})^{-\mathbf{1}}\mathbf{A}' \tag{6.4}$$

$$\Delta E_{94,weighed} = \left[\left(\frac{\Delta L^*}{2S_L}\right)^2 + \left(\frac{\Delta C^*_{ab}}{2S_C}\right)^2 + \left(\frac{\Delta H^*_{ab}}{S_H}\right)^2\right]^{1/2} \tag{6.5}$$

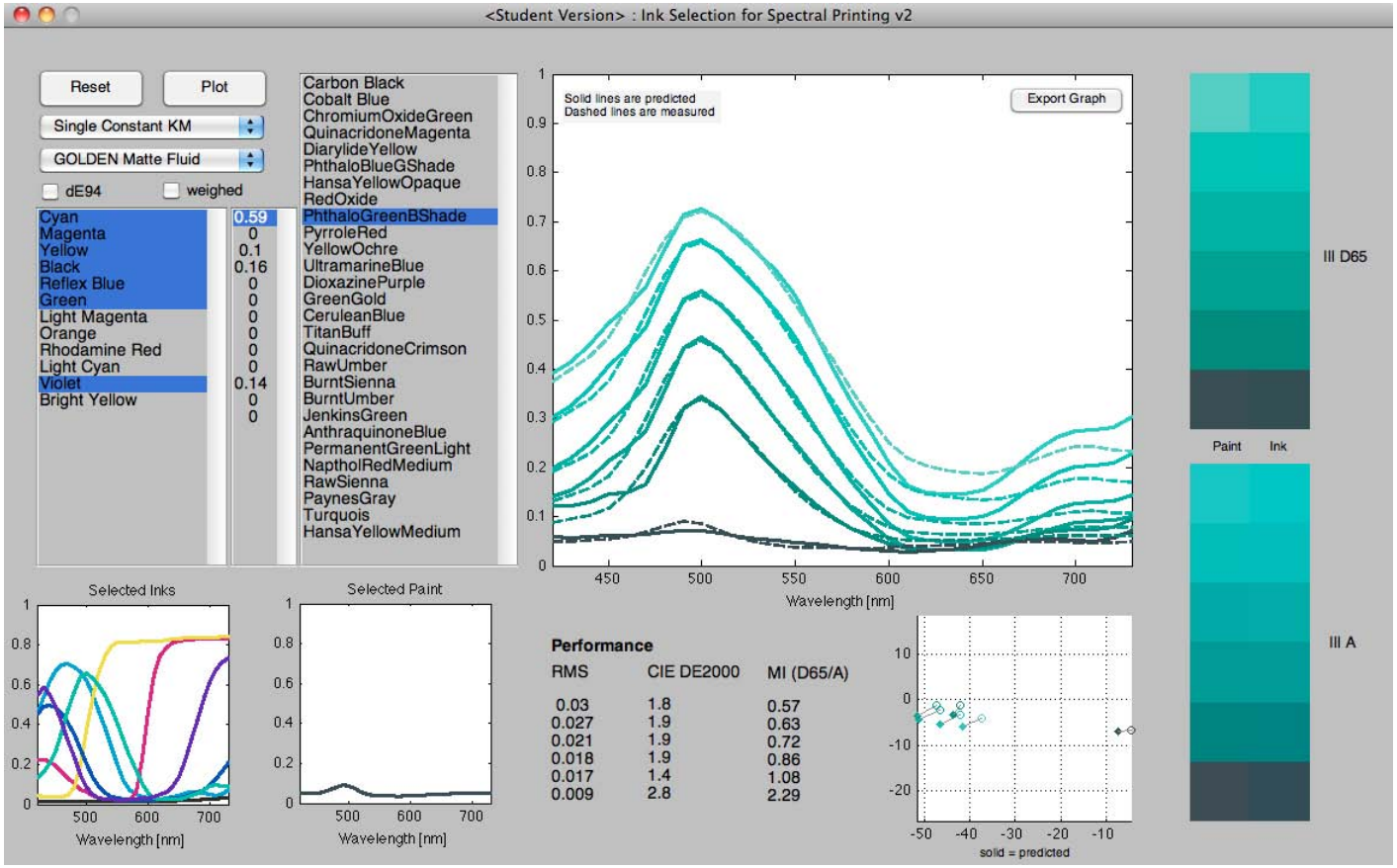

Figure 6.7: Graphical User Interface for Ink and Paint selection

6.3.4 Reducing the Number of Inks in the Ink Set

Finding combinations of ink and paint sets is a complex task. In order to reduce the complexity, the number of inks in the ink set was reduced by taking out inks that are less important to produce spectral matches. Figure 6.8 shows the process of reducing the number of inks in the system.

6.3.4.1 Light Inks

From the twelve primary inks, Light Cyan and Light Magenta were investigated first. The purpose of having light colors in the HP Indigo system is the smooth reproduction of light tones. This is especially important for photo printing applications. Figure 6.9 shows that the light inks have basically the same curve shape as the process colors Cyan and Magenta. They appear to be the same pigment but formulated in different concentrations. For each light ink, a matching spectra from the printed single-ink ramps could be found. Since the reproduction of smooth tones is not the primary interest of this research, Light Cyan and Light Magenta were removed from the ink set. These inks would not contribute spectral degrees of freedom to match artist paints. Therefore, the number of inks is reduced from 12 to 10 as shown in step one in Figure 6.8.

6.3.4.2 Yellow Inks

The set of inks shown in Figure 5.2 indicate the two yellow inks are pretty similar (Figure 6.10). Step two in the flowchart shown in Figure 6.8 is evaluating the two yellow inks.

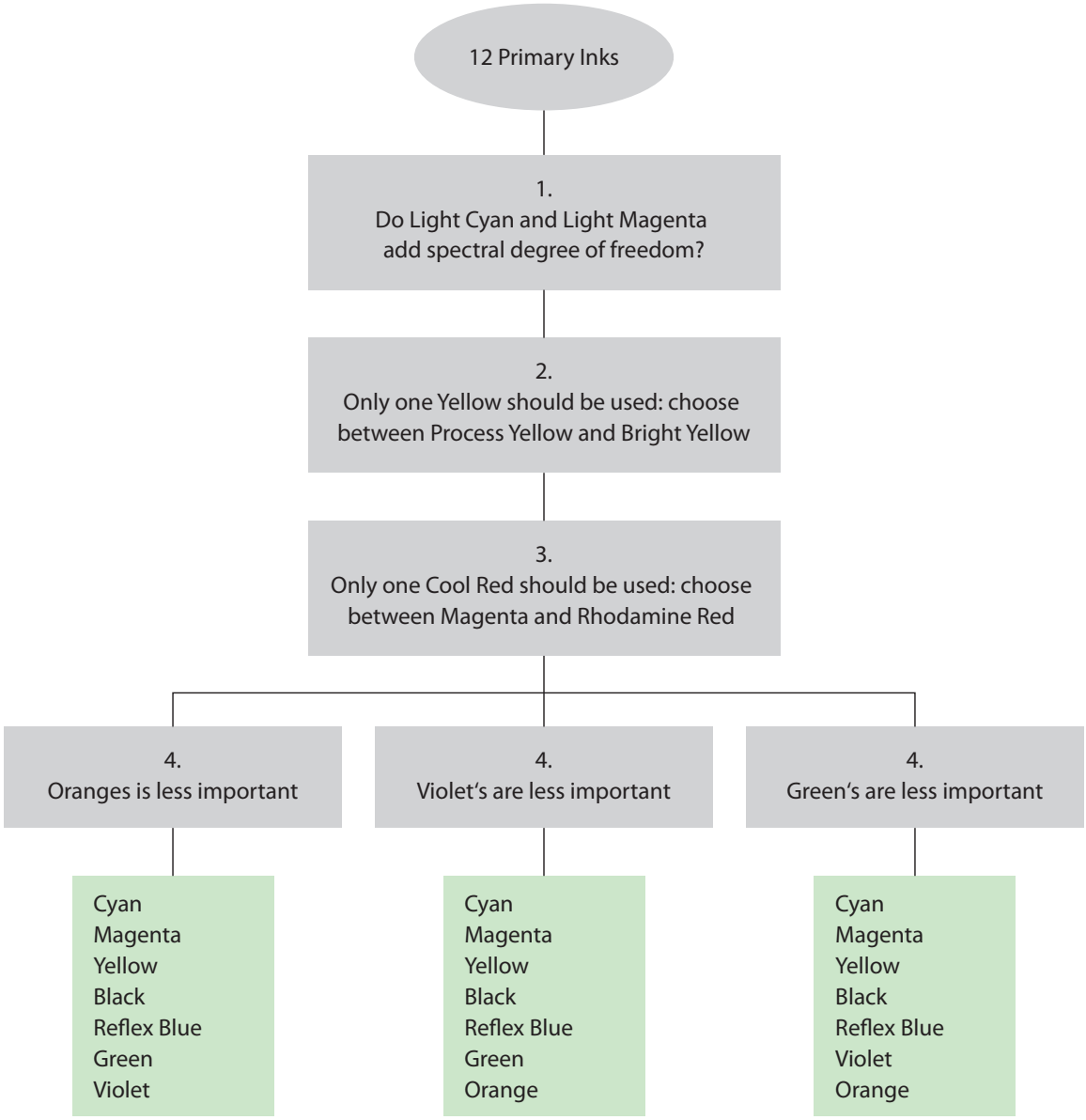

Figure 6.8: Ink Selection Flowchart

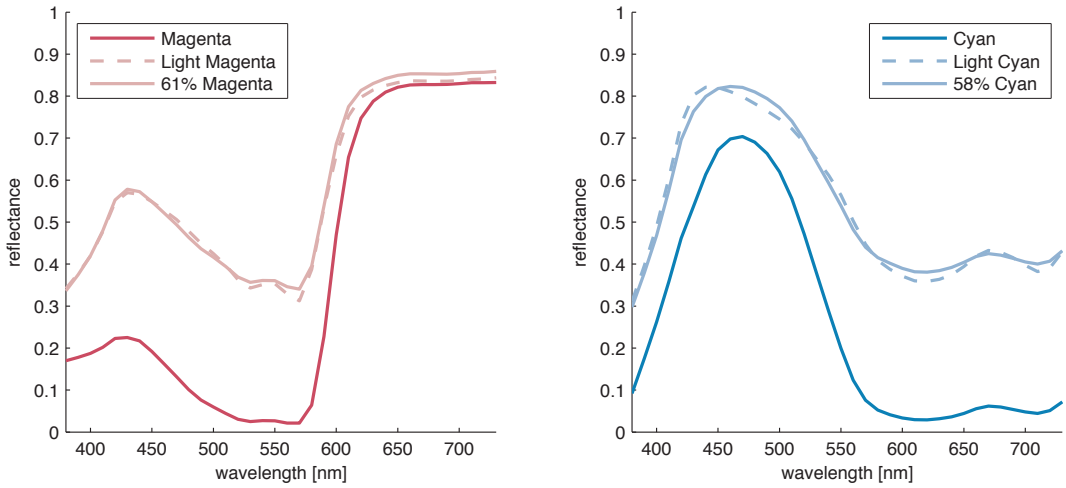

Figure 6.9: Evaluating Light Cyan and Light Magenta

Since the number of inks that can be used for printing is very limited, only one yellow should be used. The *better* yellow needs to be found to include in the ink set. At first, the Bright Yellow seems to be closer to an ideal yellow than the Process Yellow. Its better absorption at short wavelength and the steep flank around 500nm make it a *good* yellow. Nevertheless, for the purpose of this research, this is not the selection criterion. Formulating a printing yellow that matches artist paints by mixing the yellow from other primary inks is not possible. Therefore, the selection process reverses into the question: *Is there an artist pigment that matches one of the printing yellows?*

Figure 6.11 compares different yellow paints to the two printing yellows. As the top left graph shows, none of the Yellows found in the *GOLDEN Matte Fluid Acrylic* paint set is close to a printing yellow. Some research in the internet showed that the Hansa Yellow Light paint from the Heavy Body paint series reports CIELAB values that are pretty close

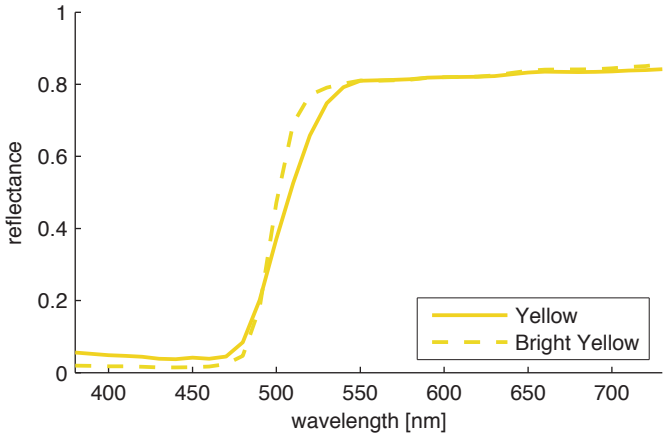

Figure 6.10: Comparing Yellow Inks

to the printing yellow [Golden, 2011a]. A trip to the art store and a few paint-drawdowns later, the measurements show that this yellow paint is already a much better match. The top right graph shows the Hansa Yellow Light from the *GOLDEN Heavy Body Acrylic* paint set. A closer look at the *GAMBLIN Oil Color* set shows that Cadmium Lemon paint is close to Bright Yellow ink. Cadmium Yellow Light also shows close similarity to Yellow ink. The paint set of *LIQUITEX Heavy Body Acrylic* does not have a Cadmium Lemon but does have a Cadmium Yellow Light which already performed well in the *GAMBLIN Oil Color* paint set. Due to practical reasons explained earlier, the focus of this research is the use of acrylic paints. Figure 6.12 shows the spectral reflectance of Cadmium Yellow Light paint and the Process Yellow ink on the left and a CIELAB a*b*-plot on the right. The spectral curve is very similar between 450nm and 550nm. This is particularly important because this impacts mainly the hue angle. The large difference above 550nm is caused because the printing yellow is less chromatic than the paint yellow.

But more importantly, the hue angle shows a good match. The plot on the right of Figure 6.12 illustrates this effect. While there is only a small difference on the a* axis, both ramps move along the b* axis with decreasing concentrations. Selecting Cadmium Yellow Light and Process Yellow completes step two in the flowchart shown in Figure 6.8.

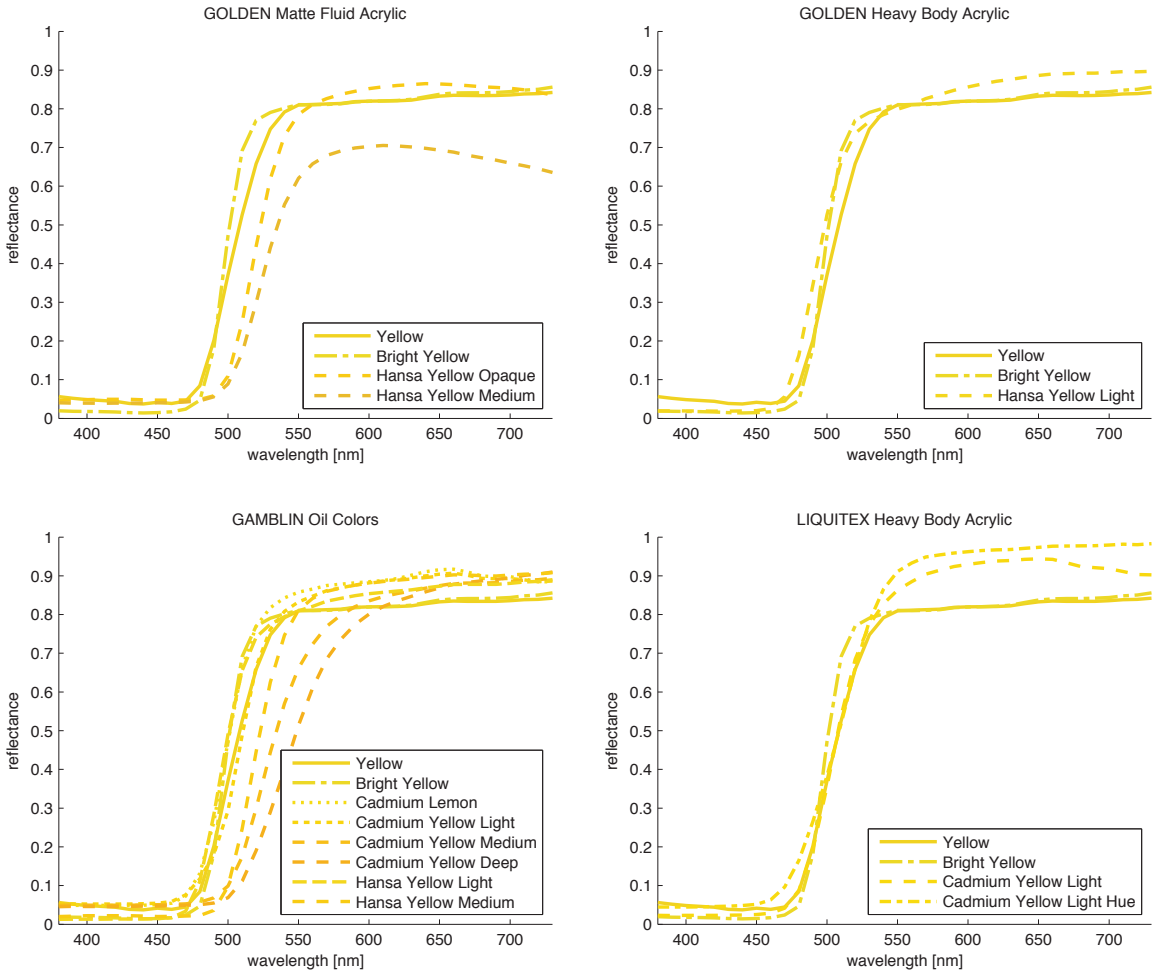

Figure 6.11: Comparing Yellows of different Paint Sets

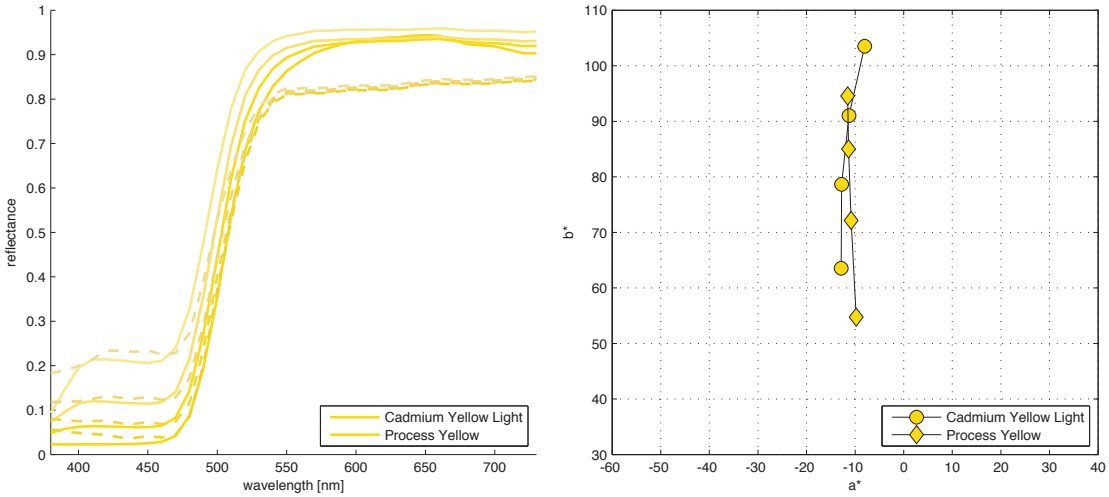

Figure 6.12: Cadmium Yellow Light and Process Yellow Ramp

6.3.4.3 Cool Red Ink

As Figure 5.2 shows, Magenta and Rhodamine Red have similar curve shapes. They mostly differ in the short wavelength range below 500nm and have a different slope around 600nm (Figure 6.13). Regarding the short wavelengths, Rhodamine Red is a *better Magenta* than the Process Magenta. Again, this is not the selection criterion for the purpose of spectrally matching artist materials. To decide which cool red ink should be used, the focus turns to the reddish paints. Finding a good red paint is important for a paint palette. Evaluating the reddish paints shows that the Magenta ink delivers better results than Rhodamine Red Ink. There are several cool red paints to choose from but not many warm reds. Cadmium Red Medium is the warmest red of the evaluated paints. As shown in Figure 6.13, Cadmium Red Medium can be well matched by using Magenta and Yellow Ink. This is not the case using Rhodamine Red. The other warm pigment,

Naphthol Red Medium, can not be matched as well as Cadmium Red Medium.

A factor which also needs to be considered is runnability of the inks during print production. As stated in the IndiChrome v7.0 user manual, Rhodamine Red ink can cause problems in production [Hewlett-Packard, 2009]. During production runs of 1000 pages and more, slight contamination of other inks may occur. These color shifts are not expected to be larger than ΔE^*_{94} = 1.5 [Hewlett-Packard, 2009]. If the use of Rhodamine Red can be avoided, it would eliminate a potential problem. Since Rhodamine Red does not play an important role for most red paints, Process Magenta ink is selected in step three, shown in Figure 6.8.

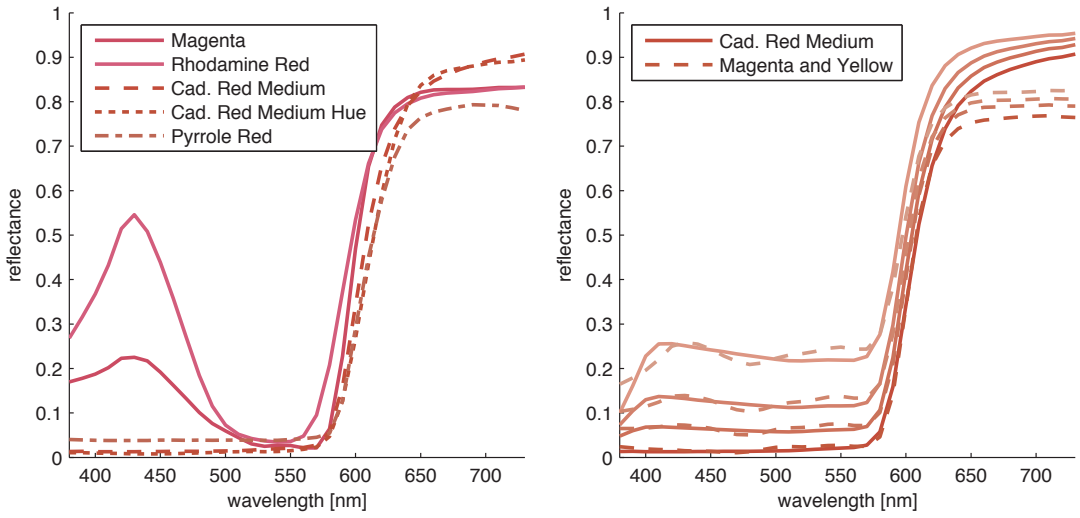

Figure 6.13: Left: Comparing Ink and Paint. Right: Matching Cadmium Red Medium Paint with Magenta and Yellow Ink

6.3.5 Ink and Paint Selection Using the Reduced Ink Set

The previous section about reducing the complexity of the ink set already defined a red (Cadmium Red Medium) and a yellow (Cadmium Yellow Light) paint. Hence, the paint palette will include these two paints. The ink set already defined yellow and magenta as a part of the final selection. The following steps go around the paint palette shown in Figure 6.2. The goal is to find a paint palette with a good color gamut that can be matched spectrally.

6.3.5.1 Warm Green

Permanent Green Light

Permanent Green Light is a warm green pigment. It has a flat spectral reflectance at longer wavelength and a peak at about 520nm (see Figure 6.14). It can be matched colorimetrically by using CMYK inks. Due to the flat spectrum at longer wavelength, green ink would be required to produce a spectral match. Even by using green ink, a very good spectral match cannot be achieved.

Jenkins Green

Jenkins Green is a low chromatic, mixed pigment paint. Its flat spectral reflectance is difficult to match. However, a reasonable spectral match could be achieved by using cyan, yellow, black and green ink (see Figure 6.14). Nevertheless, because this is a low chromatic mixed pigment paint, it will not be considered for the paint palette.

Chromium Oxide Green

Chromium Oxide is a pigment with a unique spectral reflectance. Due to this special characteristic, it cannot be matched with any combination of ink. The spectral match is shown in Figure 6.14.

Green Gold

Green Gold is a mixed pigment paint. It is a very warm paint that reflects a lot of light at longer wavelengths. It has a strong yellowish cast. A good spectral match could be achieved by using Cyan, Yellow, Black, Green and Orange ink. The plot of the spectral match is shown in Figure 6.14.

Cool Green

Phthalo Green Blue Shade

This pigment has a peak reflectance at about 500nm, similar to green ink. Therefore, green ink is important to reproduce Phthalo Green Blue Shade. Besides green, cyan, yellow and black also contribute to match this pigment. By using CMYK plus Green ink, a good spectral match of Phthalo Green Blue Shade can be achieved. Without the green ink, a good colorimetric but not a spectral match can be achieved (Figure 6.15).

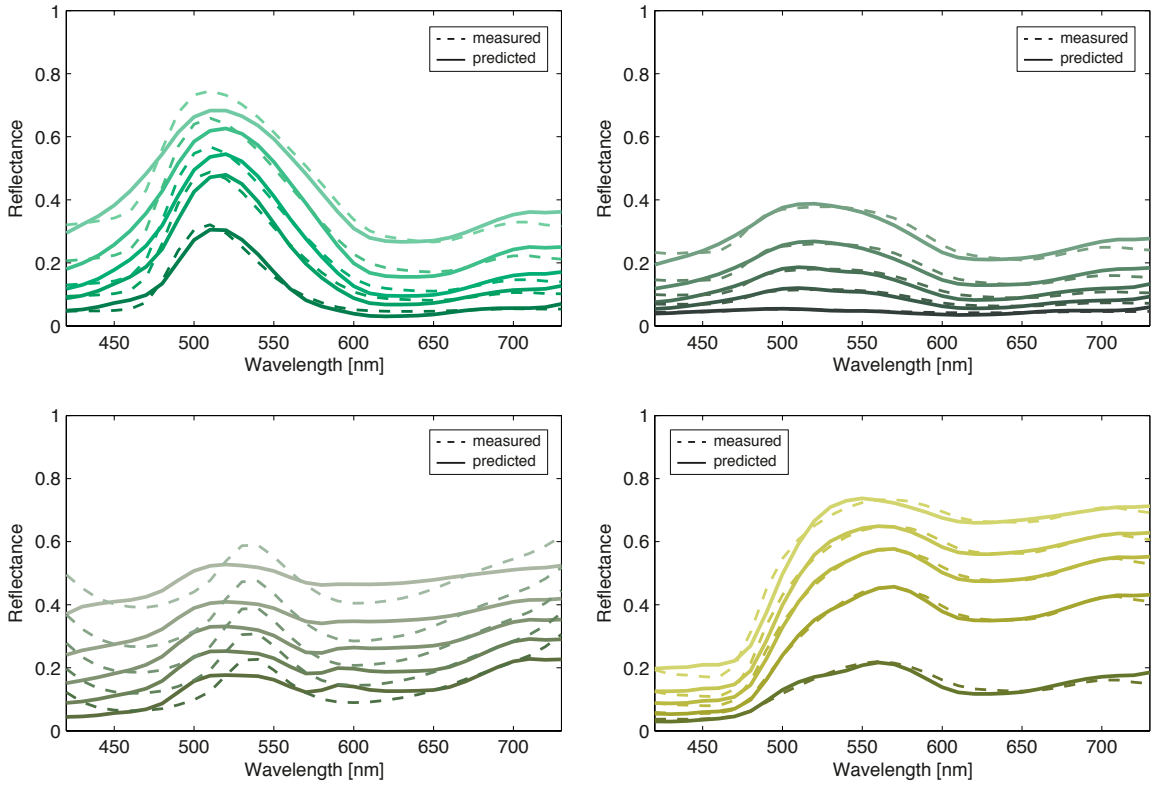

Figure 6.14: Top Left: Permanent Green Light, Top Right: Jenkins Green, Bottom Left: Chromium Oxide Green, Bottom Right: Green Gold

Cool Blue

Cerulean Blue

Cerulean Blue is a pigment with strong reflectance at longer wavelengths. Therefore, it is difficult to match because there is no similar blue ink with such a tail (see Figure 5.2). The upper graph in Figure 6.16 shows the colorimetric match. The ramp clearly indicates that metamerism is causing a color shift when viewed under Illuminant A. As the lower graph of Figure 6.16 shows, a spectral match using all available inks is not possible. The

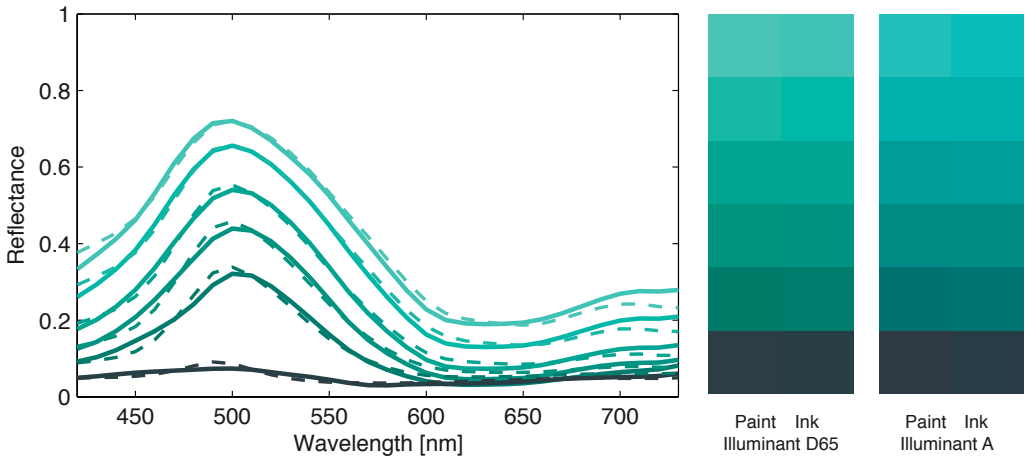

Figure 6.15: Phthalo Green Blue Shade

Cerulean Blue paint shown as dashed line cannot be matched by any combination of inks. This results in a very bad colorimetric match when optimized for a spectral error.

Phthalo Blue Green Shade

Phthalo Blue Green Shade contains Phthalocyanine pigment and is therefore close to cyan ink which is made from Phthalocyanine as well. Both are based on the PB15 pigment family. Therefore, Phthalo Blue Green Shade can be matched pretty well by primarily using Cyan but also Magenta, Black and Reflex Blue. The ramps on the right side of Figure 6.17 show that the best RMS match is also a very close colorimetric match (that is not affected by metamerism).

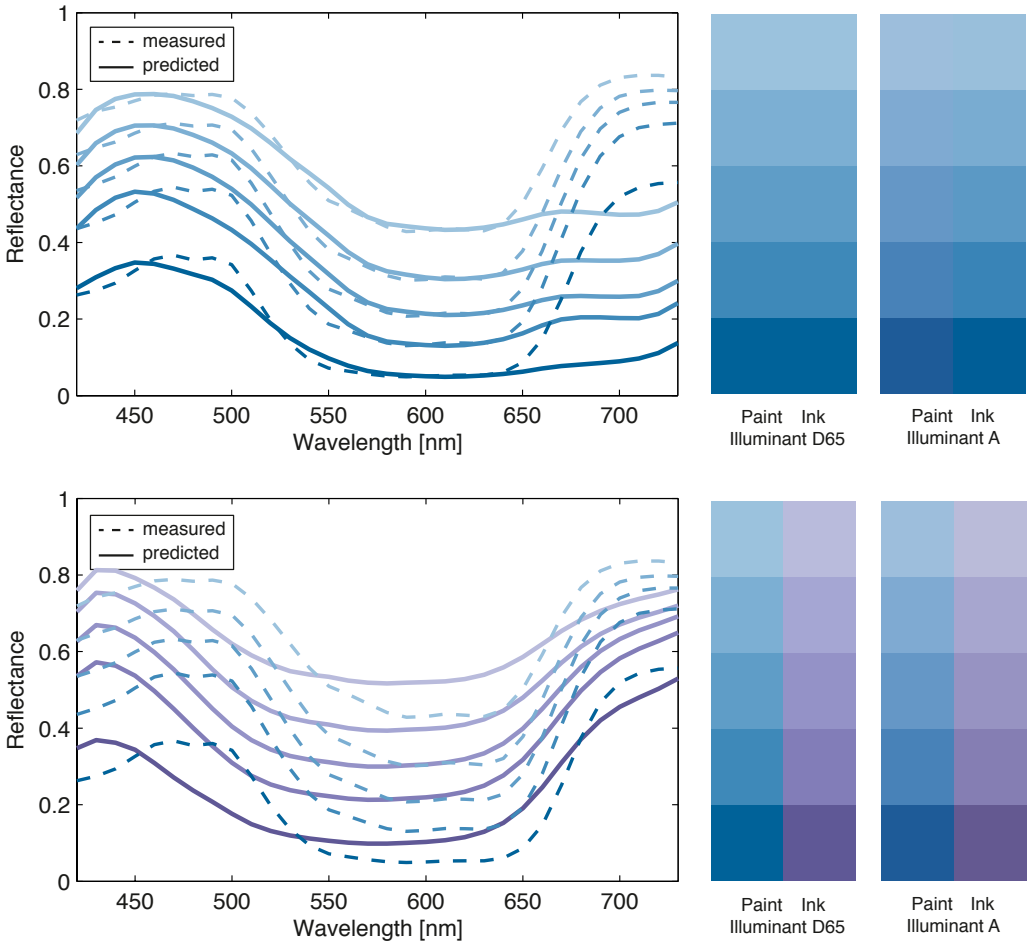

Figure 6.16: Cerulean Blue

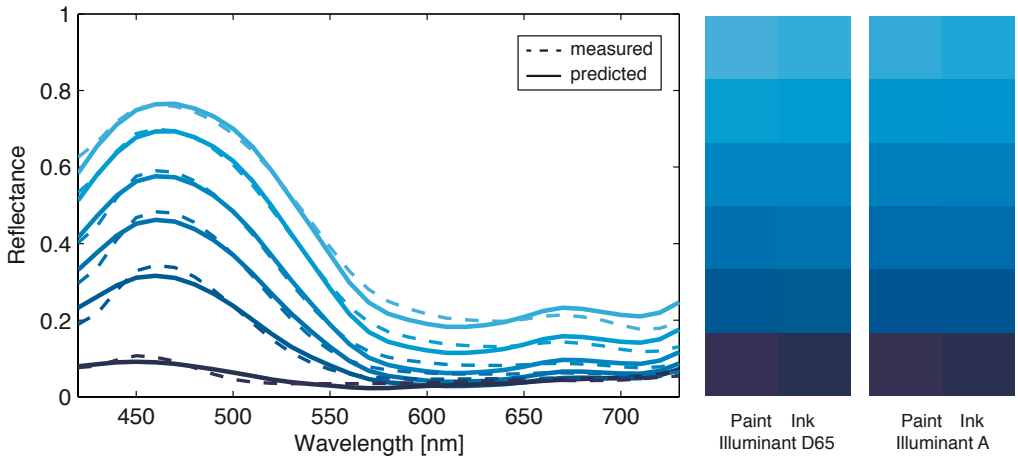

Figure 6.17: Phthalo Blue Green Shade

Prussian Blue

Prussian Blue is a pigment which can not be found in most current acrylic palettes. Therefore, the paint ramp shown in Figure 6.18 was mixed from oil colors. As the graph clearly shows, this pigment has a very flat spectral curve at longer wavelengths. Such a flat curve is difficult to match with the ink set. The patches on the right in Figure 6.18 show that the spectral match is slightly darker which is mainly caused by the spectral error at medium wavelengths. Nevertheless, a very good colorimetric match can be achieved when optimizing for a minimum colorimetric error. Due to the curve shape of Prussian Blue and the printing inks, the colorimetric match is not significantly affected by metamerism.

Turquoise (Phthalo)

Turquoise (Phthalo) is a paint that also contains the Phthalocyanine pigment from the PB15 family. Therefore, a good spectral match can be achieved by using Cyan, Magenta,

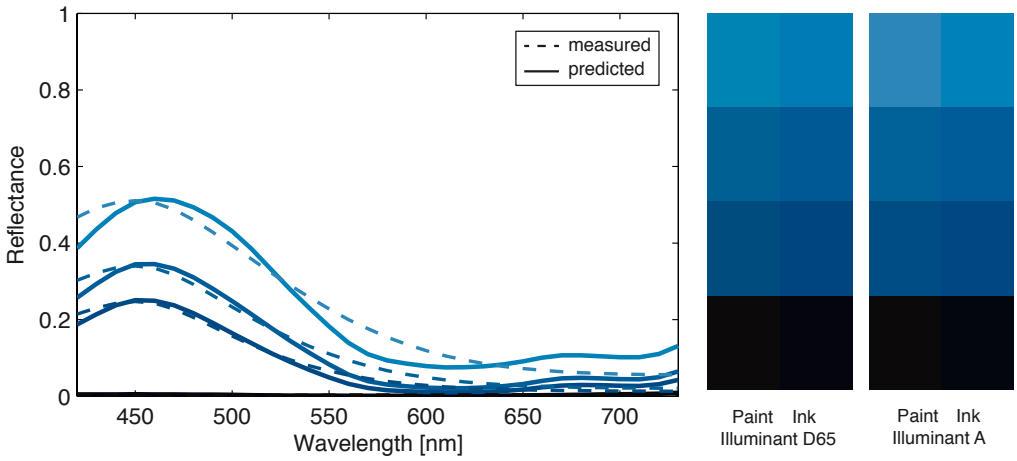

Figure 6.18: Prussian Blue

Black and Green ink. This is shown in Figure 6.19.

Warm Blue

Ultramarine Blue

Ultramarine is an important pigment in the history of art. It has been a very popular pigment among artists for many centuries. Its most distinctive spectral property is its long-wavelength tail which is sensitive to changing illuminant conditions. In CMYK color reproduction, none of the pigments shows a similar tail. The CMYK ink set needs to be extended with an ink showing such a long-wavelength tail in order to match it spectrally. A look at the primary inks shown in Figure 5.2, indicates that Reflex Blue ink show a similar tail at longer wavelength. Figure 6.20 compares the paint to the ink ramp. The 80% paint ramp can be matched quiet closely with the 91% Reflex Blue Ramp. As the graph shows, the matches of the lighter mixtures are not as good. This is because the

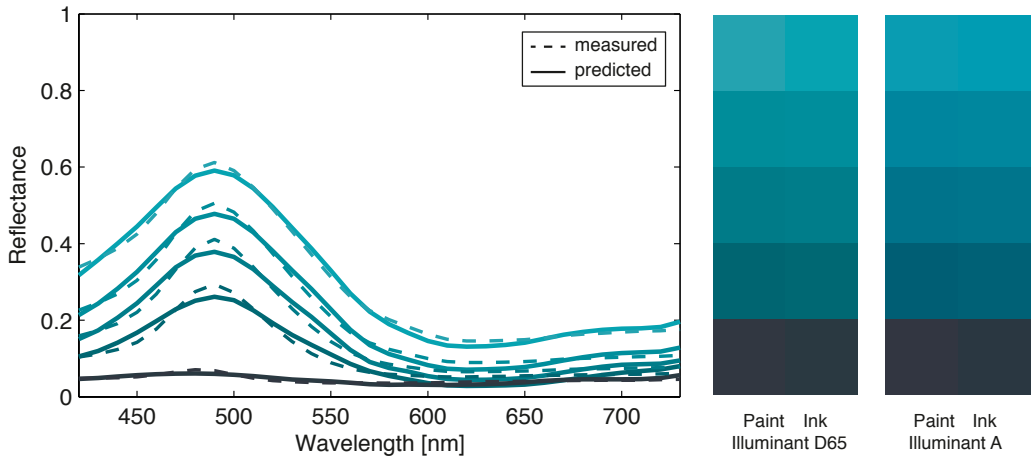

Figure 6.19: Turquoise (Phthalo)

halftone screening of the ink ramp behaves very different than mixing the Ultramarine Blue paint with Titanium Oxide paint. There is not much that can be done about that. Lighter Ultramarine Blue tones will probably not experience close spectral matches. To match Ultramarine Blue paint, Reflex Blue ink needs to be included in the ink set.

Cobalt Blue

Cobalt Blue is another pigment that has been very popular among artists. This pigment is well known to cause problems in current color reproduction workflows. The problem of metamerism is worse than with Ultramarine Blue. Matching Cobalt Blue would be important. Nevertheless, none of the primary inks shown in Figure 5.2 includes the same characteristics at longer wavelength as Cobalt Blue. Figure 6.21 shows the Cobalt Blue ramp as dashed lines and the solid lines as the matches. The upper graph shows that a good colorimetric match can be achieved. Similar to Cerulean Blue, the metamerism between

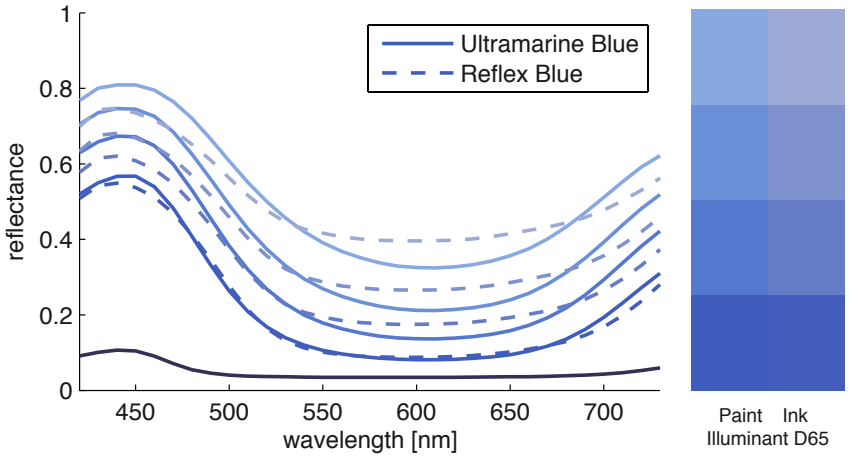

Figure 6.20: Ultramarine Blue and Reflex Blue

the pigment ramp and matches show up clearly when viewed under Illuminant A. The bad performance of the spectral match becomes very apparent in the lower graph. The spectral match is far away and causes a large colorimetric error when matched with the present ink set. Unfortunately, spectrally matching Cobalt Blue is impossible with the available inks.

Violet

In the Violet sector, there are not many paint pigments available. The set of evaluated pigments only includes Dioxazine Purple. To match this pigment, important inks are mainly Violet but also Reflex Blue, Magenta and Black. Figure 6.22 shows the benefit of printing more than the standard CMYK inks. The match on the left shows a good colorimetric match using CMYK only. The spectral match on the right shows what adding Violet and Reflex Blue ink can achieve in terms of spectral matching. Due to the good spectral match, color inconstancy will not show up under changing lighting conditions. To

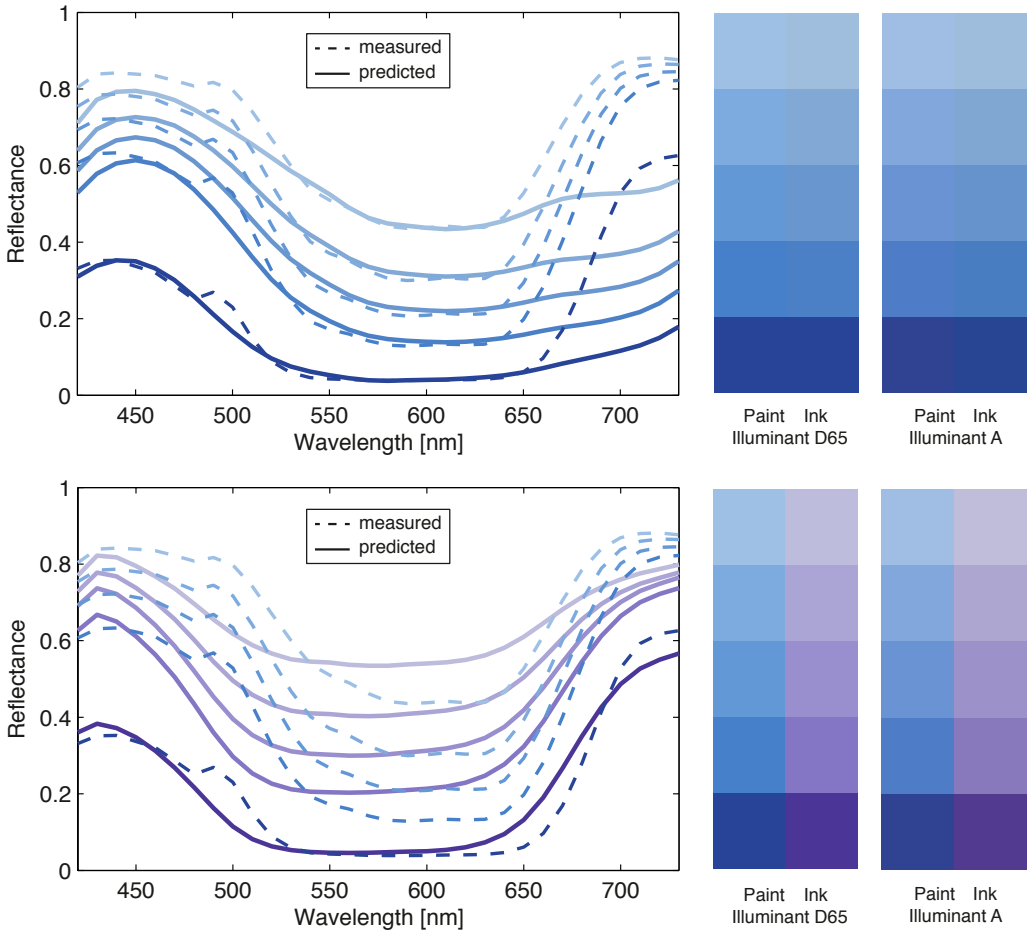

Figure 6.21: Matching Cobalt Blue

match purple paint, Violet ink needs to be in the ink set to achieve a spectral match.

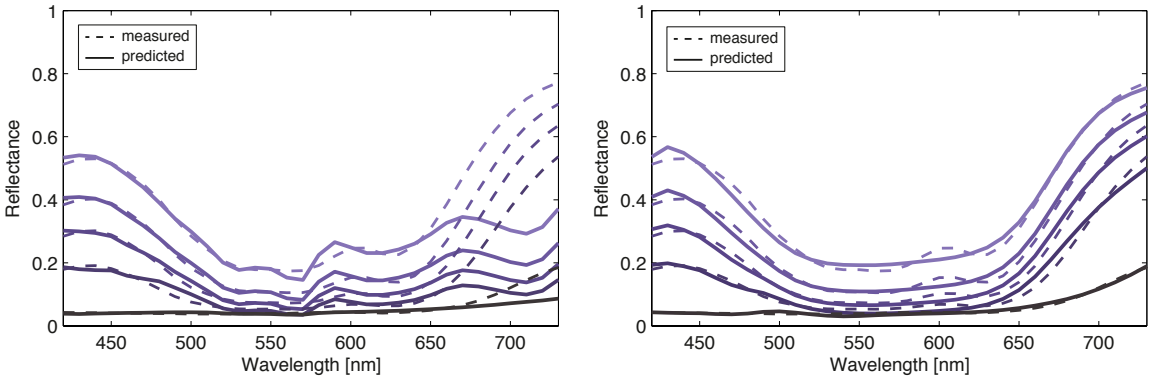

Figure 6.22: Matching Dioxazine Purple with CMYK (left) and 7 Inks (right)

Cool Red

Quinacridone Magenta

Quinacridone Magenta is a single pigment paint. With the given set of inks it is difficult to match the flank of the curve between 580 and 680nm. Therefore, the spectral and colorimetric matches show some error. Spectral curves and ramps of the spectral match are shown in Figure 6.23. The evaluation with the GUI showed that a colorimetric match would exhibit more metameric error under changing viewing conditions.

Quinacridone Crimson

Quinacridone Crimson is a paint mixed from two Quinacridone pigments. It can be matched by using Magenta, Yellow, Orange and Violet ink. Figure 6.24 shows that the spectral and colorimetric matches of Quinacridone Crimson are good. Due to the good

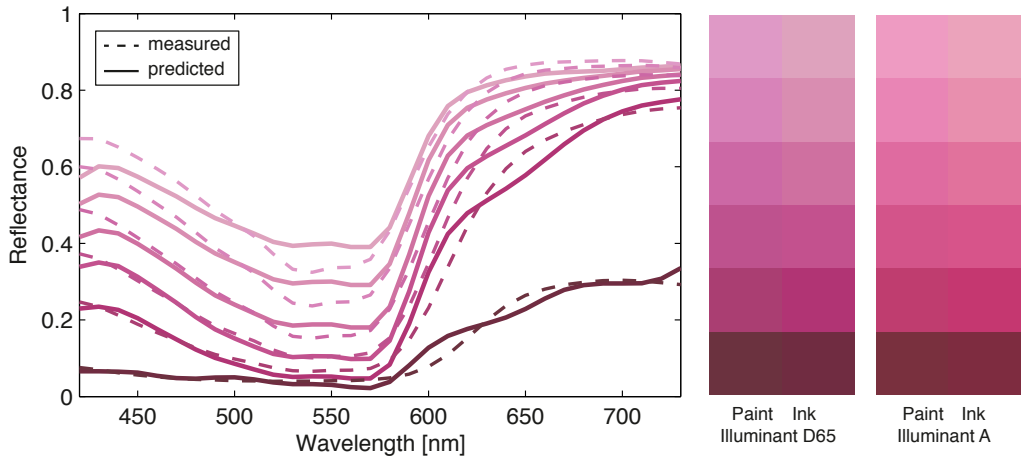

Figure 6.23: Quinacridone Magenta

spectral match, the ramp patches match under Illuminant A as well.

Warm Red

Warm red paints were already evaluated in section 6.3.4.3 where Magenta and Rhodamine ink was evaluated. The analysis showed that Cadmium Red Medium can be matched by using Process Magenta and Yellow ink.

Warm Orange

The evaluated paints offer only one warm orange paint. This is Pyrrole Orange which is a single pigment paint. As shown in Figure 6.25, matching Pyrrole Orange with CMYK inks results in a poor spectral match. Not only a spectral but also a colorimetric match is impossible because it is beyond the CMYK printing gamut. Matching Orange paint recalls the problem of matching yellow. Either there is an ink that matches the paint or not.

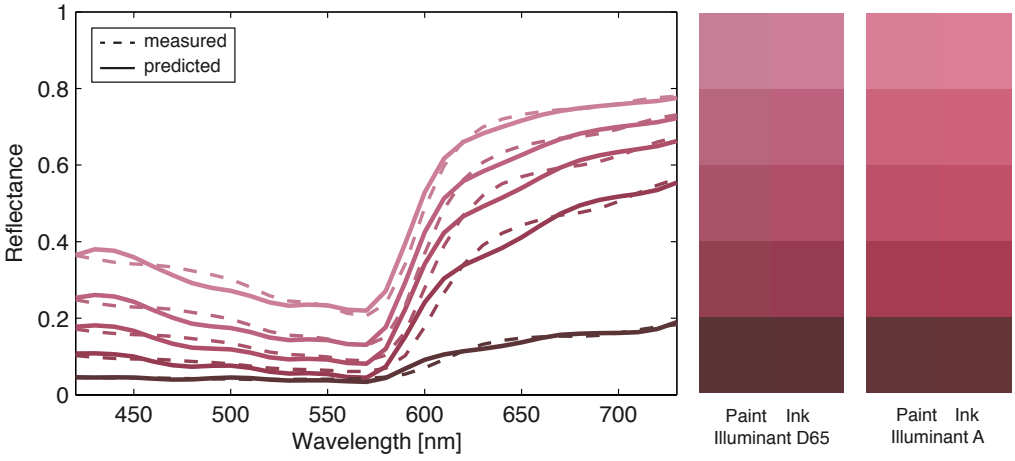

Figure 6.24: Quinacridone Crimson

Mixing inks to match Orange will always result in a bad spectral match. In this case (right plot in Figure 6.25) adding Orange ink does not yield a satisfying result because Pyrrole Orange is a warmer than the Orange ink. Therefore, Pyrrole Orange cannot be matched with the present ink set.

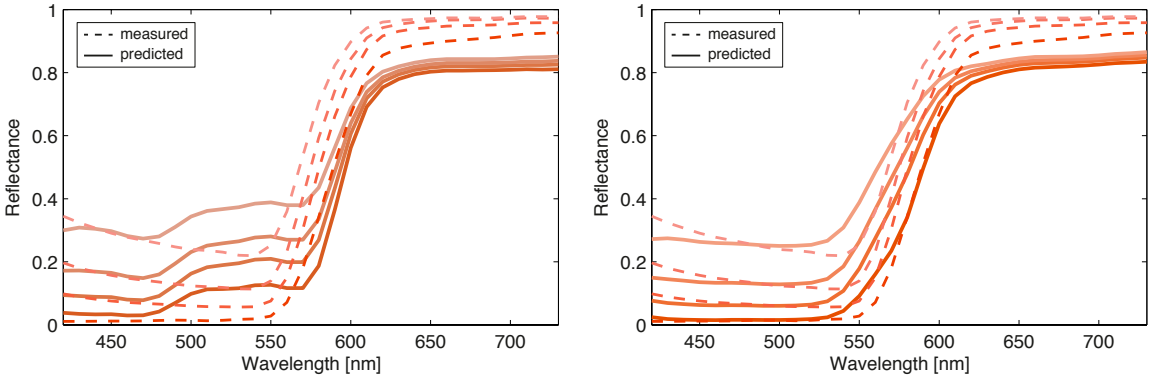

Figure 6.25: Pyrrole Orange matched with CMYK (Left) and Pyrrole Orange matched with CMYK plus Orange Ink (Right)

Cool Orange

Similar to the warm orange, there is only one cool orange pigment – Cadmium Orange. As described before, Orange can not be spectrally matched by mixing printing inks. Therefore, the orange ink ramp was evaluated to find out if it can match Cadmium Orange. Figure 6.26 compares patches from the Orange ink ramp that best match Cadmium Orange. The difference in reflectance above 600nm shows that the Orange Ink is less chromatic but it is located at the same hue angle as Cadmium Orange. Taking into account that the Orange paint is beyond the printer gamut, the colorimetric match is acceptable. Cadmium Orange and Orange ink are an important pair to enlarge the gamut of the paint palette in the orange sector.

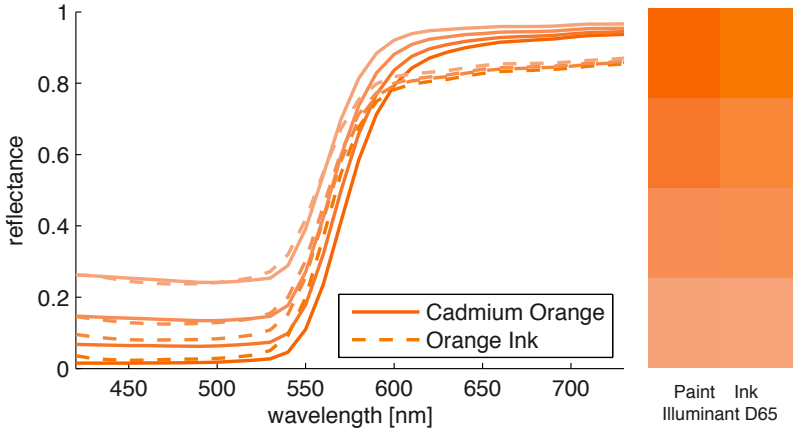

Figure 6.26: Cadmium Orange matched with the Orange Ink Ramp

6.3.6 The Final Paint Palette

Defining a paint palette is not only about finding the paints with the best possible match – it is also about finding a palette with a good color gamut. It should be a realistic representation of what an artist would use to create artwork. Nevertheless, it is not easy to find a palette that would work for all artists. An artist palette is based on the personal preferences of the artist and his painting style. During different time periods in history, artists used different raw materials to create their art. The goal of the present research is to find a palette that spans a wide color gamut and uses common pigments that are available to artists today.

As the analysis of the different paints showed, Cyan, Magenta and Yellow are important to match most pigments. For the purpose of print production, the black ink must also be used. Black ink is important to reproduce the flat spectral curves of grays mixed from carbon black and white paint. For the practical application of printing any book, black ink is also required to print text. This defines the four common CMYK inks to be a part of the ink set. Hence, the inks selection comes down to choose maximum three out of the four inks that are left after reducing the ink set. As the flowchart in Figure 6.8 shows, Reflex Blue, Green, Violet and Orange need to be evaluated to complete the ink set.

As the analysis of the inks and paints showed, Reflex Blue comprises important properties to match Ultramarine Blue. Since Ultramarine Blue is a very important pigment in a lot of artwork, Reflex Blue is a must have. Using Violet ink would allow the match of Dioxazine Purple. Violet ink is also helpful to improve the performance of mixing cool

red inks. Without Violet ink there would be only brownish and low chromatic purple colors in the gamut of the paint palette.

Since Violet and Reflex Blue are required, the question reduces to the choice between Orange and Green. Mixing Orange paint is very difficult. A highly chromatic orange cannot be mixed with a warm red and a cool yellow. Demanding an Orange paint would require the use of Orange ink. Green on the other hand is also important. Figure 6.27 shows the ink gamut when either orange or green would be added to the ink set. As the plot shows, both inks play an important role in enhancing the color gamut in the orange or green sector. Technically, green and orange would yield a similar gain in terms of ink gamut. Therefore, the decision mainly depends on the paint palette. Color mixing experiments showed that Phthalo Blue Green Shade and Cadmium Yellow Light can create good green mixtures without having a green paint. On the other hand, mixing Cadmium Red Medium and Cadmium Yellow Light does not result in a very chromatic orange. To support decision making, several artists and paint experts were consulted for their preference of having a green or orange paint in their palette [Bosket, 2011, Gottsegen, 2011, Golden, 2011b]. Generally, these experts considered Orange as the more important color in the palette. Based on these recommendations, it was decided to neglect green and favor orange.

Summing up, a paint palette that can be spectrally matched by a set of seven inks would include the paints shown in Figure 6.28. The selected ink set to match these pigments is: Cyan, Magenta, Yellow, Black, Reflex Blue, Orange and Violet.

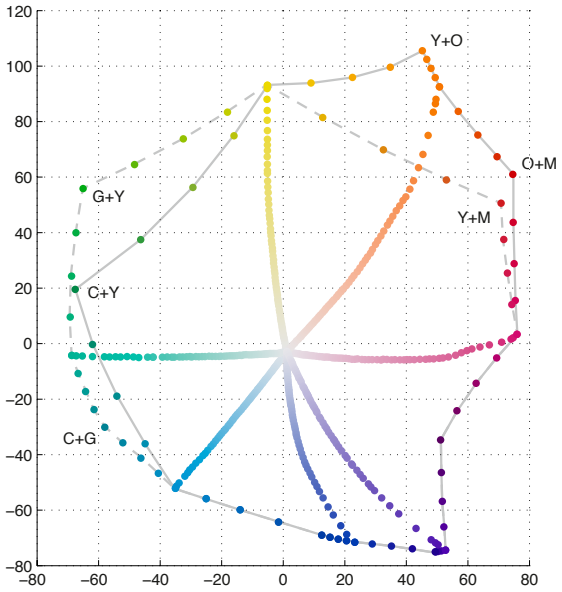

Figure 6.27: Predicted Gamut Plot for Ink Selection (Colors were predicted using the YNSN model with predicted solid overprints)

6.3.7 Summary

A wide range of artist paints was evaluated. Some pigments have spectral properties that cannot be spectrally matched with the current set of HP Indigo ElectroInk®. New inks would have to be developed to match paints like Cobalt Blue or Cerulean Blue. Hence it was exciting to find that Ultramarine Blue can be matched with a printing ink. The evaluation showed that Cyan, Magenta, Yellow and Black are important inks and support the spectral match of many paints. Violet ink enables a spectral match in the purple sector of the paint palette. The trade-off between orange and green was decided in favor of orange since most artists preferred to enhance the paint gamut towards orange rather than green.

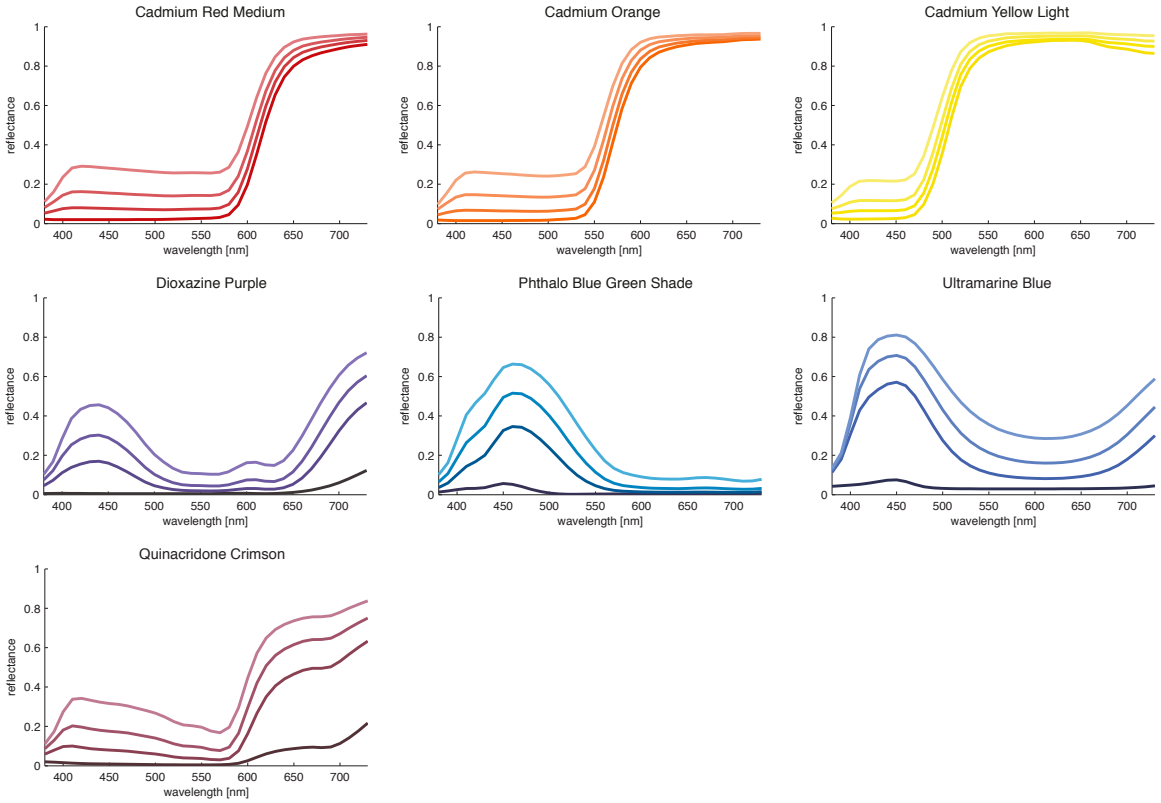

Figure 6.28: Ramps of Paint Palette

Chapter 7

Characterization of the Printing Process and Spectral Modeling

This chapter describes the process of characterizing the printing process including test targets, screen angle and ink sequence selection. The data obtained from the second press run are then used for spectral modeling of the printing system. The performance of the spectral modeling of the present system using the CYNSN model is evaluated at the end of this chapter.

7.1 Test Target for Cellular YNSN Model

The goal of the second press run was to characterize the seven ink printing process. To do so, several test targets were created. To perform the effective area coverage correction for the YNSN model, ramps were printed for every ink. The Cellular Neugebauer model requires measured reflectances for all nodes. Besides the 128 neugebauer primary colors, all three and four node combinations were printed. For seven inks, many patches have to be created. Three nodes (0%, 50%, 100%) result in $3^7 = 2187$ patches, four nodes in

$4^7 = 16384$ patches. More than four nodes would create too many patches and would not be practical. The same process control elements as used in the first press run were included. The test targets are shown in Appendix B.

7.2 Press Settings

This section describes the settings that were used to print the test targets. It also shows the process of decision making to define the settings. Screen angles, ink sequence as well as an overview over the press settings are discussed.

7.2.1 Screening Angles

Selecting good screening angles for multi-color printing is a very important step. Ideally, the difference between two colors should be as big as possible. In conventional four color lithographic processes, the screening angles are chosen according to the following schematic: At first, the most dominant color is set to $45\,^\circ$ (often Black). The other two dominant colors (Cyan and Magenta) are set to angles as far apart as possible. This usually results in $15\,^\circ$ for Magenta and $75\,^\circ$ for Cyan. At last, the least dominant color (Yellow) is placed between Cyan and Black at $65\,^\circ$ [Sigg, 2007].

The process of screen angle selection is well known and established in conventional printing technologies. However, conventional screening technologies apply to digital printing with some restrictions. Due to the low resolution of 812 spots per inch on the HP Indigo, more complex screening technologies need to be used. Additional effects like

Table 7.1: Vector Correlation Matrix of Ink Set

	Cyan	Magenta	Yellow	Black	Reflex Blue	Orange	Violet
Cyan	1	0.22827	0.32011	0.59461	0.90155	**0.12722**	0.55986
Magenta		1	0.8221	0.8521	**0.36854**	0.93667	0.7366
Yellow			1	0.90796	0.27985	0.9143	**0.54547**
Black				1	0.62067	0.84311	0.81314

dithering can enhance the behavior of the screening. A further limitation is the fact that the HP Indigo can print only four different screen angles. Therefore, some inks have to share screen angles. The default screen angles for CMYK are shown in Table 7.2. Since these screen angles have proved to work well on this press, the same angles were used for the prints. To define the screening angles for the additional inks, the method of calculating the vector correlation of the spectral reflectance of the inks was chosen. Equation 7.1 shows the calculation of the vector correlation where Ψ is the reflectance of ink1 and ink2. A table of the vector correlations between the different inks is shown in Table 7.1.

Since the CMYK inks are kept at the default screening angles, only the three additional inks are evaluated. First, the most obvious pair of inks sharing a screen angle is Cyan and Orange since these two inks have the least vector correlation. The other two inks are more difficult to define. Yellow shows a low vector correlation for Reflex Blue and Violet. Therefore, the vector correlation of Magenta plays a role. Magenta should not share a screen angle with Violet. Therefore Yellow and Violet share a screen angle. The other pair is Magenta and Reflex Blue.

$$\rho = \sum_{\lambda=400nm}^{700nm} \Psi_{\lambda,ink1}\Psi_{\lambda,ink2} \sqrt{\sum_{\lambda=400nm}^{700nm} \Psi^2_{\lambda,ink1}}^{-1} \sqrt{\sum_{\lambda=400nm}^{700nm} \Psi^2_{\lambda,ink2}}^{-1} \tag{7.1}$$

The pairs of screen angles are also shown Figure 7.1. The a*-b* plot indicates that ideally complementary colors share a screen angle. The pair of most concern is Reflex Blue and Magenta. Unfortunately, this is a compromise that is not ideal but a better solution could not be found.

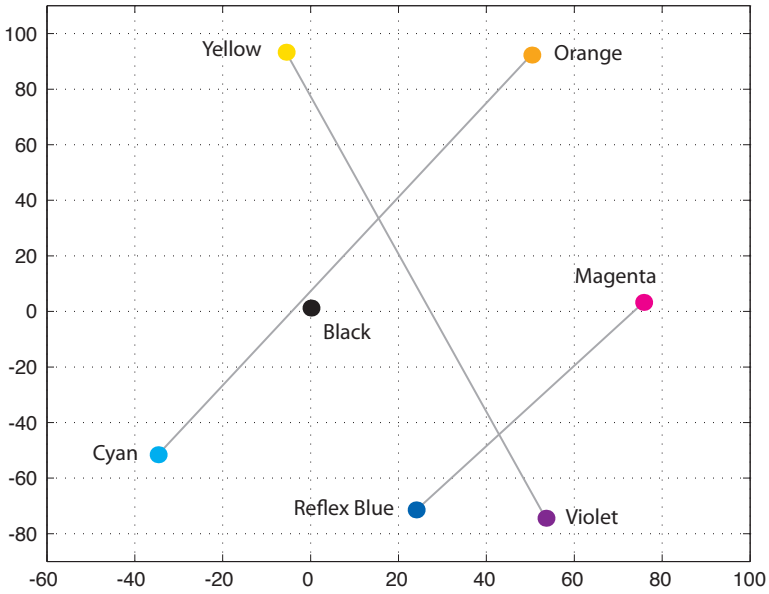

Figure 7.1: a* - b* Plot of Ink Set

7.2.2 Ink Sequence

The sequence in which the inks are laid down does impact the gamut of the print. There are 7! = 5040 possible sequences to print seven inks. At first, the brute force method of

predicting the full set of Neugebauer Primaries to calculate the volume of the gamut was considered. Since the prediction of the many dark Neugebauer Primary colors turned out to be inaccurate, a better solution had to be found.

Printing inks are not truly transparent. Toner based inks like the liquid toner used in HP Indigo presses are known to scatter light. Printing a light and strong scattering ink onto darker ink would increase the lightness of the darker ink rather than decrease it like a fully transparent ink would. Therefore, a larger gamut can be achieved by printing a dark ink onto a scattering light ink. To evaluate the scattering properties of the inks, the test target from the first press run was used. Since the first ink on the paper was black, this target is ideal to evaluate the scattering properties of each ink. Figure 7.2 shows solid chromatic inks printed on black ink. To rank the inks by scattering, the area below each spectral curve was calculated. The larger the area below the curve, the more scattering that occurred. The ink sequence ranked by scattering was defined as: Orange, Yellow, Magenta, Violet, Cyan, Reflex Blue and Black.

A summary of all press setting used in the second press run is shown in Table 7.2.

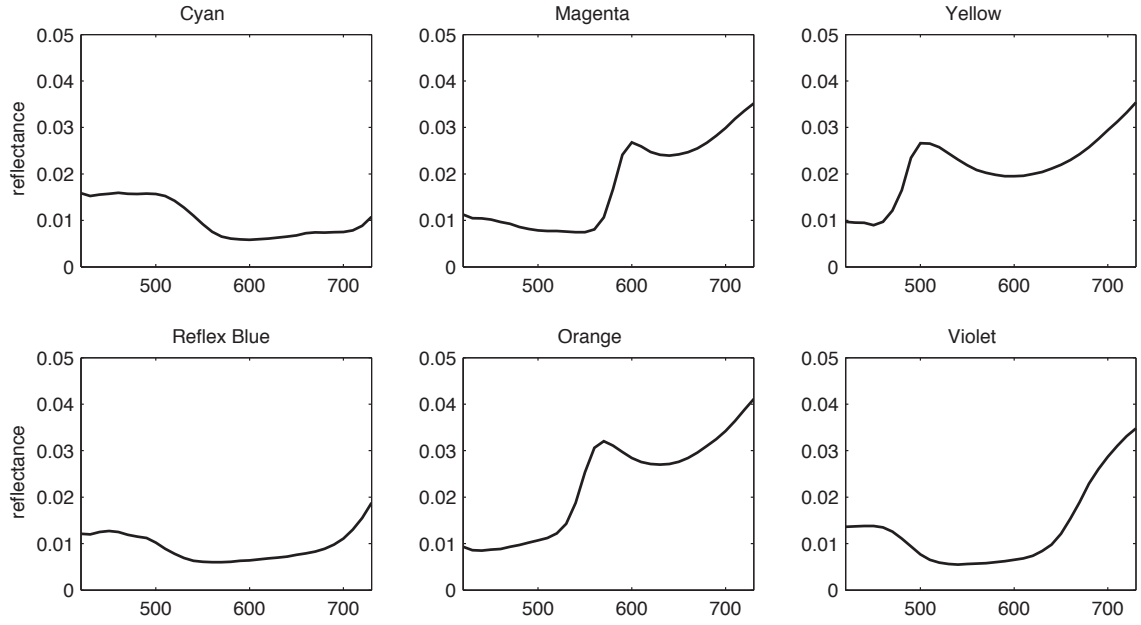

Figure 7.2: Scattering of Inks Printed on Black

Table 7.2: Press Settings Press Run 2

Ink	**Screen Angle**	**Density (Status G)**	**Ink Sequence**
Cyan	Cyan (4 °)	1.45	5
Magenta	Magenta (64 °)	1.45	3
Yellow	Yellow (18 °)	1.10	2
Black	Black (34 °)	1.75	7
Reflex Blue	Magenta	1.60	6
Orange	Cyan	1.90	1
Violet	Yellow	1.45	4

7.3 Spectral Modeling

7.3.1 Yule Nieslen n-Factor

It was explained in Section 4.2.3 that the Yule-Nielsen n-factor can improve the accuracy of the Neugebauer printing model. To evaluate this n-factor correction, n-factors from zero to twenty were evaluated. For each n-factor the effective area correction was calculated by linear regression as described in Section 4.2.2. The YNSN model was then used to calculate the spectral reflectance of each patch of the ink ramp. Every ink ramp was treated independently from the other inks. This can be considered a reasonable assumption [Wyble and Berns, 2000]. Figure 7.3 shows the effect of the n-factor for all the ink ramps. The lowest error appears to be at an n-factor of 2. Figure 7.4 shows the prediction of each ramp using the chosen n-factor. The performance of the ramp prediction is shown in Table 7.3. An n-factor of 2 results in low CIEDE2000 and RMS errors for all ramps. As Figure 7.4 indicates, the errors for the black ramp are the largest.

7.3.2 Area Coverage Correction

Using a look up table (LUT) to correct the theoretical to effective area coverages is known to improve the accuracy of the prediction. Section 4.2.2 describes how the effective area coverage can be calculated by using least squares linear regression. Using this calculation, the left graph of Figure 7.5 shows the LUT for area coverage correction of the YNSN model. Since this correction is used to compensate for the error that occurs between two Neugebauer Primary colors, the CYNSN model requires a different LUT. Because each

Table 7.3: Performance of Predicted Ink Ramps (n=2)

Ink Ramp	Metric	Area Coverage						
		0.1255	0.2510	0.3765	0.5020	0.6235	0.7490	0.8745
Cyan	ΔE_{00}	0.3	0.5	0.5	0.6	0.6	0.4	0.4
	RMS	0.0027	0.0054	0.0072	0.0082	0.0093	0.0088	0.0068
Magenta	ΔE_{00}	0.7	0.8	0.9	1.0	0.9	0.8	0.3
	RMS	0.0051	0.0068	0.0074	0.0087	0.0082	0.0077	0.0031
Yellow	ΔE_{00}	0.2	0.2	0.2	0.3	0.2	0.2	0.3
	RMS	0.0026	0.0022	0.003	0.0049	0.0038	0.0038	0.0051
Black	ΔE_{00}	0.3	0.6	0.8	1.0	1.2	1.3	1.4
	RMS	0.0038	0.0063	0.008	0.0088	0.0091	0.0077	0.006
Reflex Blue	ΔE_{00}	0.4	0.6	0.7	0.7	0.5	0.4	0.6
	RMS	0.0037	0.005	0.0061	0.0066	0.0061	0.0055	0.0069
Orange	ΔE_{00}	0.2	0.3	0.4	0.4	0.2	0.2	0.1
	RMS	0.003	0.0044	0.0056	0.0055	0.0047	0.0033	0.0016
Violet	ΔE_{00}	0.4	0.5	0.5	0.4	0.4	0.4	0.6
	RMS	0.0036	0.0049	0.0055	0.0043	0.0043	0.0035	0.0058

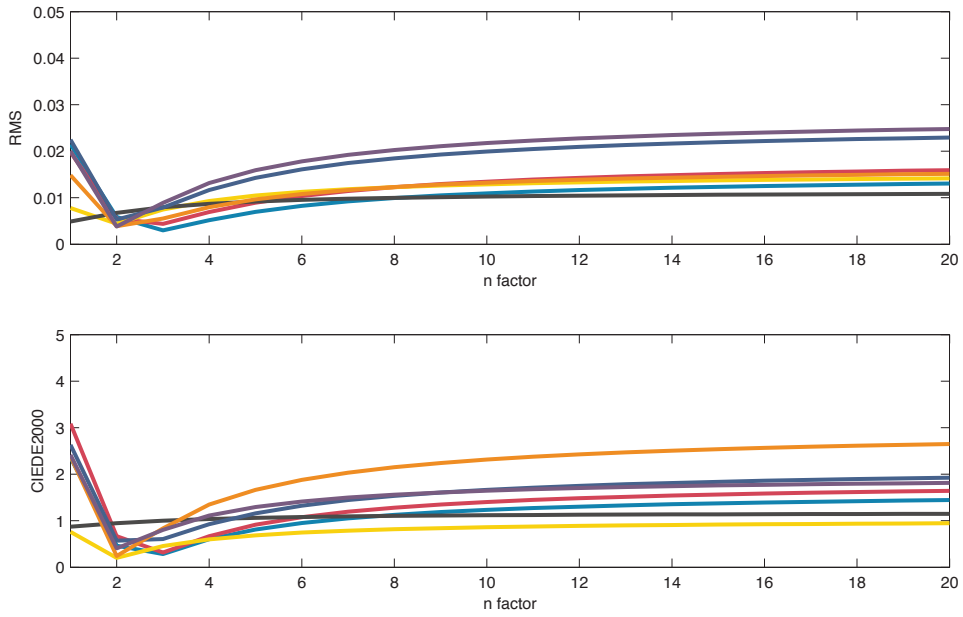

Figure 7.3: Evaluation of the Yule-Nielsen n-Factor

subcell is considered as a local YNSN model, it requires a separate LUT. The area correction for the CYNSN model with 2 subcells is shown in Figure 7.5 in the graph on the right side.

7.3.3 Performance of Spectral Modeling

The performance of the spectral modeling was evaluated with a set of 2400 random patches printed at the same time as the calibration patches used for the YNSN and CYNSN model. Theoretical area coverages of the random patches were converted to effective area coverages using cubic spline interpolation. These effective area coverages are the input data for the forward models. Accuracy and speed for the YNSN and CYNSN model with two subcells was compared. In Table 7.4 the colorimetric error is shown as

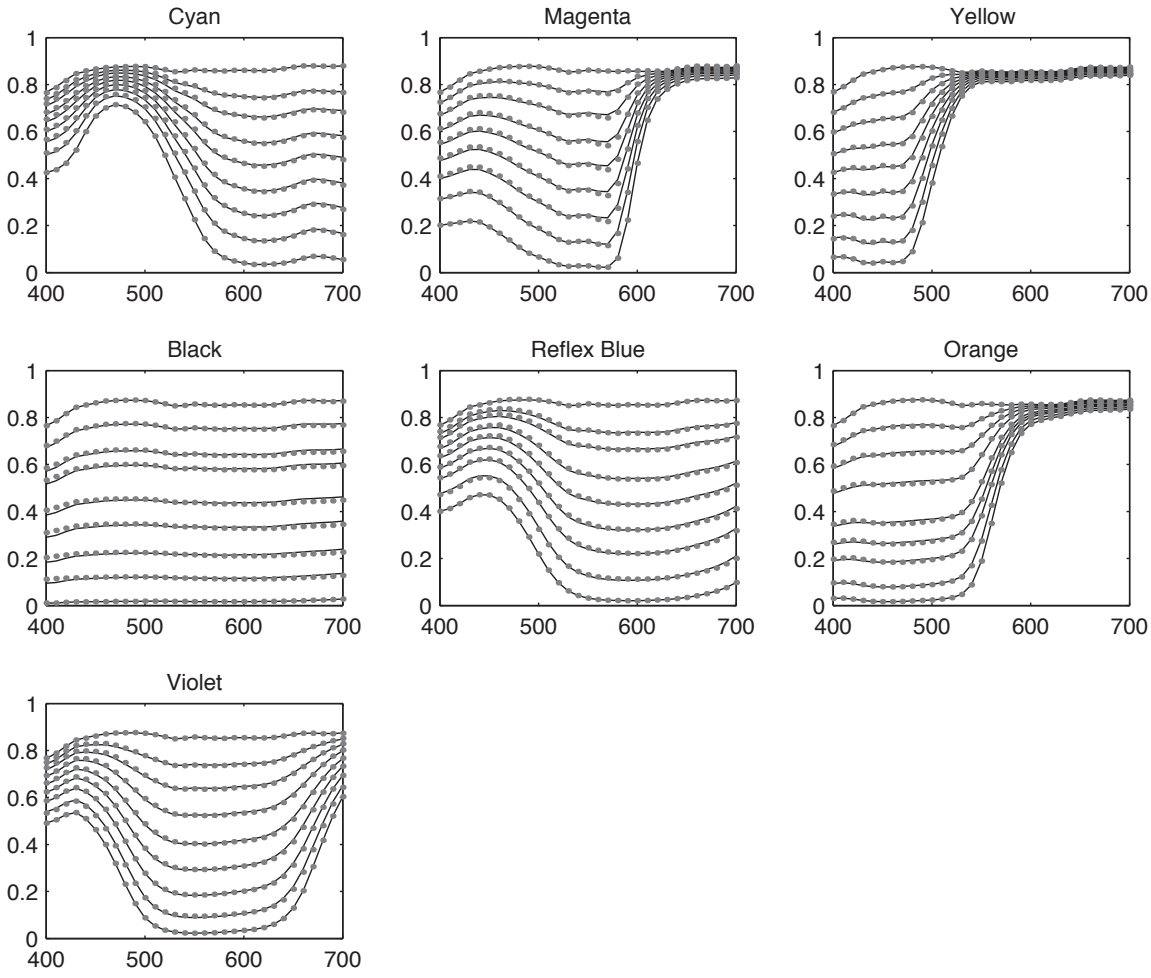

Figure 7.4: Prediction of Ink Ramps with a Yule-Nielsen Factor of n=2 (Gray Dots indicate the predicted reflectance of the Ink Ramp)

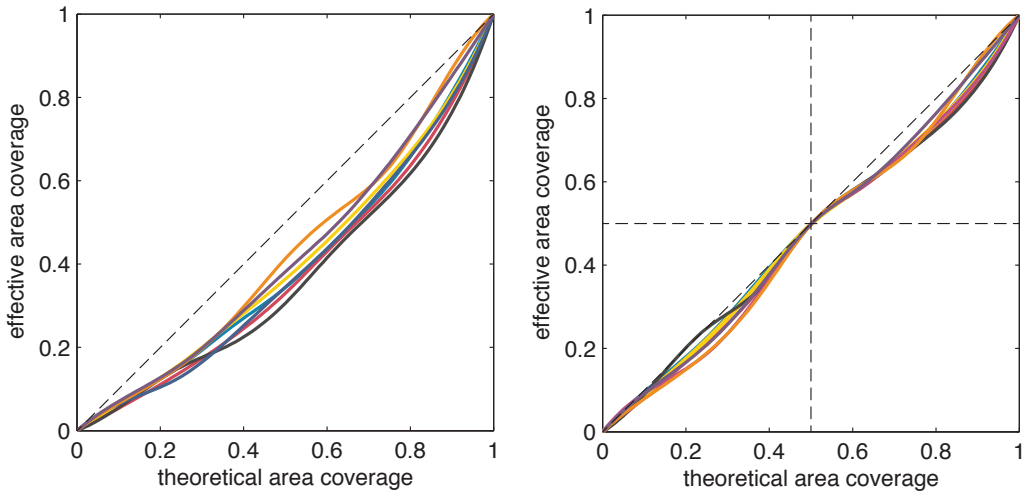

Figure 7.5: Left: Area Coverage Correction for YNSN, Right: Area Coverage Correction for CYNSN

ΔE_{00} difference. These numbers show that the CYNSN model improves the performance as expected. The mean color difference improves from 2.52 to 1.89 ΔE_{00}. Standard deviation and percentiles show similar improvements. A summary of the Root Mean Square (RMS) error is shown in Table 7.5. The RMS errors show the same improvement from the YNSN to the CYNSN model. The mean RMS error improves from 0.0140 to 0.0103. Since the CYNSN model requires the selection of the corresponding subcell, more computational effort is required than for the YNSN. The implementation in MATLAB showed that the YNSN model runs more than twice as fast as the CYNSN model with MATLAB functions showed in Appendix C. This performance could be improved by optimizing the code but the selection of the subcell requires some additional effort.

Due to its better accuracy, the CYNSN model was used for further evaluation. Histograms for ΔE_{00} and RMS are shown in Figure 7.6. A large portion of the 2400

Table 7.4: CIEDE2000 Performance of the YNSN Forward Model

	Mean	Std Dev	90 Percentile	95 Percentile
YNSN	2.52	1.93	4.98	6.42
CYNSN 3 Nodes	1.89	1.56	3.8	4.87

Table 7.5: RMS Performance of the YNSN Forward Model

	Mean	Std Dev	90 Percentile	95 Percentile
YNSN	0.0140	0.0095	0.0268	0.0314
CYNSN 3 Nodes	0.0103	0.0077	0.0207	0.0259

random patches show an accuracy of 3 ΔE_{00}, 0.02 RMS or less. The five spectral curves with the largest ΔE_{00} error are shown in Figure 7.7 (Note the range of the y-axis with a maximum of 10% reflectance). All the patches with the worst accuracy are very dark. This is expected since small spectral errors lead to large errors in dark patches. A factor that is not considered here is the repeatability of the instrument. The X-Rite Eye-One iSis likely is affected by noise when measuring dark patches. (The set of 2400 random patches was averaged from four printed targets.) Therefore, these dark measurements can be affected by measurement errors.

In Figure 7.8 the errors of the 500 patches with the worst ΔE_{00} error are shown as L*C* plot. The arrows point from the measured to the prediction patch. In the bottom left corner there is a cluster of dark patches with large colorimetric errors. For a majority of the patches, the prediction tends to be more chromatic and slightly darker.

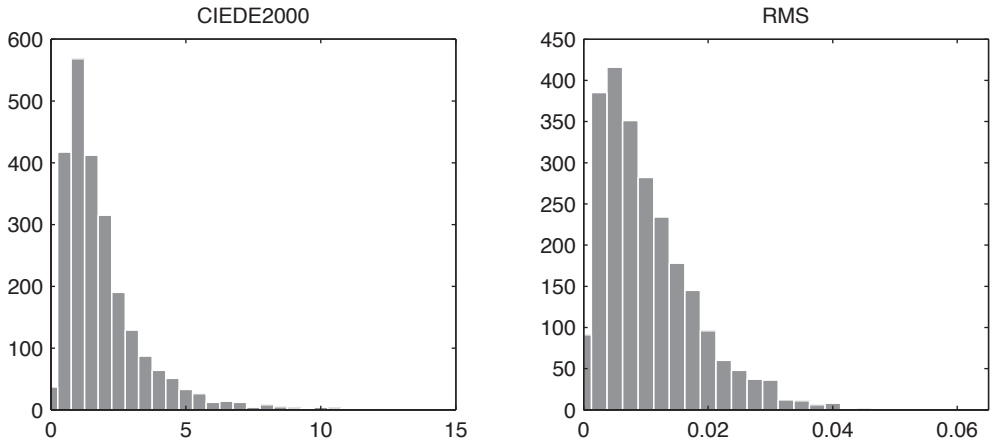

Figure 7.6: Histogram of CIEDE2000 and RMS error of the CYNSN Forward model

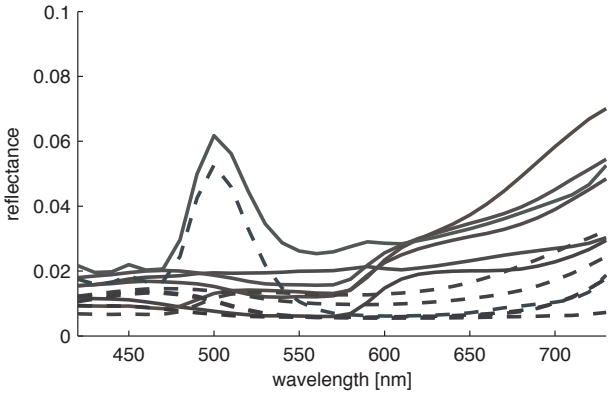

Figure 7.7: Five CYNSN predictions with the largest CIEDE2000 error of the random patches

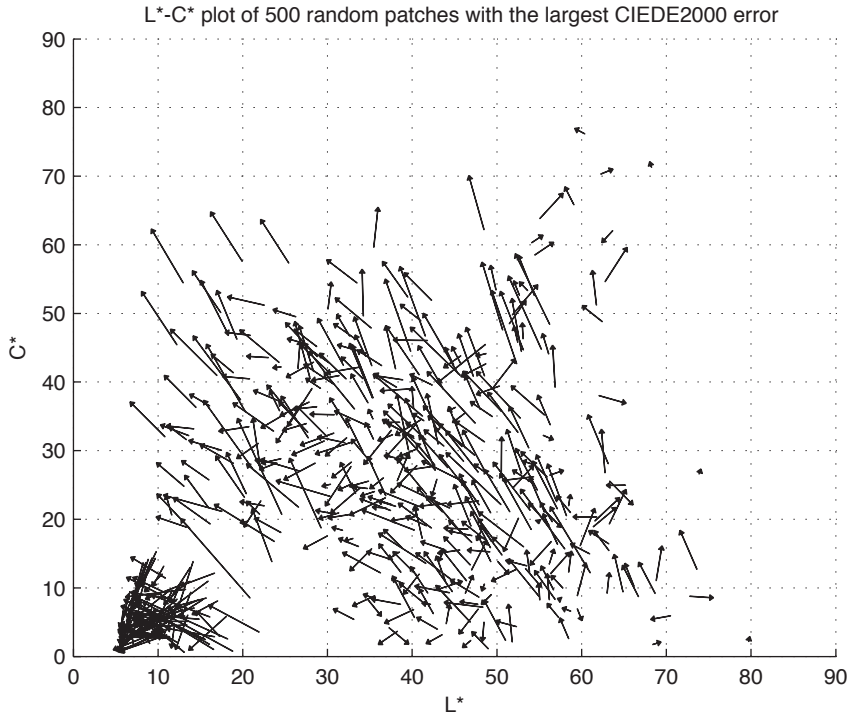

Figure 7.8: L*C* plot of 500 random patches largest CIEDE2000 error

7.4 Summary

The Spectral Neugebauer model was used to model the HP Indigo printing system. Its accuracy was improved by the Yule-Nielsen correction and the cellular extension. The effective area correction also improved the accuracy of the model. Using two subcells in the CYNSN model delivered a good performance while keeping the number of Cellular Neugebauer primaries at a reasonable level. Due to the subcell selection, the cellular model requires more computational effort to predict the spectral reflectance. The CYNSN model with effective area correction and two subcells proved to be a good choice to accurately model the HP Indigo printing system.

Chapter 8

Computational Evaluation

The focus of this chapter is the evaluation of the seven-color printing system using the selected ink set. First, gray metamers printed during the second press run are used to evaluate the accuracy of the prediction of these sensitive patches. Then, a custom paint target is used to evaluate the performance of paint mixtures sampling the paint gamut. For visual evaluation, spectral color separation is performed on synthetic spectral images.

8.1 Metamers

Metamers can be used to evaluate an ink set to see how different kinds of mixtures can create the same appearance under one illuminant and one observer condition. All the three-ink combinations were evaluated to build gray metamers. These gray metamers were included in the second press run. Therefore, only the data from the first press run were available to perform the predictions. These predictions were then printed in the second press run. To predict the grays, the YNSN model (missing Neugebauer primary colors

were predicted) was used to estimate the area coverages. These estimated grays were optimized to be metameric to a spectral curve of the black ink ramp with a lightness of $L^* = 70$. Since the full set of Neugebauer primary colors was not known at this point, test targets were created to evaluate different mixtures surrounding the predicted gray. (It was assumed that the prediction was not very accurate due to the incomplete set of measured Neugebauer primary colors.) Such a target is shown in Figure B.4 in the appendix. Since the prediction of the area coverages were not accurate, the measured reflectances of every patch was compared to the black ink ramp. Because grays are very sensitive to small variations in concentration, optimizing the concentration of the black ramp helped to find the best metamers. Hence, a lightness of $L^* = 70$ could not be achieved for some samples. Figure 8.1 shows spectral curves of the metamers. To visualize the metamers, the background of every plot shows the black ink reflectance rendered for sRGB. The top left corner of the plots are rendered to show the three-ink reflectances rendered for D50. The same curves rendered for Illiminant A (for chromatic adaptation the CIECAT02 transformation matrix was used) are visualized in the top right corner of the plots.

Whereas common four color CMYK printing can only create one metamer, the use of the present set of seven inks allows the creation of many different metamers. Reflex Blue and Violet ink especially contribute to the metamers because of their behavior at longer wavelengths.

These metamers are also suitable to evaluate the accuracy of the CYNSN forward model. These gray samples are very sensitive to small amounts of errors. Therefore, these

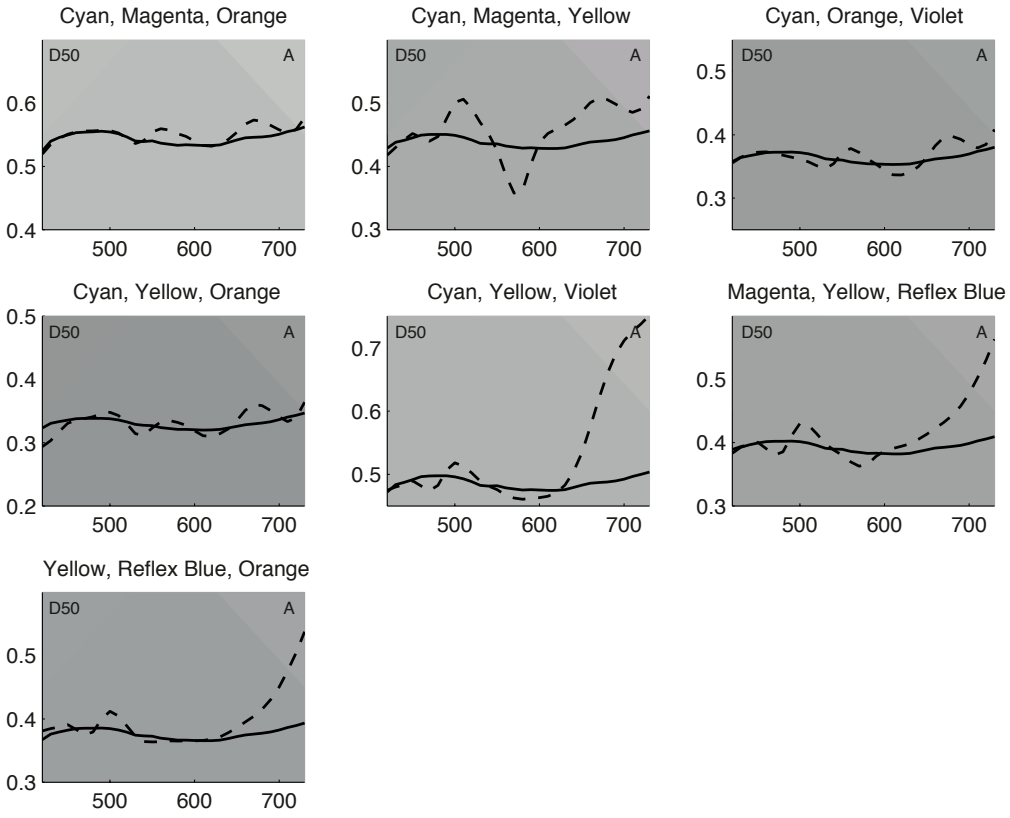

Figure 8.1: Gray Metamers built with sets of three-ink combinations. Solid lines show grays built with black ink and dashed lines show grays mixed with combinations of three chromatic inks.

samples are the most difficult to predict accurately. The area coverages from the gray patches selected before were used again. The area coverages from these patches were used as input data into the CYNSN forward model. Figure 8.2 illustrates the error of the prediction. The solid spectral curves are the measured reflectances whereas the dashed lines are the predicted reflectances. Color differences are shown in the background of every plot. The left half of the background shows the measured gray patch and the right half shows the predicted color. The two largest errors were predicted for the gray sample using Cyan, Yellow and Orange ink (CIEDE2000 of 4.5) and Magenta, Yellow and Reflex Blue (CIEDE2000 of 3.8). The fact that some gray mixtures perform better than others can be explained by going back to Figure 7.1. The gray metamers with the poorest performance all contain two inks sharing one screen angle. Either the pair Cyan-Orange, or Magenta-Reflex Blue. This demonstrates that sharing screen angles is causing problems for the spectral modeling of the system. The gray mixtures used here to evaluate the system likely represent the most difficult colors where accuracy matters the most.

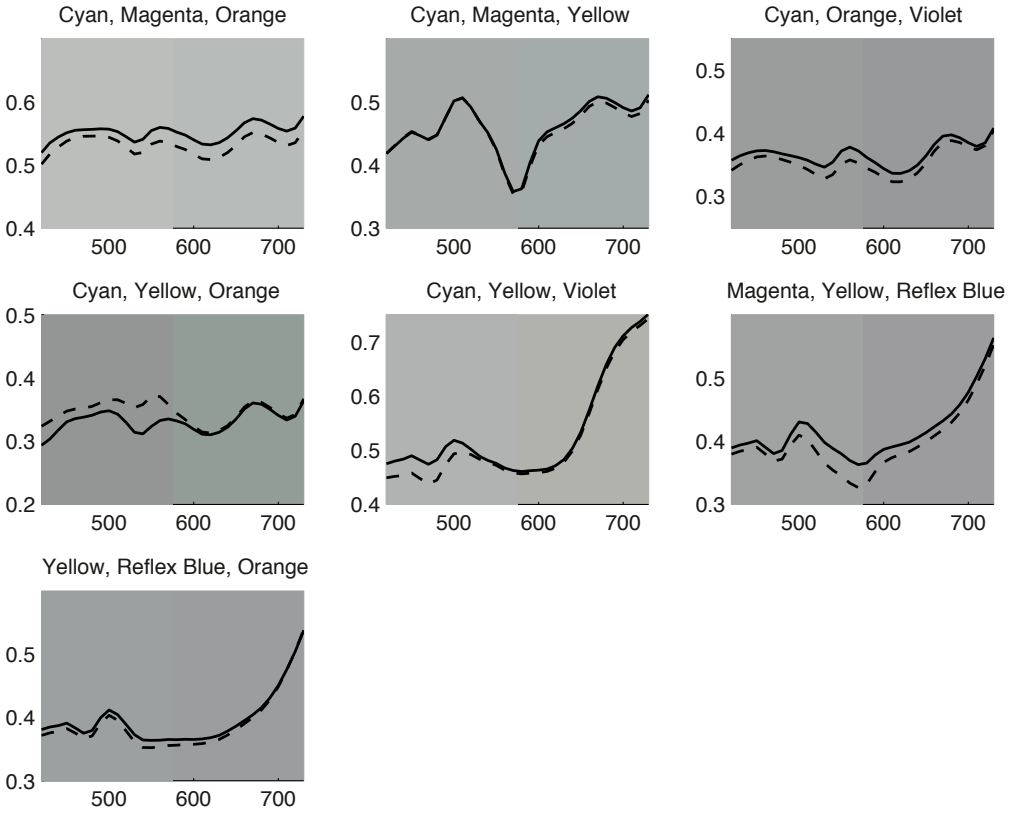

Figure 8.2: Accuracy of the CYNSN model for gray samples. Solid lines are measured grays and dashed lines show grays predicted with the CYNSN model. The left half of the background of every plot represents the measured and the right half the predicted gray for visual comparison.

8.2 Paint Target

In order to evaluate the performance of the spectral separation using samples that best represent the paint gamut, a custom test target was created. The target shown in Figure 8.4 was built from spectral reflectances derived from physical paint mixtures (see Figure 8.3) only using the paints of the selected paint palette. This ensures that the spectral reflectances used for evaluation well represent reflectances naturally occurring in artwork created with the selected paint palette. The background of each plot in Figure 8.4 is rendered to represent the color difference between the painted patch and the estimated spectral reflectance of the print. The left half shows the color of the print and the right half the measured color under D50. As the solid lines (paint patches) and the dashed lines (print patches) confirm, the spectral match of most patches is accurate. Errors in the reddish patches are likely caused by the optimization. The optimization is a combination of spectral and colorimetric matching. The colorimetric error for spectral miss-matches of reddish colors as shown in Figure 8.4 are fairly small. Therefore, the optimization introduces a fairly large spectral error in order to get a better colorimetric match. A more sophisticated separation algorithm might improve these spectral matches. The mean color difference of all 40 patches is 1.1 ΔE_{00} with a median of 0.4 ΔE_{00}. In terms of spectral error, a mean RMS of 0.0245 and a median of 0.0218 RMS was measured. Over all, a good spectral and colorimetric match can be achieved for in-gamut paint mixtures.

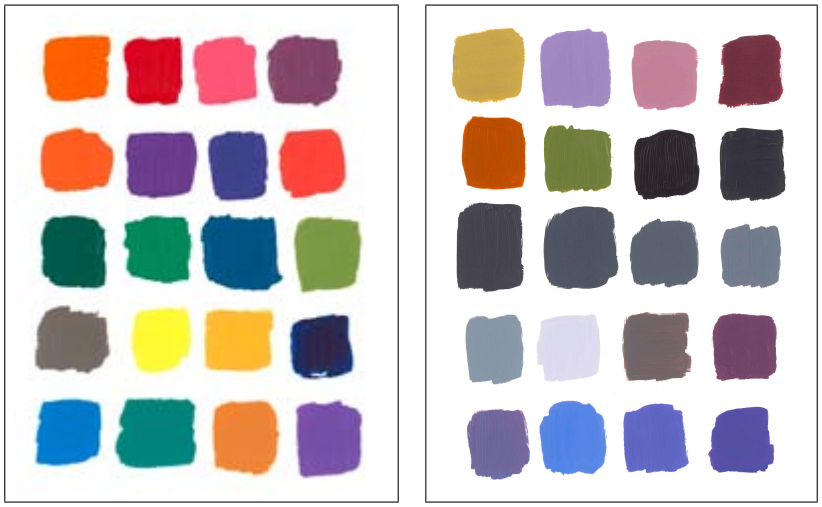

Figure 8.3: Paint Target

8.3 Images

8.3.1 Spectral Separation of Images

So far the evaluation focused on the performance of the spectral modeling of the printing system. Applying these computations to images is an important step to take full advantage of the capabilities of spectral color reproduction. However, the separation of spectral images is a much more complex process than computing color patches. With images, the interaction of pixels placed next to each another and the size of the images adds a lot of complexity to the separation. As stated before, the inversion of the CYNSN model using non-linear optimization in MATLAB is slow. The MATLAB function *fmincon()* allows good control for constrained, nonlinear multivariable optimizations. Unfortunately, selecting the subcell in the objective function is time consuming – especially due to the

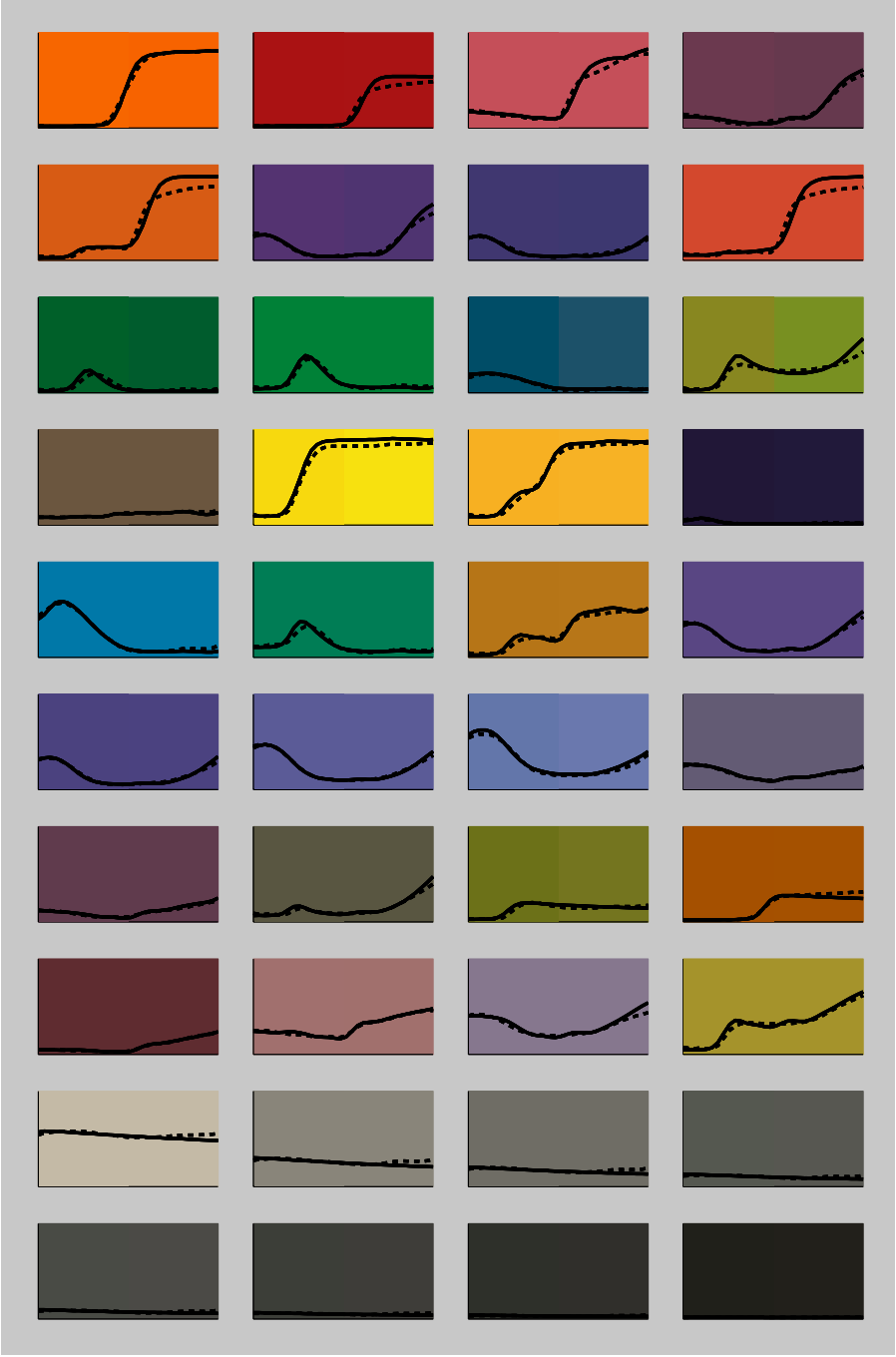

Figure 8.4: Target of paint patches created with the selected paint palette. Solid lines represent the spectral reflectance of the paint patches and the dashed line the spectral match created by inverting the CYNSN model. The left half of the background of each plot represents the predicted and the right half the measured color viewed under D50.

fact that it needs to be repeated for every iteration. Speed is not so important to compute a small number of samples, but once the optimization is applied to images, speed matters. Images used in a print production workflow should have a resolution of 300 dots per inch or more for high quality printing. Therefore, a letter-sized page covered with an image would require the computation of about 8.5 million pixels. Computing these kinds of images would take several days or weeks using MATLAB on desktop computer. Thus, MATLAB could not be used to perform the spectral separation of images. Prior research by Taplin [Taplin, 2001] dealt with the same problem. His research showed that using a programming language closer to the hardware (he implemented the CYNSN-inversion in C) could execute the task much faster. The researcher is aware of the fact that more sophisticated algorithms were developed subsequent to Taplin. But since computational performance is not the main scope of this project, the brute-force inversion of the Neugebauer model was chosen. To do so, the existing implementation written by Taplin was used (a selection of other approaches is listed in the bibliography:
[Urban and Grigat, 2008], [Tzeng, 1999] [Urban et al., 2008], [Derhak, 2006],
[Guo et al., 2010]). The provided C code from Taplin [Taplin, 2001] was extended from a six- to a seven-ink system. To achieve a spectral match while maintaining colorimetric accuracy, the code runs two stages of optimization. First, the RMS error is minimized. The second optimization minimizes the colorimetric error while an adjustment range of +/- 5% within the first optimization ensures spectral accuracy. For efficient use of today's multi-core processor architectures, the code was enhanced to allow parallel processing in

multiple threads. The modified code allows the spectral separation of up to 420 pixels/sec. on a 3.2 GHz Dual Quad-Core Intel Xenon MacPro. A spectral image of about 5 Mega-Pixels can be separated into a seven channel image in less than 3.5 hours. For the purpose of this research this can be considered as a useful performance.

8.3.2 Spectral Images

Capturing spectral images is an area of ongoing research for many years. Imaging artwork to get spectral reflectance for every pixel is a very complex process. At first, spectral images from a system performing spectral reconstruction based on a multi-channel camera [Zhao and Berns, 2007] were used. This system delivers highly accurate colorimetric images and a spectral reconstruction of the original reflectance. The reconstruction of the spectral reflectance shows good results for a large portion of the pixels. Nevertheless, there are also pixels where the spectral reconstruction introduces error into the spectra. These pixels do not show up in the initial image, but they cause problems when the non-linear optimization is trying to match these particular reflectances. This caused the optimization to fail and predict area coverages with large errors. These bad pixels showed up in the final image as noise. Therefore, these spectral images were not used to evaluate the performance of the spectral separation.

A solution was found by using spectral reconstruction based on the selected paint palette. These synthetic spectral images are a realistic representation of high quality images with smooth spectral reflectances. As input data, the ramps of the paint palette and

a colorimetric image were used. Software developed by Abed performed an estimation of spectral reflectance from colorimetry [Abed, 2012]. These synthetic images have low noise, are constrained to the paint gamut and are therefore well-suitable to test the spectral separation. These images are shown in Figures 8.5 and 8.6. The images are referred to as Tree, Flower, Salai and LasVegas as indicated in the caption of the images. When using too many inks, the synthetic spectral images tend to get noisy. Therefore, each image was restricted to a palette with five paints. These palettes are shown in Table 8.1.

Figure 8.5: Spectral Images used for evaluation. Left: Tree, Right: Flower

8.3.3 Image Analysis

8.3.3.1 Tree Image

The spectral reflectance of Tree was estimated using the paint palette shown in Table 8.1. Figure 8.7 compares the spectral reflectance of the original and the estimated reflectance of the print rendered for Illuminant D50 and Illuminant A. Under Illuminant D50 (top

Figure 8.6: Spectral Images used for evaluation: Left: Salai, Right: LasVegas

Table 8.1: Paint Palettes of Images

Tree	**Flower**
Cadmium Red Medium	Cadmium Red Medium
Cadmium Orange	Cadmium Orange
Cadmium Yellow Light	Cadmium Yellow Light
Dioxazine Purple	Dioxazine Purple
Phthalo Blue Green Shade	Ultramarine Blue
Salai	**LasVegas**
Cadmium Red Medium	Cadmium Red Medium
Cadmium Yellow Light	Cadmium Orange
Dioxazine Purple	Cadmium Yellow Light
Phthalo Blue Green Shade	Phthalo Blue Green Shade
Ultramarine Blue	Quinacridone Crimson

row) the images show a good color match. This is expected since the spectral separation optimizes for RMS and colorimetric error under D50. The fact that between the left image of row one and two a color shift is apparent, indicates that the image is not color constant. Interesting is the match of the two images under Illuminant A. It shows that the original and the print of this color inconstant image still match. This is mostly visible in the purple sky and the earthy-yellow ground. The Color Checkers in row three (Illuminant D50) and four (Illuminant A) were included in the image and show the same result. Especially the bottom row of gray patches shows that print and original behave very similar under changing viewing conditions. The gray patches turn reddish under Illuminant A for the original as well as for the print.

8.3.3.2 Flower Image

The Flower image was rendered the same way as the Tree image but with a different paint palette shown in Table 8.1. Since this image uses Ultramarine Blue and Dioxazine Purple that both reflect light in the long wavelength end of the visible spectrum, colors including these paints are likely sensitive to color inconstancy. As the comparison in Figure 8.8 shows, the blue-purple colors shift towards red between D50 and Illuminant A. Most importantly, the color shift between the original and the predicted image are constant. The estimated printed reflectance under Illuminant A also shifts purple-blues towards a more reddish color as the original does under this illuminant. The reproduction is therefore not significantly affected by metamerism when comparing to the original.

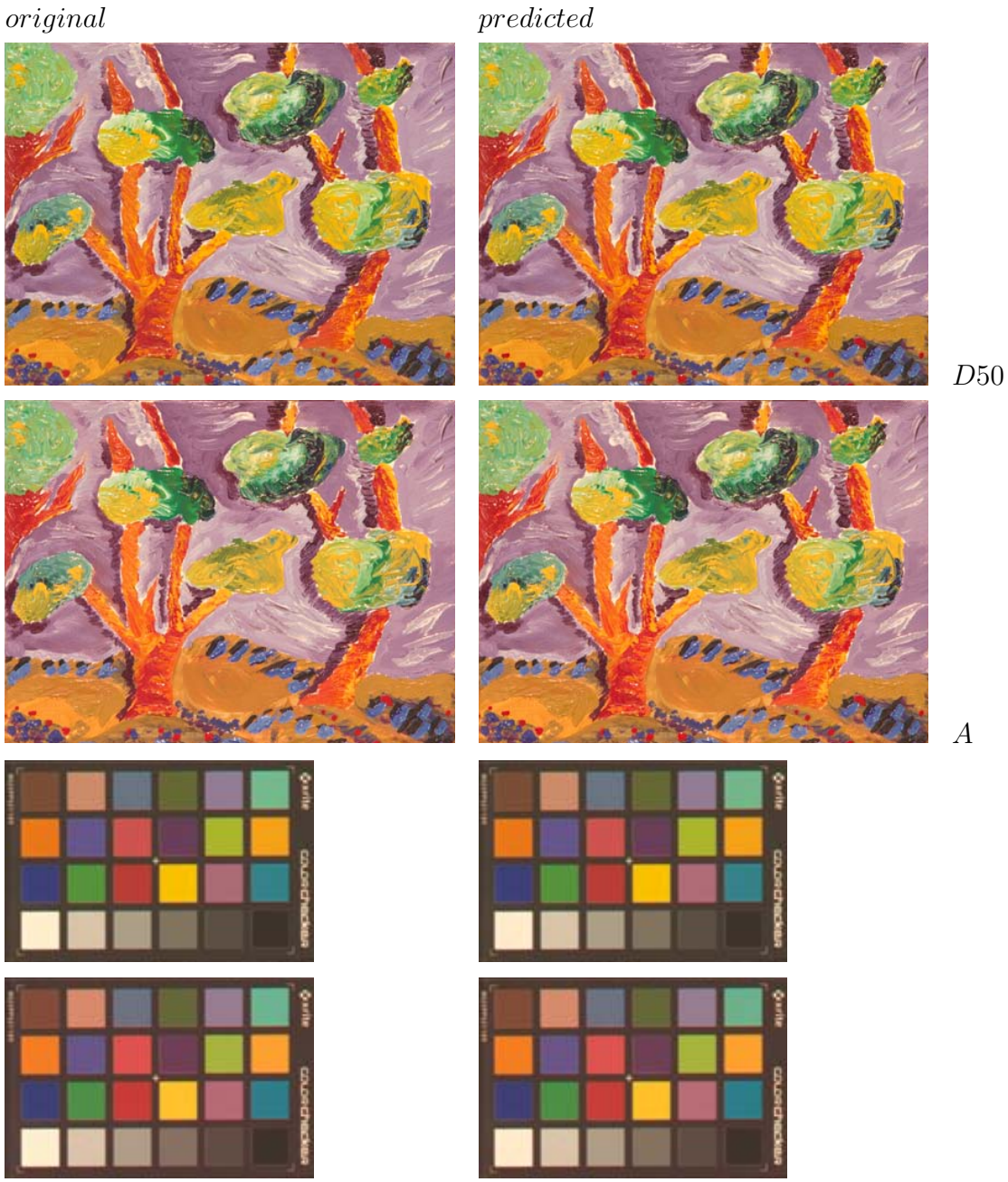

Figure 8.7: Rendering of the Tree image for different lighting conditions. The upper row compares the original spectral image on the left with the predicted printed image on the right under Illuminant D50. The second row compares the original spectral image on the left with the predicted printed image on the right under Illuminant A. The color checkers were included in the image. Row three corresponds to row one and row four to row two. (CIECAT02 chromatic adaptation was used for the images shown under Illuminant A.)

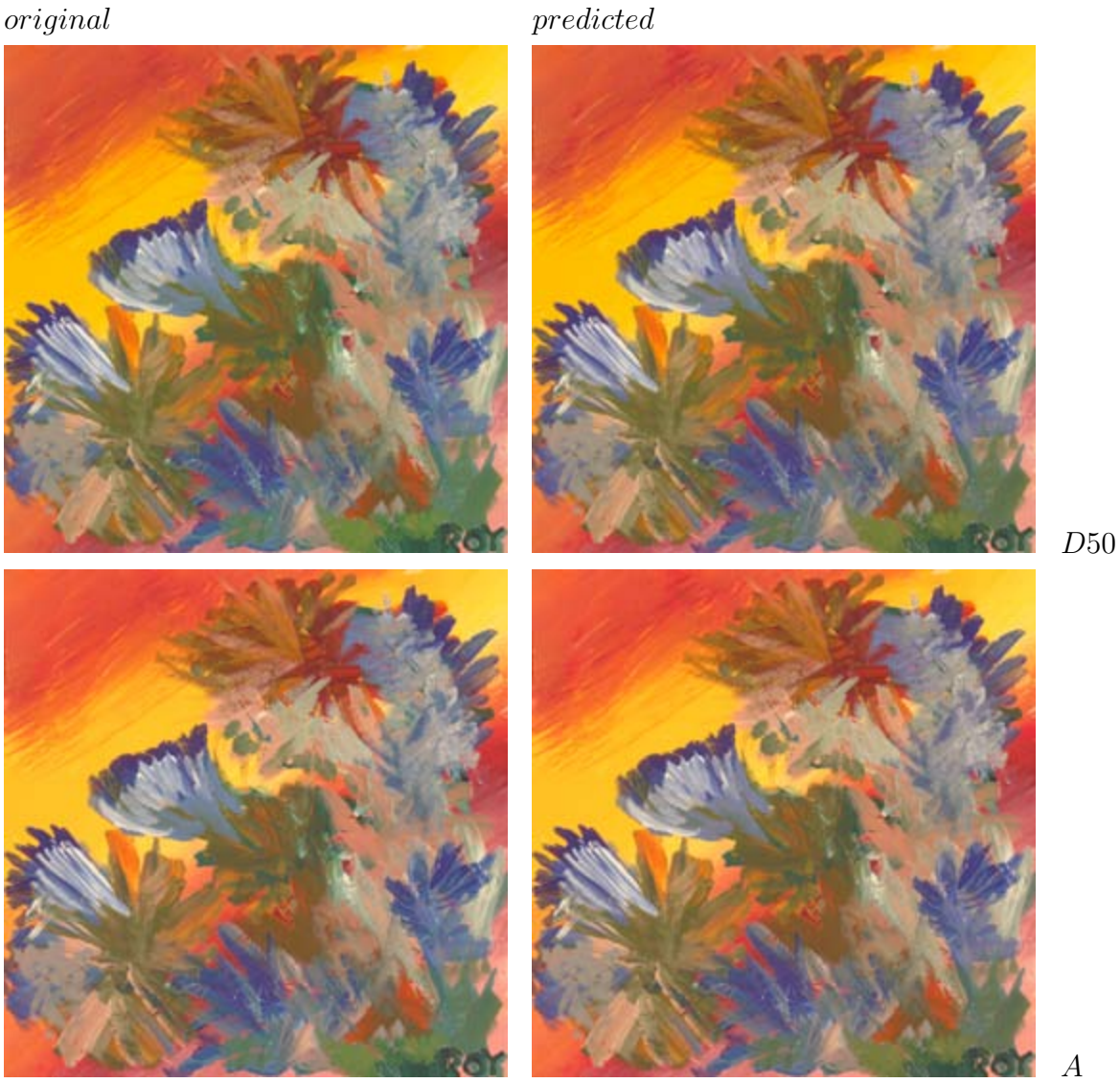

Figure 8.8: Rendering of the Flower image for different lighting conditions. The upper row compares the original spectral image on the left with the predicted printed image on the right under Illuminant D50. The second row compares the original spectral image on the left with the predicted printed image on the right under Illuminant A.(CIECAT02 chromatic adaptation was used for the images shown under Illuminant A.)

8.3.3.3 Salai Image

The Salai image uses two blue paints in its palette: Ultramarine Blue and Phthalo Blue Green Shade (these pigments were also used in the actual painting). Phthalo Blue Green Shade was added to mix better greens and Ultramarine Blue because it is known to be color inconstant. When comparing the rendered images of Figure 8.9, the most apparent color shift occurs in the blue mountains and the sky in the background. The reddish color shift between D50 and Illuminant A indicated that these blues were likely created with Ultramarine Blue and Dioxazine Purple. Another apparent color shift can be seen in the green trees. They are also color inconstant in changing viewing conditions but original and reproduction change in the same way. The color inconstant original on the left compared to the predicted reproduction on the right indicates the power of spectral color reproduction. Print and original colors shift in the same way and are therefore not significantly metameric. A closer look at the reproduction shows artifacts in the blue and the red regions of the dress. These artifacts are caused by the non-linear optimization in the spectral separation. They could either be caused by out of gamut colors or bad converging of the optimization. This problem was not further investigated.

8.3.3.4 LasVegas Image

The LasVegas image is a digital photograph with a synthetic texture (Water Color Filter of Photoshop CS5). As the paint palette shown in Table 8.1 indicates, this image is likely to be color constant for the most part. It does not include Ultramarine Blue or Dioxazine

Figure 8.9: Rendering of the Salai image for different lighting conditions. The upper row compares the original spectral image on the left with the predicted printed image on the right under Illuminant D50. The second row compares the original spectral image on the left with the predicted printed image on the right under Illuminant A. (CIECAT02 chromatic adaptation was used for the images shown under Illuminant A.)

Purple. None of the pigments shows a tail at longer wavelength or any other exceptional characteristics. Due to the paint selection, this image has a large gamut except in the purple sector which does not play an important role in this image. Figure 8.10 compares the rendered image under Illuminant D50 and Illuminant A. Most image areas are color constant. An area where a color shift occurs is the street that tends to be more reddish under Illuminant A. This color shift is maintained in the reproduction shown in the bottom right image. This image shows that depending on the paint palette and the image, spectral color reproduction does not yield a big advantage over colorimetric color reproduction as long as a large gamut can be reproduced. When balancing between colorimetric and spectral color reproduction, this image with its particular paint palette would not gain enough to justify going the extra mile of spectral color reproduction. A wide gamut printing process using colorimetric color management would likely yield a result which would be as good as the spectral workflow for most applications. Observer and illuminant metamerism does not affect every original in the same way.

8.4 Comparing the Seven Ink Printing System to CMY Printing

For comparing the seven ink printing system to printing with conventional Cyan, Magenta and Yellow (CMY), the custom paint target was used. The separation of the CMY system was performed similarly to the seven ink system. In contrast to the two stage spectral separation, the CMY separation optimizes for the smallest colorimetric error only (D50 /

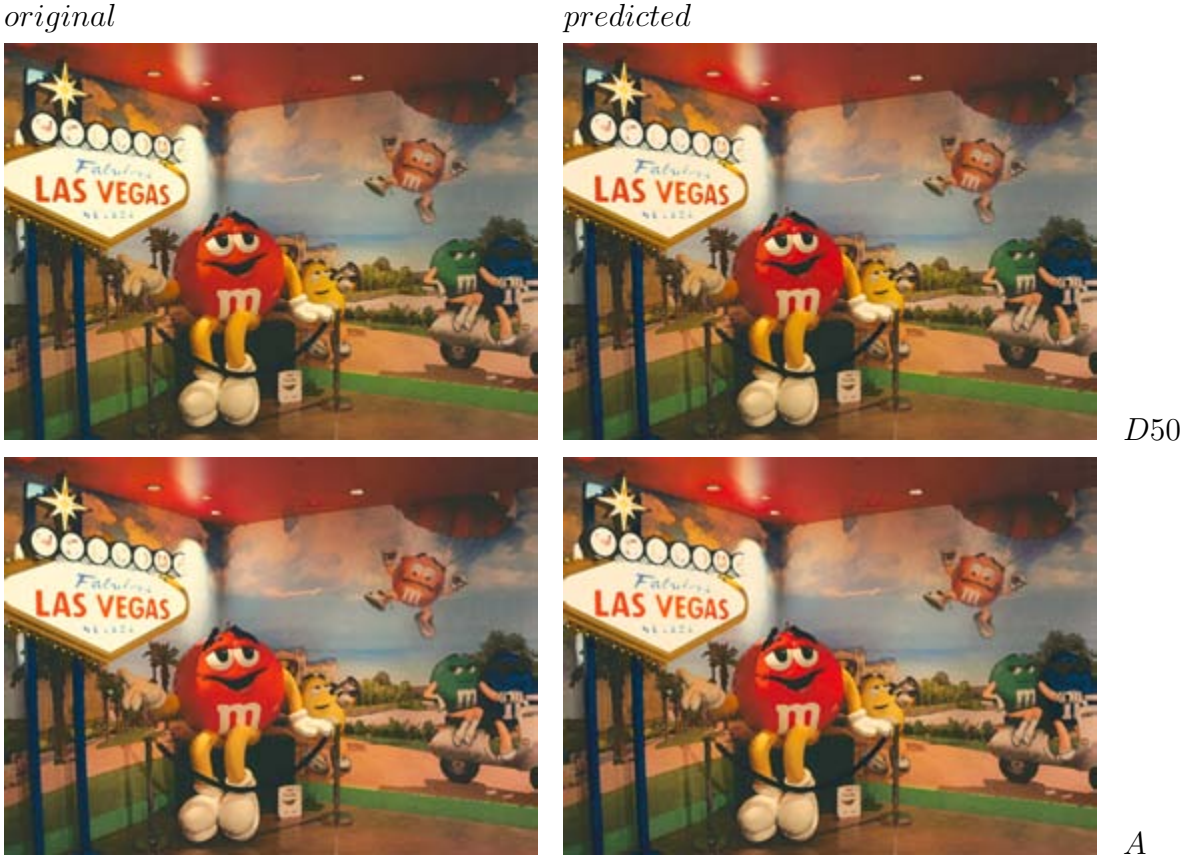

Figure 8.10: Rendering of the LasVegas image for different lighting conditions. The upper row compares the original spectral image on the left with the predicted printed image on the right under Illuminant D50. The second row compares the original spectral image on the left with the predicted printed image on the right under Illuminant A. (CIECAT02 chromatic adaptation was used for the images shown under Illuminant A.)

2°). This imitates the color separation implemented in ICC profiles. The black ink used in conventional printing was ignored because it would be difficult to implement Gray Component Replacement (GCR) and Under Color Removal (UCR) into the current system to simulate an ICC workflow. The main purpose of the CMY separation is to compare the metameric potential between the seven and three ink system. Comparing the separation of gray patches to current ICC color separation in general is difficult since there are many different implementations to handle low chromatic or neutral colors (GCR, UCR, Ink Saving Algorithms). Therefore, the gray patches from the custom paint target shown in Figure 8.11 will likely be less metameric for many ICC color separations.

The solid lines show the spectral reflectance of the measured paint and the dashed line the best colorimetric match (D50 / 2°) for CMY. The backgrounds of the plots are split into three segments. Each segment represent an sRGB rendition of a spectral curve viewed under Illuminant A (Figure 8.11) and Illuminant D50 (Figure 8.12). It is expected that the largest metameric errors in the CMY system occur in paint patches mixed with Cadmium Orange, Ultramarine Blue or Dioxazine Purple. The effect of not using orange ink becomes apparent in patches #1, #15 and #28. The lack of inks with long-wavelength tails in CMY are obvious in patches #6, #20, #21, #22 and #23. The matches under Illuminant A are in general darker because the spectral power distribution of Illuminant A and the spectral curves of paints reflect less light in total if the tail at longer wavelengths cannot be reproduced. There is one patch which needs particular attention. For patch #12, the CMY match is better than the seven ink match. This is caused because the spectral

separation is trying to match the tail at longer wavelengths sacrificing the colorimetric match. Therefore, patch #12 is a good example of a curve shape where the spectral separation algorithm introduces an error which does not occur in the simpler CMY separation. This error is a problem of the separation algorithm and not of the ink set.

A computational evaluation showed that the average metameric index (D50 to Illuminant A, CIEDE2000) reduced from 1.2 using CMY to 0.7 using seven inks. The largest difference in metameric index was a drop from 6.4 to 1.9. These calculations do not include the eight gray samples in the last and second to the last row of the target. A detailed overview of the performance of all chromatic patches is shown in Table 8.2.

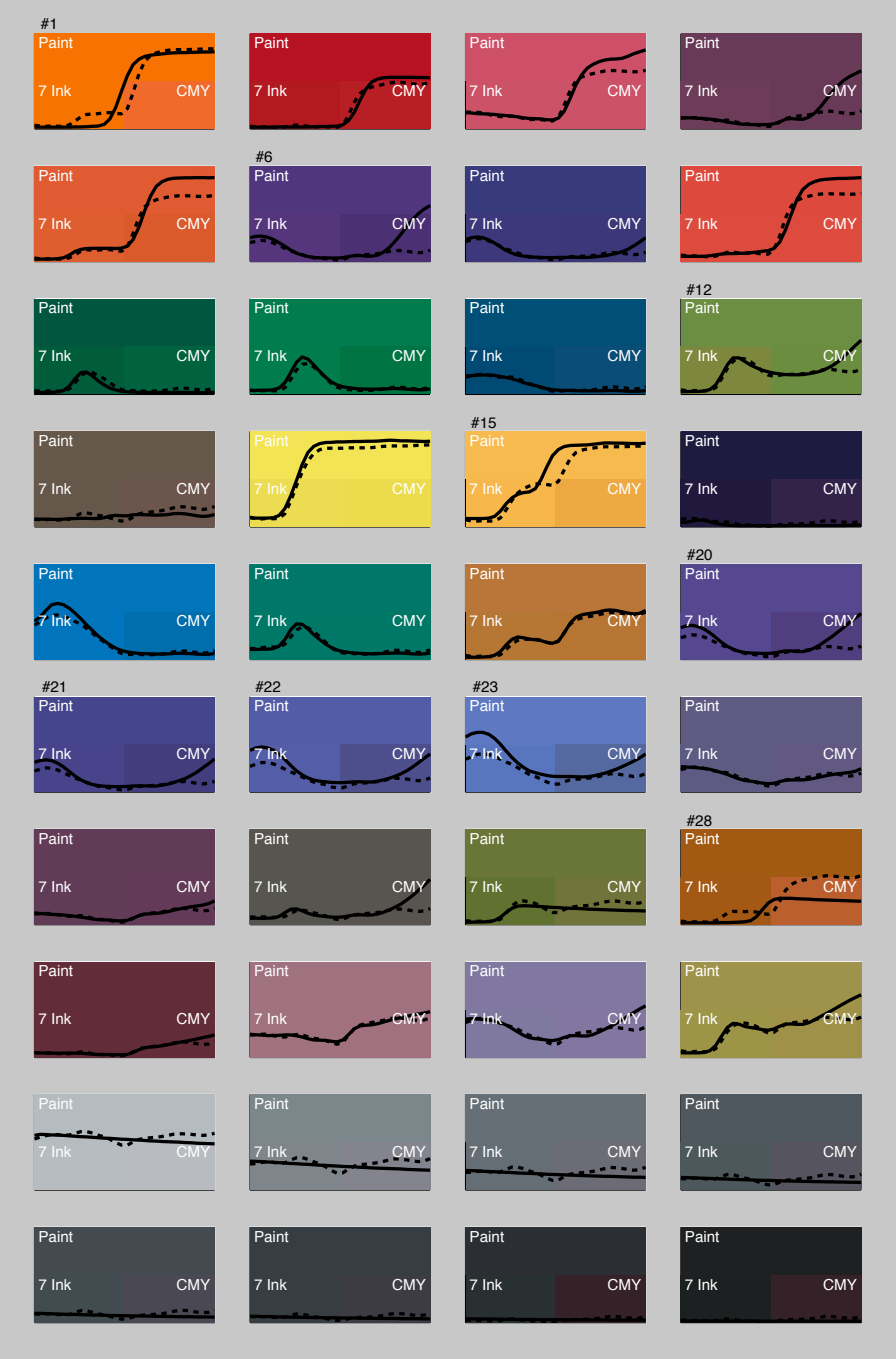

Figure 8.11: This Paint target compares the seven ink printing system to conventional Cyan, Magenta Yellow (CMY) printing. The solid line shows the reflectance of the measured paint sample and the dashed line shows the best colorimetric match under Illuminant D50. The background color segments of each plot represent the rendered appearance for Illuminant A. (CIECAT02 chromatic adaptation was used to render the appearance of the colors under Illuminant A.)

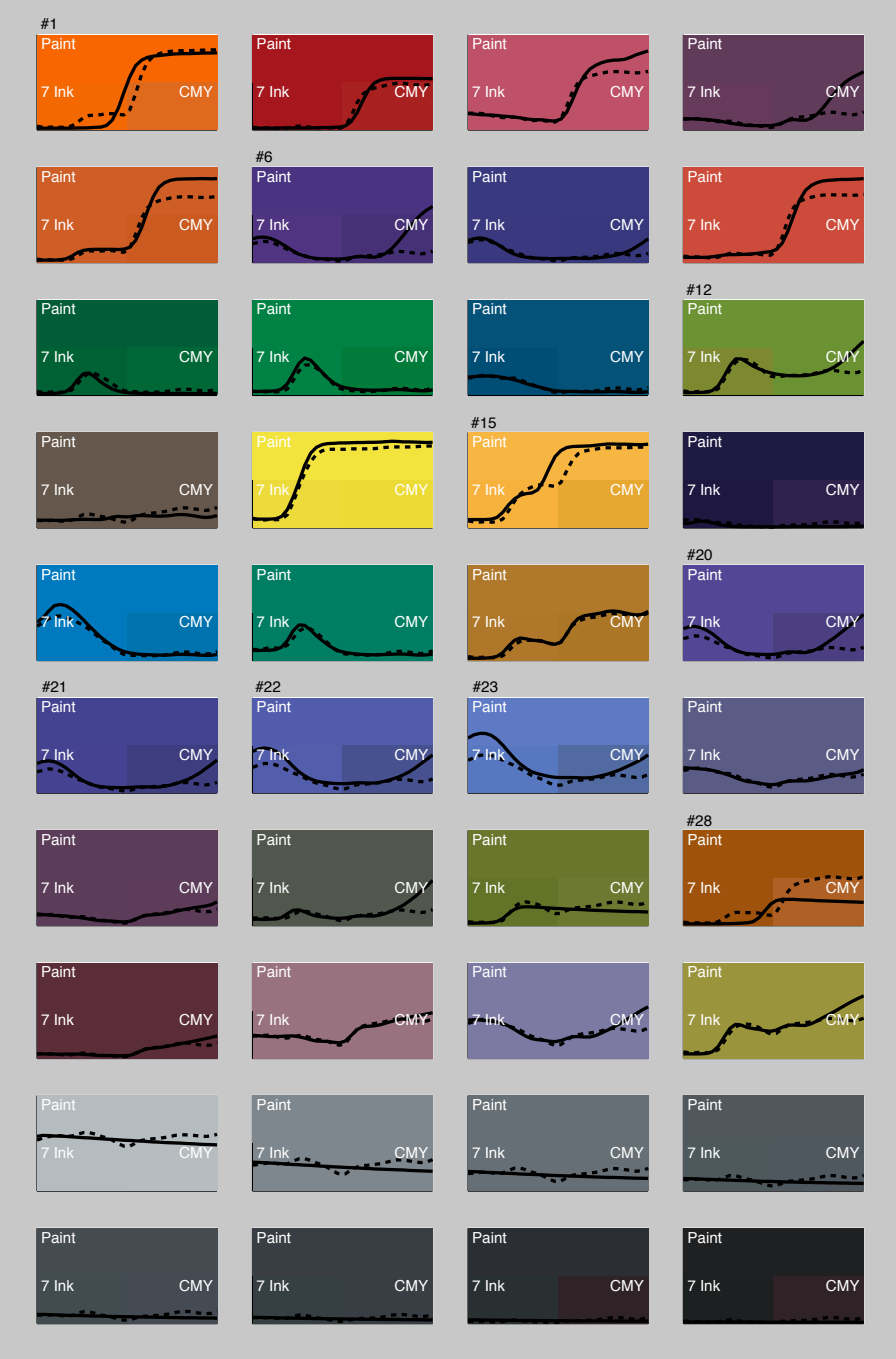

Figure 8.12: This Paint target compares the seven ink printing system to conventional Cyan, Magenta Yellow (CMY) printing. The solid line shows the reflectance of the measured paint sample and the dashed line shows the best colorimetric match under Illuminant D50. The background color segments of each plot represent the rendered appearance for Illuminant D50.

Table 8.2: Table comparing the performance of the seven ink and the CMY ink system.

		7-Ink			CMY		
Color	#	CIEDE2000	MI D50 to A	RMS	CIEDE2000	MI D50 to A	RMS
	1	1.9	0.2	0.0211	5.2	2.2	0.1101
	2	0.4	1.2	0.0522	1.4	1.5	0.0442
	3	0.3	1.5	0.0419	0.2	0.7	0.0891
	4	1.8	0.4	0.0232	0.1	5.1	0.1539
	5	0.6	0.1	0.0798	1.4	0.3	0.1119
	6	1.4	0.6	0.0306	2.0	0.9	0.1614
	7	0.3	0.7	0.0119	0.7	0.5	0.0424
	8	0.2	0.4	0.0785	0.2	0.4	0.0936
	9	3.4	0.7	0.0245	5.8	2.5	0.0315
	10	0.2	0.6	0.0207	3.2	5.8	0.0292
	11	2.0	0.9	0.0111	0.4	0.2	0.0189
	12	6.4	0.1	0.0512	0.3	0.2	0.0886
	13	0.2	0.6	0.0098	2.1	0.9	0.0467
	14	2.0	0.5	0.0539	2.0	0.5	0.0556
	15	0.8	1.1	0.0316	4.8	0.7	0.1073
	16	1.0	0.2	0.0069	3.6	0.4	0.0269
	17	0.2	2.0	0.0202	3.6	0.6	0.0512
	18	0.4	0.6	0.0268	0.3	0.5	0.0264
	19	0.7	0.8	0.0308	0.9	4.6	0.0221
	20	0.1	0.7	0.0186	3.9	5.7	0.1177
	21	0.1	0.7	0.0149	3.3	0.6	0.0771
	22	0.0	1.3	0.0111	5.8	1.8	0.1048
	23	1.7	0.2	0.0254	7.3	1.2	0.1253
	24	0.1	0.6	0.0071	0.4	0.9	0.0208
	25	0.3	1.7	0.0106	0.2	1.2	0.0239
	26	0.8	0.2	0.0232	0.3	0.2	0.0906
	27	2.1	0.5	0.0188	0.9	2.3	0.0520
	28	0.4	0.7	0.0275	5.8	1.2	0.1575
	29	0.2	0.8	0.0051	0.2	5.3	0.0256
	30	0.3	0.3	0.0117	0.1	3.6	0.0269
	31	0.3	0.9	0.0315	0.3	0.4	0.0733
	32	0.4	0.5	0.0280	0.2	0.5	0.0807

8.5 Summary

The computational evaluation of the performance of the seven ink printing system was performed by evaluating gray metamers, a paint palette and spectral images. First, it was shown that the seven ink system enables a range of different gray metamers. These metamers are very sensitive to changing viewing conditions or variations during the printing process. The gray metamers were also used to evaluate the performance of the CYNSN forward model. While several grays were predicted accurately, a few showed a visible color difference between the measured and the predicted gray. A custom paint target was created from paint mixtures using the selected paint palette. This custom target representing in-gamut colors could be matched with good spectral and colorimetric accuracy. A mean color difference of 1.1 ΔE_{00} could be achieved while maintaining a mean RMS of less than 2.5%. The evaluation of synthetical spectral images representing artwork created with selected paints showed that a reproduction could be created without metamerism visible to the human eye. Therefore, the original should be reproduced with good spectral and colorimetric accuracy.

Chapter 9

Conclusions

The evaluation of a wide range of artist pigments and a set of printing inks showed that there are paint and ink combinations capable of producing spectral matches. Some artist pigments display very distinctive curve shapes that cannot be matched with the current set of HP Indigo ElectroInk®. New inks would have to be developed to match pigments like Cobalt Blue or Cerulean Blue. It was found that Ultramarine Blue can be spectrally matched with printing inks. The evaluation showed that Cyan, Magenta, Yellow and Black are important inks to support the spectral match of a wide range of artist pigments. The three additional inks in the final ink set were Reflex Blue, Orange and Violet. A paint palette with a wide color gamut that can be spectrally reproduced with the ink set was found.

The spectral modeling of the printing process showed that the CYNSN model with two sub cells and an effective area coverage correction could predict the spectral reflectance with good accuracy. The inversion of the CYNSN model required a lot of

computational power. Therefore, an existing implementation of a non-linear optimization in the language C had to be used to perform the spectral separation of images within a useful time. Nevertheless, this performance would not be practical in a commercial application.

The seven ink printing system used in this research was able to produce a range of several gray metamers. Most of these sensitive grays could be matched with good accuracy. A custom paint target including in-gamut colors could be matched with good spectral and colorimetric results. Synthetic spectral images showed that an accurate reproduction can be achieved. The good spectral accuracy of the print led to the same color constancy as the original. These images rendered for different illuminant conditions showed no visible metamerism between original and reproduction.

Chapter 10

Recommendations for Further Research

The present research is one piece in a large mosaic leading to a spectral color reproduction workflow. There is still a wide variety of problems that have to be solved in order to implement spectral color reproduction into a production environment. A big problem of this research was the inversion of the spectral model characterizing the printing process. Despite the fact that this has been an area of ongoing research for many years, a solution for a fast, true spectral color separation has not yet been found. Another limitation of this research is gamut mapping. After finding the best spectral match, the optimization searches for the smallest colorimetric difference. Optimizing for minimal ΔE_{ab} is a simple but not an optimal gamut mapping strategy for this application. Spectral color gamut mapping is a complex problem that has to be solved before a spectral workflow can be implemented. Since some spectra can be matched with different ink mixtures, a many-to-one mapping problem occurs. Even if the spectral reflectances are smooth, this problem causes image noise in the ink separations when the spectral separation is

performed on a pixel by pixel basis. This research showed that pigments that have been popular by artists can not be matched with the present ink set. In order to reproduce a wider range of pigments, new inks would have to be formulated with the intention to match these pigments. Printing more that four inks is a big challenge in print production. On conventional printing systems, most screening technologies generate some kind artifacts when printing with more than four inks. This problem will likely disappear with the fast evolving ink-jet production systems that use frequency modulated screening more successfully than most current production systems. Spectral color reproduction can only be used when there are appropriate input data. Spectral capturing has not yet evolved to a point were spectral data can be captured in an accurate and efficient manner. This has also been an area of ongoing research for many years.

Bibliography

[Abed, 2012] Abed, F. (2012). Personal communication.

[Berns et al., 2000] Berns, R. S., Billmeyer, F. W., Saltzman, M., and Billmeyer, F. W. (2000). *Billmeyer and Saltzman's principles of color technology*. Wiley, New York, 3rd ed edition.

[Bosket, 2011] Bosket, T. (2011). Art-affects. Presentation at Munsell Color Science Laboratory, RIT.

[Chen, 2006] Chen, Y. (2006). *Optimal design of ink spectra for multiple-ink color reproduction.* PhD thesis, RIT.

[CIE, 2011] CIE (2011). Cie, international commission on illumination, http://cie.co.at.

[Derhak, 2006] Derhak, M. W. (2006). Spectral colorimetry using labpqr: An interim connection space. *The Journal of Imaging Science and Technology*, 50(1):53–63.

[Gamblin, 2011] Gamblin, R. (2011). Artists oil colors, www.gamblincolors.com.

[Golden, 2011a] Golden (2011a). Golden artist colors, www.goldenpaints.com.

[Golden, 2011b] Golden, M. (2011b). email conversation.

[Gottsegen, 2011] Gottsegen, M. (2011). email conversation.

[Green, 2010] Green, P. (2010). *Color Management: Understanding and Using ICC Profiles*. Wiley.

[Guo et al., 2010] Guo, J., Xu, H., and Luo, M. R. (2010). Novel spectral characterization method for color printer based on the cellular neugebauer mode. *Chinese Optics Letters*, 8(11):1106–1109.

[Hewlett-Packard, 2009] Hewlett-Packard (2009). *HP IndiChrome Ink Mixing System v7.0*.

[Hunt, 2004] Hunt, R. W. G. (2004). *The reproduction of colour*. John Wiley & Sons, Chichester, West Sussex, England, 6th ed edition.

[ICC, 2010] ICC (2010). Specification icc.1:2010.

[ICC, 2011] ICC (2011). International color consortium, http://color.org.

[Kang, 2006] Kang, H. R. (2006). *Computational color technology*. SPIE Press, Bellingham, Wash.

[Kohler and Berns, 1993] Kohler, T. and Berns, R. S. (1993). Reducing metamerism and increasing gamut using five or more colored inks. *Reducing metamerism and increasing gamut using five or more colored inks*.

[Küppers, 1993] Küppers, H. (1993). *Die Farbenlehre der Fernseh-, Foto und Drucktechnik*. DuMont Buchverlag.

[Liquitex, 2007] Liquitex (2007). *The Acrylic Book*. Liquitex Artist Materials.

[Neugebauer, 1937] Neugebauer, H. E. J. (1937). Die theoretischen grundlagen des mehrfarbendrucks. *Zeitschrift für wissenschaftliche Photographie, Photophysik und Photochemie*, 36(4).

[Neugebauer, 2005] Neugebauer, H. E. J. (2005). The theoretical basis of multicolor letterpress printing. *Color Research and Application*, Volume 30(5).

[Okumura, 2005] Okumura, Y. (2005). Developing a spectral and colorimetric database of artist paint materials. Master's thesis, RIT.

[Pantone, 1998] Pantone (1998). Us patent 5,734,800 - six-color process system.

[Rosen, 2003] Rosen, M. R. (2003). *Navigating the roadblocks to spectral color reproduction: data efficient multi-channel imaging and spectral color management*. PhD thesis, RIT.

[Sigg, 2007] Sigg, F. (2007). Some considerations about screen angles. *Rochester Institure of Technology*.

[Sigg and Viggiano, 2011] Sigg, F. and Viggiano, S. (2011). Predicting the color of an overprint of two spot colors using a mathematical model. *TAGA*.

[Staniforth, 1985] Staniforth, S. (1985). Retouching and colour matching: The restorer and metamerism. *Studies in Conservation*, 30:101–111.

[Taplin, 2001] Taplin, L. A. (2001). Spectral modeling of a six-color inkjet printer. Master's thesis, RIT.

[Tzeng, 1999] Tzeng, D. (1999). Spectral-based color separation algorithm development for multiple-ink color reproduction. Master's thesis, RIT.

[Urban and Grigat, 2008] Urban, P. and Grigat, R.-R. (2008). Spectral-based color separation using linear regression iteration. *Color Research and Application*, 31(3):229–238.

[Urban et al., 2008] Urban, P., Rosen, M. R., and Berns, R. S. (2008). Spectral gamut mapping framework based on human color vision. *CGIV 2008 and MCS'08 Final Program and Proceedings*.

[Viggiano, 2010] Viggiano, S. (2010). *New Models for the Reflectance Spectra of Halftone-based Color Hardcopy*. PhD thesis, RIT.

[Wilcox, 1994] Wilcox, M. (1994). *Blue and Yellow Don't Make Green*. North Light Books.

[Wyble and Berns, 2000] Wyble, D. R. and Berns, R. S. (2000). A critical review of spectral models applied to binary color printing. *Color Research and Application*, 25(1):4 – 19.

[Zhao and Berns, 2007] Zhao, Y. and Berns, R. S. (2007). Image-based spectral reflectance reconstruction using the matrix r method. *Color Research and Application*, 32(5):343–351.

Appendices

A. Test Target Press Run 1

Figure A.1 shows the test target for the first press run. The upper target is used to evaluate the properties of the ink on paper, the lower target is used to evaluate the scattering of the colors over black ink. It is important that black ink is printed first. Process control elements are included at the top and the bottom of the page.

Figure A.1: Test target press run 1

B. Test Target Press Run 2

Figure B.1 shows the test target for the second press run to measure all Cellular Neugebauer primary colors with 3 nodes (0%, 50%, 100%).

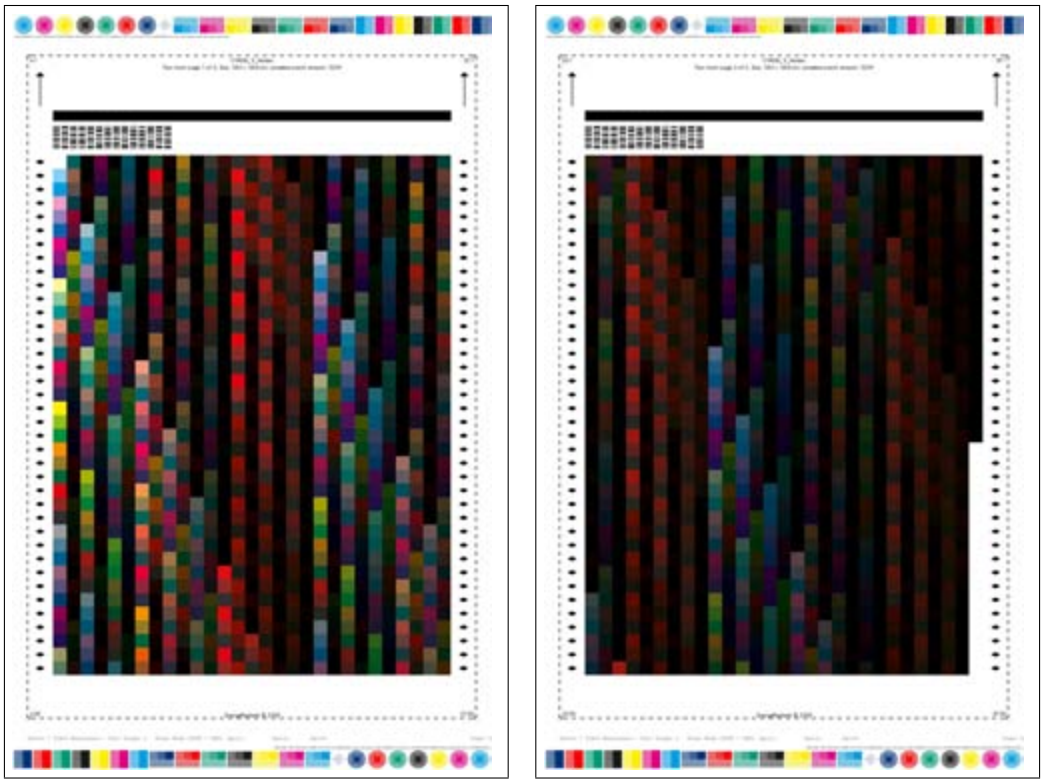

Figure B.1: Cellular Neugebauer Primaries for 3 Nodes

The random patches shown in Figure B.2 were used to evaluate the performance of the spectral printer model.

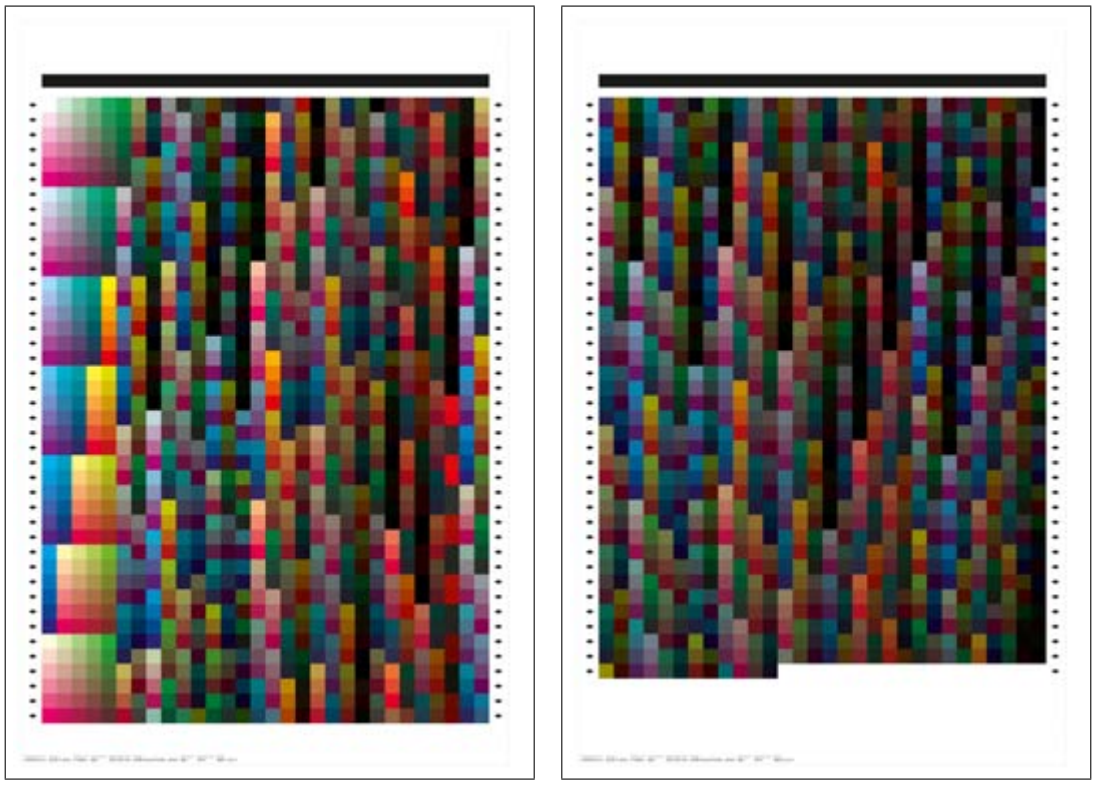

Figure B.2: Random Patches to Evaluate the Spectral Model

Figure B.3: Left: Ink ramps for effective area coverage correction. Right: IT8-7.4 CMYK Target for CMYK ICC profile

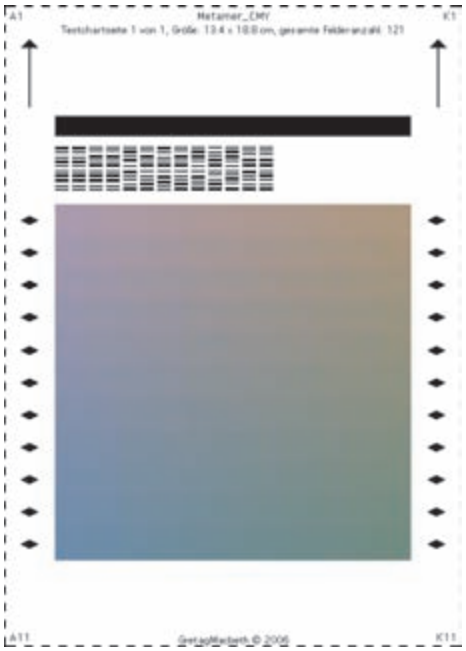

Figure B.4: Target to evaluate a gray metamer

C. Matlab Functions

```
function [ out ] = saunderson_Ri_to_R_SPEX( in, K1, K2 )
% ========================================================================
% Calculate R from Ri for specular excluded measurements
% ========================================================================
% Input values:   in = internal reflectance,
          K1 and K2: constants
% wavelenghts in columns and different measurements in rows
% ========================================================================

[row,col] = size(in);
out = ( (ones(row,col) - repmat(K1,row,col)) .* (ones(row,col) - ...
    repmat(K2,row,col)) .*in ) ./ (ones(row,col) - repmat(K2,row,col).*
        in);
end
```

```
function [ out ] = saunderson_Rm_to_Ri_SPEX( in, K1, K2 )
% ========================================================================
% Calculates Ri from Rm for specular excluded measurements
% ========================================================================
% Input values:   in = measured reflectance,
          K1 and K2: constants
% wavelenghts in columns and different measurements in rows
% ========================================================================

[row,col] = size(in);
out = in ./ ( (ones(row,col) - repmat(K1,row,col)) .*...
    (ones(row,col) - repmat(K2,row,col)) + repmat(K2,row,col) .* in ) ;
end
```

```
function [ out ] = KS_from_Ri_opaque( in )
% ========================================================================
% Function to calculate KS from Ri for opaque materials
% ========================================================================
% Input values:
```

```
% KS:                        internal spectral reflectance Ri [nx31]
% ========================================================================

[row,col] = size(in);
out = ((ones(row,col) - in).^2 ) ./ (in.*2);

end
```

```
function [ out ] = Ri_from_KS_opaque( KS )
% ========================================================================
% Function to calculate Ri from KS for opaque materials
% ========================================================================
% Input values:
% KS:                           K/S values [nx31]
% ========================================================================

[row, col] = size(KS);
out = ones(row,col) + KS - (KS.^2 + KS*2).^.5;

end
```

```
function [ R_pred ] = YNSN_Forward_Model( a, inks )
% ========================================================================
% Yule-Nielsen Spectral Neugebauer Forward Model
%
% This function is from the Masters Thesis "Spectral Modeling of a
% Six-Color Inkjet Printer" by Lawrence A. Taplin, Munsell Color
% Science Laboratory, 2001
% ========================================================================
% Input values:
% Matrix of neugebauer area coverage:  inks.neug_matrix [128x7]
% Neugebauer reflectances^(1/n):       inks.neugePrim_n [128x31]
% Number of inks:                      inks.no [1x1]
% Yule-Nielsen value:                  inks.n [1x1]
% area coverage:                       a [1x7]
%
% wavelenghts are in columns and samples in rows
% ========================================================================

area_coverage = ones(2^inks.no,1) * a;
```

```
20  R_pred = (inks.neugePrim_n' * prod(area_coverage.*inks.neug_matrix + (1-
        area_coverage) .* ~ inks.neug_matrix,2)).^inks.n;
21
22  end
```

```
1   function [ pred ] = CYNSN_Forward_Model_3Nodes( a, inks )
2   % ========================================================================
3   % Cellular Yule-Nielsen Spectral Neugebauer Forward Model
4   %
5   % This function was adapted from the c-code function cynsn() shown in
6   % the Masters Thesis "Spectral Modeling of a Six-Color Inkjet Printer"
7   % by Lawrence A. Taplin, at the Munsell Color Science Laboratory, 2001
8   % ========================================================================
9   % Input values:
10  % Matrix of cellular area coverage:    inks.cellular_neug_matrix [2187x7]
11  % Matrix of neugebauer area coverage: inks.neug_matrix [128x7]
12  % Cellular primary reflectance^(1/n): inks.cellular_neug_refl_n[2187x31]
13  % Number of inks:                      inks.no [1x1]
14  % Number of nodes:                     inks.nodes [1x1]
15  % Yule-Nielsen value:                  inks.n [1x1]
16  % area coverage:                       a [1x7]
17  %
18  % wavelenghts are in columns and samples in rows
19  % ========================================================================
20
21  t       = repmat(inks.cellular_neug_matrix(1,1),1,inks.no) ;
22  p       = a > t ;
23  h_ac    = a ./ t ;
24  h_ac(h_ac>ones(1,inks.no)) = 1 ;
25  h_ac(h_ac<ones(1,inks.no)) = inks.cellular_neug_matrix(1,1) ;
26  l_ac    = h_ac - t ;
27  b       = (a - l_ac) ./ (h_ac - l_ac) ;
28  pred    = zeros(1,size(inks.cellular_neug_refl_n,2)) ;
29
30  for i=0:1:(2^inks.no -1)
31      pri = 0;
32      off = 0;
33      for j=0:1:(inks.no-1)
34          if (bitand(uint8(i+1), bitshift(1, j))) == 0
35              pri = pri + (1 + p(j+1)) * inks.nodes^j ;
36          else
37              pri = pri + (0 + p(j+1)) * inks.nodes^j ;
38          end
```

```
39      end
40
41      if pri == 0
42          pri = inks.nodes^inks.no ;
43      end
44
45      w = 1;
46      for j=0:(inks.no-1)
47          if (bitand(uint8(i+1), bitshift(1, j))) == 0
48              w = w * b(j+1) ;
49          else
50              w = w * (1-b(j+1)) ;
51          end
52      end
53      pred = pred + inks.cellular_neug_refl_n(pri+off,:) .* w ;
54  end
55      pred = pred.^inks.n ;
56  end
```

```
1   function [ a_est, RMS_error, total_time_elapsed ] =
        YNSN_Inverse_Area_Pred_RMS( refl, start, ink, cie )
2   % ========================================================================
3   % Function to execute the non-linear optimization to invert the
4   % YNSN printing model
5   % ========================================================================
6   % Input values:
7   % Spectral reflectance to match:        relf [1x31]
8   % Start values for optimization:        start [1x7]
9   % Struct with Neugebauer data:          ink
10  % Struct with CIE data
11  % ========================================================================
12
13  % define the options for fmincon()
14  options = optimset(...
15  'Display','off', ...
16  'TolX',1e-5, ...
17  'MaxIter',500,...
18  'TolFun',1e-5,...
19  'Algorithm','active-set');
20
21  % define constraints for fmincon
22  A = ones(1,ink.no);
23  b = ink.no;             % Total Area Coverage
```

```
24 lb = zeros(1,ink.no);  % lower bound of area coverage
25 ub = ones(1,ink.no);   % upper bound of area coverage
26 nlcon = [];
27
28 tic      % start timer
29 [a_est,RMS_error]=fmincon('Objective_Function_Inverse_Optimization_RMS',
       start,A,b,[],[],lb,ub,nlcon,options,refl,ink);
30 total_time_elapsed = toc; % read timer
31
32 end
```

```
1  function [ rms_error ] = Objective_Function_Inverse_Optimization_RMS(
       area, refl, ink)
2  % ========================================================================
3  % Objective Function to invert the YNSN printing model
4  % ========================================================================
5  % Input values:
6  % Area coverage:                          area [1x7]
7  % Spectral reflectance to match:         relf [1x31]
8  % Struct with Neugebauer data:           ink
9  % ========================================================================
10
11 refl_est   = YNSN_Forward_Refl_Pred(area, ink);
12 rms_error  = RMS(refl', refl_est);
13
14 end
```

```
1  function [ p ] = vectorCorrelation_InkSel( ink1, ink2 )
2  % ========================================================================
3  % Function to calculate vector correlation of two vectors
4  % ========================================================================
5  % Input values:
6  % First vector (reflectance):             ink1 [nx31]
7  % Second vector (reflectance):            ink2 [nx31]
8  % ========================================================================
9
10 p = sum(ink1 .* ink2)' ./ ...
11     ( (sum(ink1.^2)).^(1/2) .* (sum(ink2.^2)).^(1/2) )' ;
12
13 end
```

```
function [ SX, KX ] = KM_SX_KX( R_WB, R_BB, white, black )
% ========================================================================
% Function to calculate SX and KX for the two constant Kubelka-Munk
% Black-and-White method
% ========================================================================
% Input values:
% Reflectance of ink with white backing:  R_WB [1x31]
% Reflectance of ink with black backing:  R_BB [1x31]
% Reflectance of black backing:           white [1x31]
% Reflectance of white backing:           black [1x31]
% ========================================================================

[no, ~] = size(R_WB);
white = repmat(white,no,1);
black = repmat(black,no,1);

a  = ( (R_WB-R_BB).*(1 + white.*black) - (white-black).*(1 + R_WB.*R_BB)
     ) ./ ( 2.*(R_WB.*black - R_BB.*white) )
b  = sqrt(a.^2 - 1)
SX = (1./b) .*( acoth((a-R_WB)./b) - acoth((a-white)./b) );
KX = SX.*(a-1);

end
```

```
function [ RMS_weight ] = RMS_weight( r1, r2, weight)
% ========================================================================
% Calculate the weighed Root Mean Square Error of two curves
% ========================================================================
% Input values:   r1     = spectral reflectance
%         r2     = spectral reflectance
%         weight = vector to weight the spectral difference
% ========================================================================

sq_err = ( (r1-r2) .* repmat(weight,1,size(r1,2)) ).^2 ;
RMS_weight = (mean(sq_err(:)))^(.5);

end
```

```
function [ out ] = parse_ColorPortFile( filename_array )
% ========================================================================
% Function to parse a file saved in X-Rite ColorPort v2
% when multiple file names are passed the function returns
% the mean of all files as a struct
% ========================================================================
% Input values:
% Charr array with filenames:          filename_array
% ========================================================================

for i=1:1:size(filename_array,1)
    all(:,:,i) = load(filename_array(1,:));
end

all_mean    = mean(all,3);
out.area    = all_mean(:,1:7) / 100;
out.lab     = all_mean(:,8:10);
out.lch     = all_mean(:,11:13);
out.refl    = all_mean(:,17:end);

end
```

```
function [  ] = plotSpectra( curve, refl, cie, yText )
% ========================================================================
% Plots spectral curve with the corresponding color in sRGB
% ========================================================================
% Input: curve, spectra, cie, 'lable for y-axis'
% ========================================================================

[row,col] = size(curve);
figure;
hold on
for i=1:1:row
plot(cie.lambda,curve(i,:),'Color',ref2srgb(refl(i,:)',cie.cmf,cie.
    illD65),'LineWidth',1.5)
end

xlabel('wavelength [nm]')
ylabel(yText)
hold off
```